ASSESSMENT OF HUMAN THERMAL COMFORT DURING SHORT-TERM EXPOSURE IN HOT AND HUMID URBAN OUTDOOR AREAS

HUANG TAIYANG

PhD

The Hong Kong Polytechnic University

2022

The Hong Kong Polytechnic University

Department of Building Environment and Energy Engineering

Assessment of Human Thermal Comfort During Short-term Exposure in Hot and Humid Urban Outdoor Areas

Huang Taiyang

A thesis submitted in partial fulfillment of the requirements for the degree of Doctor of Philosophy

August 2021

CERTIFICATE OF ORIGINALITY

I hereby declare that this thesis is my own work and that, to the best of my knowledge and belief, it reproduces no material previously published or written, nor material that has been accepted for the award of any other degree or diploma, except where due acknowledgement has been made in the text.

_____________________________(Signed)

Huang Taiyang (Name of student)

Abstract

Abstract of thesis entitled:	Assessment of human thermal comfort during short-term exposure in hot and humid urban outdoor areas
submitted by:	Huang Taiyang
for the degree of	Doctor of Philosophy

at The Hong Kong Polytechnic University in August 2021.

City residents have to frequently expose themselves to the outdoor environment. For example, people in a living community need to pass through the outdoor areas from home to groceries, restaurants, or subway stations. In daily life, the outdoor space usually acts as a transition area that people enter when moving from one building to another. This outdoor exposure is inevitable and the duration of the exposure is relatively short. For the improvement of residents' comfort and livability and in the urban transitional outdoor areas, it is crucial to carry out assessments on human thermal perceptions and develop appropriate models to predict thermal comfort in the short-term outdoor exposure. The thesis intends to investigate human thermal comfort during short-term (less than 15 minutes) exposure in the hot and humid urban outdoor areas by conducting on-site experiments, including meteorological monitoring and survey. Data acquired from the experiments were analyzed to develop models to predict human thermal sensation and thermal comfort during short-term exposure. Extra field experiments were performed as verification of the regression quality and predicting accuracy of the predicting models.

The thesis consists of three main sections: 1) The investigation on research subjects' thermal perceptions, including thermal comfort and thermal sensation conditions after a 15-min exposure in several outdoor sites located at a university campus. The experiments were conducted in 23 days from Mar-2016 to Dec-2016. A total number of 1,107 questionnaires were collected. 2) The investigation on research subjects' thermal perceptions, including thermal comfort, thermal sensation and thermal acceptability conditions during a 10-min exposure in two outdoor sites located at a university campus. The experiments were conducted in 14 days from Feb-2018 to Oct-2018. 197 research subjects participated in the repeat experiments and a total number of 1,182 questionnaires were collected in this experiment. 3) The development of TSV and TCV prediction models incorporating the data acquired from the above-mentioned outdoor experiments. Stepwise regressions were conducted to filter the independent variables in predicting TSV and TCV. Multiple linear regression was adopted to determine the impact coefficient of each selected predictor and obtain the final predicting models.

Results indicate that the major meteorological parameters differences that exist between the shaded sites and the sunlit sites are in solar irradiance and air velocity. Statistical analyses show that during both the 10-min exposure and the 15-min exposure, the shaded area are significantly more comfortable than the sunlit area. It is also revealed that respondent thermal perceptions are closely related to the subjects' perceptions of solar radiation and wind speed. Mean Thermal Sensation Vote fitted well respectively with PET or UTCI in linear regressions. A positive relationship existed between Thermal sensation vote and outdoor-indoor meteorological differences and the second-order polynomial regression is suitable for fitting Thermal comfort vote and Thermal acceptability vote with outdoor/indoor environmental differences. Yet additional considerations on the factors that have impacts on the occupants' actual thermal responses should be covered for the enhancement of the predicting accuracy of human thermal perceptions. To improve the predicting model, stepwise regression was employed and four independent variables were finally selected, including PET (or UTCI), indoor/outdoor PET (or UTCI) difference, subjective sunlight level and wind level. The four variables were correlated with TSV and TCV using multiple linear regression to determine the impact coefficients. Subjective sunlight level and wind level were converted into mean radiant temperature and air velocity, respectively according to the corresponding linear regression formulae. Eventually, the TSV and TCV prediction formulae are obtained including four predictors: PET (or UTCI), indoor/outdoor PET (or UTCI) difference, mean radiant temperature and wind velocity, all of which can either be calculated by the meteorological and surveyed data or directly collected from measurements and subject interviews. Predicting accuracies of the 4 predictor models are acceptable (57.9% ~ 72.7% in accuracy) according to the verifications. It is also found that the inclusion of the 3 extra predictors significantly improves the regression quality (0.1 ~ 0.2 in R^2) of the predicting models. The predicting accuracies are increased in most cases (+3.6% ~

+14.1%), except that in the TCV predicting model adopting PET and △PET as predictors (-4.2%). Thermal perception predicting models adopting UTCI and △UTCI as predictors are better in predicting accuracy (+1.1% ~ +7.8%) compared with models adopting PET and △PET as predictors.

This thesis comprehensively characterizes the thermal environment and occupants' thermal perception conditions during transitional short-term exposure in different outdoor building geometries located in a hot and humid subtropical city. The study provides abundant experimental data concerning human transient state thermal perceptions in the outdoor areas in the hot and humid subtropical climate. The output of the research can be used to predict subjective thermal perceptions during short-term outdoor exposure in any combinations of environmental parameters and personal details in the subtropical regions. It is also helpful in the development of advanced design tools concerning urban outdoor microclimate, which is believed to be beneficial for developers, city planners and the government in designing a more comfortable and livable urban environment.

Publications Arising from the Thesis

Journal publications

Huang, T., Li, J., Xie, Y., Niu, J., & Mak, C. M. (2017). Simultaneous environmental parameter monitoring and human subject survey regarding outdoor thermal comfort and its modelling. *Building and Environment*, *125*, 502-514.

Huang, T., Niu, J., Xie, Y., Li, J., & Mak, C. M. (2020). Assessment of “lift-up” design's impact on thermal perceptions in the transition process from indoor to outdoor. *Sustainable Cities and Society*, *56*, 102081.

Conference paper

Huang, T., Niu, J., Mak, C. M., & Lin, Z. (2017). Comparisons of Respondent Thermal Perceptions in Underneath-elevated-building (UEB) Areas and Direct-radiated (DR) Areas. Procedia Engineering, 205, 4165-4171.

Acknowledgements

I would like to express my appreciation to my parents, who have been providing me with unconditional supports and encouragement in all aspects of my life since I was born. I feel fortunate and grateful for being your child.

I want to thank my supervisor Prof. Niu Jianlei for his patient guidance during my Ph.D. study. You are the person who leads me to the research frontier, the person that inspires me from an academic amateur to a qualified researcher. Your professionalism as a scholar has always been an encouragement for me to pursue brilliance. I also want to thank my co-supervisor Prof. Mak Cheuk-Ming and Prof. Lin Zhang for their constant supports.

I want to express my gratitude to the colleagues in the CRF project of the Hong Kong Research Grant Council, Prof. Kenny C.S. Kwok, Dr. Lee Tsz-Cheung and Dr. Zhang Hui for their valuable advice on my research in the field studies. I also want to thank Mr. Kenny Hung for his supports in the preparation and calibration of the experimental instruments and Dr. Steve Lamb for his early advice on the questionnaire design. I want to acknowledge all my colleagues in Prof. Niu's research group, Prof. Liu Jianlin, Ms. Fang Yuhang, Dr. Xie Yongxin, Ms. Li Jianong, Dr. Wu Yan, Dr. Zhang Xiyao, Dr. Wang Caixia and Dr. Thomas Tung for their help and company.

Appreciation also goes to Ms. Zhu Tianlan, Ms. Lee Siu Yan, Ms. Pun Yuet Ting and Mr. Albert Law and Ms. Chan Wai-man for the help in the field experiments and data analysis.

Table of Contents

List of Figures

List of Tables

Nomenclature

Abbreviation	**Unit**	**Explanation**
$\triangle PET_{xmin\text{-}I}$	K	PET difference using PET at the x^{th} minute outdoors less PET in the indoor area
$\triangle UTCI_{xmin\text{-}I}$	K	UTCI difference using PET at the x^{th} minute outdoors less PET in the indoor area
α_l	-	Long-wave solar irradiance absorption coefficient
α_s	-	Short-wave solar irradiance absorption coefficient
ε	-	Emissivity
ν_b	$L/(s \cdot m^2)$	The blood from core to skin
ρ	kg/m^3	Density of the tissue
ρ_b, ρ_{bl}	kg/L	Blood density
σ	$W/(m^2 \cdot K^4)$	Stefan-Boltzmann constant
ω_{bl}	$m^3/(s \cdot m^3)$	Blood perfusion rate
A	year	Age
ANOVA	-	Analysis of Variance
c	J/(kg·K)	Heat capacitance
c_b	W·s/(K·kg)	Specific heat of blood
c_{bl}	J/(kg·K)	Heat capacitance of blood
C	W/m^2	Convective heat transfer
D	mm	Diameter of black globe
DTS	-	Dynamic thermal sensation
E	W/m^2	Total evaporative heat loss
E_{Re}	W/m^2	Sum of heat flows for heating and humidifying the inspired air
E_{Sw}	W/m^2	Heat flow due to evaporation of sweat
F_{cl}	-	Analogous factors for heat transfer by convection
F_{CS}	W/m^2	Heat flows from body core to skin surface
F_i	-	Angle factors between subjects and environment
F_{pcl}	-	Analogous factors for mass transfer by water vapor
F_{SC}	W/m^2	Heat flow from skin through the clothing to the outer clothing
G	-	Gender
h_r	$W/(m^2 \cdot K)$	Radiation exchange coefficient
h_c	$W/(m^2 \cdot K)$	Convective heat transfer coefficient
H	m	Height
I_{clo}	clo	Clothing insulation

k	W/(m·K)	Heat conductivity
K_{min}	W/(m^2·K)	Minimum heat conductance of skin tissue
m	-	Constant for different mean skin temperature
m_{rsw}	W/m^2	Rate of sweat latent heat production
M	W/m^2	Metabolic intensity
MEMI	-	Munich Energy-balance Model for Individuals
MTSV	-	Mean Thermal Sensation Vote
PET	℃	Physiological Equivalent Temperature
P_a	Pa	Saturated vapor pressure for the dry bulb of air temperature
P_{sk}	Pa	Saturated vapor pressure at $T_{skin,m}$
Q_l	W/m^2	Long-wave solar irradiance
Q_s	W/m^2	Short-wave solar irradiance
r	m	Radius
R	W/m^2	Radiative heat transfer
RH	-	Relative humidity
Ridit	-	Relative to an identified distribution unit
S_{cr}	W/m^2	Net heat flow from and to the core shell
S_{sk}	W/m^2	Rate of heat storage
S	W/m^2	Heat flow storage
SET*	℃	Standard Effective Temperature
t	s	Time
T	℃	Tissue temperature
T_a	℃	Air temperature
T_{bla}	℃	arterial blood temperature
T_c	℃	Core temperature
T_{cl}	℃	Mean surface temperature of the clothing
T_g	℃	Globe temperature
T_{hy}	℃	Head core temperature
T_{mr}	℃	Mean radiant temperature
Tsk	℃	Skin temperature
Tskin,m	℃	Mean skin temperature
TAV	-	Thermal Acceptability Vote
TAV_{xmin}	-	TAV at the xth minute
TCV	-	Thermal Comfort Vote
TCV_{xmin}	-	TCV at the xth minute
TSV	-	Thermal Sensation Vote
TSV_{xmin}	-	TSV at the xth minute
UTCI	℃	Universal Thermal Climate Index
V_{10}	m/s	10-meter wind velocity

V_a	m/s	Wind velocity
V_b	$L/(s \cdot m^2)$	Rate of skin blood flow
VP	hPa	Water vapor pressure
W	kg	Weight

Chapter 1 Introduction

1.1 Background

City residents inevitably spend much time outdoors. For example, the process of walking to the workplaces, schools, taking rests and other outdoor activities. Researchers believed that outdoor activities are helpful in reducing physical stress and evocating positive feelings (Abraham et al., 2010; Bowler et al., 2010). As appealed in prior studies (Gehl, 1987; Lloyd & Auld, 2003), high-quality livable outdoor areas are needed for the well-being improvement of the city residents. Therefore, the enhancement of thermal conditions and occupants' thermal perceptions in outdoor areas has become a hot research field. There are mainly two objectives in these studies focused on outdoor thermal comfort and outdoor environment: (1) to assess the performance of certain measures in enhancing outdoor microclimate; (2) to develop appropriate models to describe outdoor thermal comfort.

Among all the relevant studies during the past decades, some of the researchers aim at enhancing local thermal microclimate conditions by utilizing different measures. An important topic is to improve the local thermal conditions and the occupants' thermal perceptions at precinct scale by altering building and landscape designs. Some researchers (Ali-Toudert & Mayer, 2006; Bourbia & Boucheriba, 2010; Georgakis & Santamouris, 2006; Johansson, 2006; Krüger et al., 2010; Matzarakis et al., 2007; Pearlmutter et al., 2007; Shashua-Bar & Hoffman, 2004) studied on the urban street canyon, including aspect ratio and solar orientation's impacts on local thermal comfort. Some studies (Hwang et al., 2011; Lin et al., 2010; Yan et al., 2014; Yang et al., 2013; Yuan & Chen, 2011) focused on sky view factor (SVF), proposing that higher SVF was advantageous in alleviating the urban heat island effect and enhancing local thermal conditions. Others (Ali-Toudert & Mayer, 2007; Klemm et al., 2015; Ng et al., 2012; Picot, 2004; Shashua-Bar & Hoffman, 2000; Shashua-Bar et al., 2011; Srivanit & Hokao, 2013) aimed at green infrastructure and investigated the cooling efficiency and the impacts on the local microclimate of street trees, green roofs and urban parks. Xia et al. (2017) carried out wind tunnel experiments, discovering that the so-called "lift-up" design was found to be beneficial in wind amplification and thermal condition improvements. Computational Fluid Dynamics (CFD) studies and field measurements conducted by Niu et al. (2015), Liu and Niu (2016) and Liu et al. (2016) acted as extra pieces of evidence that the wind amplification at the pedestrian level can be achieved by adopting the lift-up design. Huang et al. (2017) further compared the thermal comfort conditions between open space and the lift-up shaded space and discovered a 0.5 unit drop of respondent thermal sensation vote in the lift-up shaded spaces.

Another aspect of the outdoor environment and thermal comfort investigations is to build reliable models and develop appropriate indices to evaluate outdoor thermal perceptions. Indices for thermal stress evaluation and thermal perception prediction were vastly studied. The most widely adopted indices in the evaluation of outdoor thermal perceptions are OUT_SET* (De Dear & Pickup, 2000; Pickup & de Dear, 2000), physiological equivalent temperature (PET) (Höppe, 1999) and universal thermal climate index (UTCI) (Jendritzky et al., 2012). Improved from standard effective temperature (SET*) (A. P. Gagge et al., 1986), which was initially adopted for evaluating the thermal stress in an indoor setup, OUT_SET* included the effects of solar and infrared radiation in the thermal regulation model to be available for human thermal stress assessment in the outdoor environment. PET was developed by Höppe (Höppe, 1984) based on the Munich Energy-balance Model for Individuals (MEMI) (Höppe, 1993). PET equals the temperature in the imaginary indoor condition when the subject's core temperature (T_{core}) and skin temperature (T_{skin}) are the same between the imaginary and actual environments. Therefore, PET can be calculated in any given combination of meteorological parameters and individuals' details. UTCI was proposed on the basis of the "Fiala" multi-node model (Fiala et al., 2012; Fiala et al., 1999, 2001) coupled with the advanced clothing model. UTCI was developed and defined as "the air temperature of the reference environment which produces the same strain index value" (Bröde et al., 2012).

The above-mentioned thermal comfort assessing models employed the equivalent temperature as an output parameter, describing the complex outdoor environment by a single parameter. The method that adopts equivalent temperature to evaluate the outdoor environment is convenient but not directly understandable in terms of human thermal perceptions. Therefore, studies concerning correlating thermal comfort assessed with human thermal perceptions were conducted to translate the equivalent temperature output from the thermal comfort assessing models into understandable thermal perceptions. Lin and Matzarakis (2008) discovered positive linear relation between mean thermal sensation vote and PET from the correlation involving 1644 research subjects in Taiwan. The thermal sensations and PET classes for Taiwan were obtained and found significantly different in the comparisons with the classes for Western/Middle European (Matzarakis & Mayer, 1996). Other thermal comfort assessing indices like SET^* (Hwang & Lin, 2007; Lin et al., 2011; Xi et al., 2012) and UTCI (Hadianpour et al., 2018; Huang et al., 2016; Huang et al., 2017; Krüger et al., 2015; Lai, Guo, et al., 2014; Watanabe et al., 2014) were also in good linear relation with respondent mean thermal sensation vote. Mahmoud (2011) correlated mean thermal sensation vote with PET in an urban park with different microclimate qualities, obtaining a series of linear equations available for different sites of an urban park. The field study performed by Yahia and Johansson (2013) illustrated the relations between mean thermal sensation vote and PET in both summer and winter, finding that fitted equations from the hot season are distinct from that from cool seasons. Similar conclusions were made by several academics (Elnabawi et al., 2016; Lin et al., 2009; W. Liu et al., 2016; Salata et al., 2016). It is noticeable that simple correlations between thermal perceptions and thermal comfort indices obtained from different regions, climates, seasons and sites can be significantly different. It is questionable to adopt solely one single thermal comfort index to appropriately describe occupants' thermal perceptions in the complex outdoor environment.

Oke et al. (2017) pointed out that the changes of local meteorological conditions and local surface properties of the experimental regions result in different urban microclimates, which have great impacts on the occupants' thermal comfort in the outdoor environment. Living communities with various building heights and densities, different orientations of income wind flow, different types of ground and façade albedos, different characteristics in green infrastructures and different climate zones are significantly distinct in terms of their local microclimates. Moreover, individual differences in clothing, activity, recent exposure history, adaptation effect, and psychological preference are also the key influence factors on the occupants' thermal perceptions. That is the reason why studies on thermal comfort in outdoor areas are usually available only in specific conditions rather than widely effective.

In urban daily life, the outdoor spaces usually act as a transition area that people enter from indoor spaces when moving from one building to another. For example, people in a living community need to pass through the outdoor areas from home to groceries, restaurants or subway stations. The entry to the outdoor spaces is often considered a passive decision for a city resident. Exposure in the outdoor environment is usually inevitable and the duration of the exposure is relatively short, usually less than 15 minutes. Human physiological parameters still change over time and the thermally steady state is hard to reach during the short periods after entering the outdoor environment. Liao and Cech (1977) stated that abrupt exposure from a comfortable indoor area to a hot outdoor site can lead to strong negative impacts on the occupants' thermal perceptions. In a city located in the hot and humid subtropical region, changes in meteorological parameters during the transitions from indoor to outdoor are significant. The effects of the indoor-outdoor environmental changes on the occupants' thermal perceptions cannot be ignored. However, relevant studies focused on thermal comfort during the short-term transitional exposure in outdoor spaces were scarce in the literature. For a better understanding of residents' thermal comfort and the improvement of residents' livability and in the urban transitional outdoor areas, it is crucial to carry out assessments on human thermal perceptions and develop appropriate models to predict thermal comfort specifically in the short-term outdoor exposure.

1.2 Objective and significance

The study intends to investigate human thermal perceptions and thermal comfort during short-term (less than 15 minutes) exposure in the hot and humid urban outdoor areas by conducting on-site experiments, including meteorological monitoring and questionnaire survey. Data acquired from the experiments were then analyzed to develop models to predict human thermal sensation and thermal comfort during the short-term exposure. Data collected from extra outdoor experiments were used to verify the model predicting accuracy and the improvement of model regression quality by introducing three more predictors. The main objectives of the study are shown as below:

1) To comprehensively investigate human thermal perceptions during the transitional

short-term exposure in typical outdoor spaces in a hot and humid region.

2) To obtain the appropriate relations translating the complex outdoor environment and human physiological conditions into human thermal perceptions during the short-term exposure.

3) To discover the most significant factors that account for human thermal sensation and thermal comfort in the transient thermal state after entering outdoors.

4) To develop thermal sensation and thermal comfort predicting models for the transitional short-term outdoor exposure that are of great quality and with good accuracy in thermal perceptions predictions.

This study provides abundant experimental data concerning human thermal comfort in the outdoor areas in a hot and humid city. The output of the research can be helpful to reasonably predict human thermal perceptions during short-term outdoor exposure by inputting combinations of outdoor environmental parameters. It is also beneficial for developers, city planners and the government in designing a more comfortable and livable urban environment.

1.3 Thesis outline

This thesis consists of seven chapters, including one chapter for introduction, one chapter for literature review, one chapter for methodologies, three chapters for discussing the findings of the research and one chapter for conclusions and suggestions for future studies.

Chapter 1 provides the background, research gap, objectives and significance of this study.

Chapter 2 presents a literature review on the relevant studies during the past decades, including different measures to enhance microclimate, most widely used thermal comfort indices, correlations to translate thermal comfort indices into thermal perceptions and studies concerning transient state thermal comfort.

Chapter 3 introduces the major methodologies used in this thesis, including measurement instruments, questionnaire design, indices adopted for thermal comfort evaluation, mean radiant temperature calculation methods and other statistical methods for data comparison or model development.

Chapter 4 presents the study on research subjects' thermal perceptions, including thermal comfort and thermal sensation conditions after a 15-min exposure in several outdoor sites located at a university campus. Comparisons on thermal perceptions in open outdoor spaces and lift-up shaded outdoor spaces are conducted. Linear regressions between MTSV and two thermal comfort indices, PET and UTCI, in different types of building landscapes are performed.

Chapter 5 presents an investigation on the occupants' thermal perceptions, including thermal comfort, thermal sensation and thermal acceptability conditions during a 10-min exposure in two outdoor sites located at a university campus. The regressions between MTSV and indoor-outdoor thermal indices difference (△PET or △UTCI) are presented.

Chapter 6 presents the development of TSV and TCV predicting models incorporating the data acquired from the 10-min exposure outdoor experiments. Stepwise regressions were conducted to filter the independent variables in predicting TSV and TCV. The four selected independent variables were correlated with TSV and TCV using multiple linear regression to determine the impact coefficients.

Chapter 7 summarizes the conclusions of the thesis and introduces the recommendations for future work.

Chapter 2 Literature review

2.1 Studies concerning outdoor thermal comfort

2.1.1 Measures to evaluate outdoor microclimate

2.1.1.1 Field measurements

Field experiments were the most adopted method to investigate outdoor microclimate conditions and outdoor thermal comfort. Spagnolo and De Dear (2003) summarized the thermal neutral states in both indoor areas and outdoor areas in Australia. Nikolopoulou and Lykoudis (2006) performed a series of comparative analyses focused on outdoor microclimate and outdoor thermal comfort conditions in the fourteen selected European cities. Johansson (2006) performed long-term field measurements in two different locations with distinct thermal conditions, which was followed by short-term measurements in another 10 selected sites (Johansson & Emmanuel, 2006). It was recommended that trees, covered walkways and pedestrian arcades that provides additional shaded be adopted in urban geometry design to improve thermal comfort in Colombo, Sri Lanka. Lin et al. (Lin, 2009; Lin & Matzarakis, 2008; Lin et al., 2010) carried out field monitoring and subject surveys in Taiwan. Other investigations aimed at a particular region or climate were performed during the past years, such as the studies conducted in Italy (Salata et al., 2016), Netherland (Klemm et al., 2015; Taleghani et al., 2015), America (Middel et al., 2016; Song & Wang, 2015), Colombia (Villadiego & Velay-Dabat, 2014), Morocco (Johansson, 2006), Egypt (Elnabawi et al., 2016), Japan (Thorsson et al., 2007), Malaysia (Qaid et al., 2016; Thorsson et al., 2007) and China (Huang et al., 2016; Lai, Guo, et al., 2014; Lai, Zhou, et al., 2014; Yin et al., 2012). A summary of outdoor field measurements conducted worldwide was listed in Table 2.1.

Table 2.1 Summary of studies concerning outdoor field measurements

Study	Year	Region	Climate
(Spagnolo & De Dear, 2003)	2003	Sydney, Australia	Humid subtropical
(Nikolopoulou & Lykoudis, 2006)	2006	14 cities in Europe	Mainly Temperate oceanic and Hot-summer Mediterranean
(Johansson, 2006)	2006	Fez, Morocco	Hot-summer Mediterranean
(Johansson & Emmanuel, 2006)	2006	Colombo, Sri Lanka	Tropical monsoon
(Thorsson et al., 2007)	2007	Tokyo, Japan	Humid subtropical
(Lin & Matzarakis, 2008)	2008	Nantou, Taiwan	Monsoon-influenced humid subtropical
(Lin, 2009)	2009	Taichung, Taiwan	Monsoon-influenced humid subtropical

(Yin et al., 2012)	2012	Nanjing, China	Humid subtropical
(Ng & Cheng, 2012)	2012	Hong Kong, China	Monsoon-influenced humid subtropical climate
(Lai, Zhou, et al., 2014)	2014	Wuhan, China	Humid subtropical
(Lai, Guo, et al., 2014)	2014	Tianjin, China	Monsoon-influenced hot-summer humid continental
(Villadiego & Velay-Dabat, 2014)	2014	Barranquilla, Colombia	Tropical savanna
(Klemm et al., 2015)	2015	3 cities in The Netherlands	Temperate oceanic
(Taleghani et al., 2015)	2015	De Bilt, The Netherlands	Temperate oceanic
(Song & Wang, 2015)	2015	Phoenix, US	Hot desert
(Middel et al., 2016)	2016	Tempe, US	Hot desert
(Salata et al., 2016)	2016	Rome, Italy	Hot-summer Mediterranean
(Elnabawi et al., 2016)	2016	Cairo, Egypt	Hot desert
(Qaid et al., 2016)	2016	Putrajaya, Malaysia	Tropical rainforest
(Huang et al., 2016)	2016	Wuhan, China	Humid subtropical
(Huang et al., 2017)	2017	Hong Kong, China	Monsoon-influenced humid subtropical climate
(Kong et al., 2017)	2017	Hong Kong, China	Monsoon-influenced humid subtropical climate
(Chen et al., 2018)	2018	Harbin, China	Monsoon-influenced hot-summer humid continental climate
(Xu et al., 2019)	2019	Xi'an, China	Monsoon-influenced humid subtropical climate
(Fang et al., 2019)	2019	Guangzhou, China	Monsoon-influenced humid subtropical climate
(Cheung & Jim, 2019)	2019	Hong Kong, China	Monsoon-influenced humid subtropical climate
(Lau et al., 2019)	2019	Hong Kong, China	Monsoon-influenced humid subtropical climate
(Deng & Wong, 2020)	2020	Nanjing, China	Humid subtropical

2.1.1.2 Numerical simulations

Numerical simulation (Berkovic et al., 2012; Blocken, 2014; Chen et al., 2004; Nagano & Horikoshi, 2011) has also been adopted as a useful tool in the studies of outdoor microclimate and outdoor thermal comfort. This technique has the advantage of lower time and human resources compared with on-site monitoring and surveys. It has been a major method for thermal comfort studies with the increase of computational power (Toparlar et al., 2017). Takahashi et al. (2004) combined CFD (Computational Fluid Dynamics) with conduction and radiation heat exchange to evaluate the urban environment validated with measurement data in Kyoto. Simulations provide complete experimental control and can account for climates of all scales (Lai et al., 2019), while field measurements can provide validations to simulations in order to achieve confidence and useful insights. Oke et al. (2017). Rosso et al. (2018) compared air temperature acquired from field measurements and ENVI-met simulations, discovering up to 4.83K of difference in air temperature root mean square error (RMSE). J. Liu et al. (2016) demonstrated a method that combines simulated air velocity and measured parameters in the prediction of outdoor thermal perceptions in the areas underneath the elevated buildings.

2.1.2 Measures to enhance outdoor thermal comfort

The alteration of building morphology and landscape is an effective method to enhance urban microclimate. It was well proved that properly arranging landscape and employing appropriate surface materials can optimize urban local microclimate. Among the previous studies, two methods were most widely used as approaches to enhancing the pedestrian-level microclimate and improving pedestrians' thermal comfort: urban ecological infrastructure and building geometry. A list of the relevant studies is illustrated in Table 2.2.

Table 2.2 Summary of studies concerning measures to enhance outdoor thermal comfort

Measure	**Reference of study**	**Year**	**Region**	**Major conclusion**
Urban greening	(Sonne & Vieira, 2000)	2000	Melbourne	A forested nature park is cooler compared with residental buildings in both daytime and nighttime.
	(Chang et al., 2007)	2007	Taipei	Urban parks feel cooler than the nearby locations.
	(Chen et al., 2009)	2009	Tokyo	The effectiveness of green roofs differed according to the configuration of the urban blocks.
	(Ng et al., 2012)	2012	Hong Kong	Trees provides higher cooling efficiency in compared with the grass.
	(Vailshery et al., 2013)	2013	Bangalore	Street with trees showed lower T_a, the difference of which can reach 5.6 K.
	(Skoulika et al., 2014)	2014	Athens	Urban park has an important mitigation impact, with average park cooling intensity of 3.3 K.
	(Feyisa et al., 2014)	2014	Addis Ababa	The maximum Park Cooling Intensity of the evaluated parks is 6.72 °C.
	(Chang & Li, 2014)	2014	Taipei	In residential districts, more trees are suggested to plant in the urban parks.
	(Klemm et al., 2015)	2015	Netherlands	PET of urban parks was −1.9 K compared to city center.
	(Lin et al., 2015)	2015	Beijing	The enhanced urban park surroundings areas increases as the park grows in size.
	(Kong et al., 2017)	2017	Hong Kong	Urban trees and dense canopy reduce average daytime T_{mr} by at most 5.1 K in the open site.
	(Aminipouri et al., 2019)	2019	Vancouver	The cooling potential of added street trees is greater in lower density residential neighborhoods.
	(Middel & Krayenhoff, 2019)	2019	Tempe	Trees reduced afternoon T_{mr} up to 33.4 °C but exhibited a clear T_{mr} increase of up to 5 °C after sunset.
Building and ground surface	(Rosenfeld et al., 1995)	1995	New Mexico	By increasing flat roofs albedo, peak decrease of T_a during daytime can reach 4K.
	(Campra et al., 2008)	2008	Almeria	0.3K average surface air temperature drop was discovered in the city with white roofs.
	(Yang et al., 2011)	2011	Shanghai	Pavement albedo increases lead to the deterioration in subjects' thermal comfort.
	(Taleghani et al., 2014)	2014	Portland	High albedo material increased T_{mr} but reduced Ta.

	(Chatzidimitriou & Yannas, 2015)	2015	Thessaloniki	High pavement albedo reduces surface temperatures and increases globe temperatures.
Building geometry	(Toudert, 2005)	2005	N/A	N-S orientated canyons are in better thermal conditions.
	(Johansson, 2006)	2006	Fez	deep canyons feel better in summer, while shallow canyons are in better conditions in winter.
	(Emmanuel et al., 2007)	2007	Colombo	High aspect ratios of street canyons result in the lowest average T_{mr} during daytime.
	(Ali-Toudert & Mayer, 2007)	2007	N/A	The vast openness of street canyons to solar radiation lead to the high thermal stress.
	(Bourbia & Boucheriba, 2010)	2010	Constantine-Algeria	Around 3~6 K in T_a difference was discovered between the street canyons and the rural areas.
	(Giannopoulou et al., 2010)	2010	Athens	A significant improvement of cooling efficiency was found for when aspect ratios of the street canyons declined.
	(Abreu-Harbich et al., 2014)	2014	Campinas	The N-S orientated street showed lower PET during daytime compared with other conditions.
	(Niu et al., 2015)	2015	Hong Kong	Local cooling in the outdoor microclimate can be achieved by employing appropriate building morphology.
	(Huang et al., 2020)	2020	Hong Kong	Shaded areas with amplified wind and less solar radiation enhance pedestrian's thermal perceptions.

2.1.2.1 Urban greening

Urban ecological infrastructure, which mainly consists of urban greening and water surface, was believed to be beneficial in urban heat island alleviation. Urban greening brings shading shelters, liquid evaporations and wind flow optimizations, which greatly enhance the local microclimates (Kong et al., 2017). PCI, i.e. the Park Cooling Island is another hot topic that researchers have been focused on. Urban parks were proved to provide a 1-degree decrease in ambient T_a during the daytime and a 3-degree decrease in ambient T_a during nighttime compared with the nearby areas with only buildings around. (Chang et al., 2007; Skoulika et al., 2014). Klemm et al. (2015) reported a 1.9-degree PET drop in an urban park compared with other areas away from the parks. Urban parks with different plant arrangements (Sonne & Vieira, 2000), locations (Feyisa et al., 2014), greenery evaporation rate (Chang & Li, 2014) provide different levels of heat mitigation velocity. The heat mitigation velocity of the urban park is also determined by the wind direction (Dimoudi & Nikolopoulou, 2003) and park orientation (Lin et al., 2015). Green roofs and sidewalk trees are better substitutions in a developed city compared with urban parks, since the they occupy too much of the urban land. Santamouris (2014) reviewed several studies on the cooling efficiency performance of green roofs employing numerical simulation, stating that ambient T_a can be decreased by up to 3 degrees if the green roofs were adopted thoughout the city. Nevertheless, it appeared in other studies (Chen et al., 2009; Taleghani, 2018) that the positive effects that green roofs have on the urban microclimate are nearly zero since the green roofs are too high to affect the environment at the pedestrian level. The pedestrian-level local microclimate is influenced more significantly by planting trees on the sidewalks of the streets. It was proved that high street tree density is significantly helpful in decreasing T_a (Ng et al., 2012; Vailshery et al., 2013), T_{mr} (Aminipouri et al., 2019; Middel & Krayenhoff, 2019) and PET (Kong et al., 2017; Morakinyo et al., 2018; Yang et al., 2011), which are believed to be beneficial local thermal condition optimization. It is widely accepted that sidewalk trees near the urban streets provide remarkable enhancement on local thermal microclimate and the occupants' thermal perceptions.

2.1.2.2 Building and ground surface

Absorption of solar radiation by the building and ground surfaces is a major cause of local air temperature raise. Structural surfaces with low albedo are more able to absorb solar heat and lead to the urban heat island effect (Santamouris, 2013). During the past years, researchers have focused on adopting high-albedo materials on the pavements, building roofs and facades to enhance urban microclimate and mitigate the heat island effect. Simulations conducted by Rosenfeld et al. (1995) indicated that by increasing flat roofs albedo, the peak air temperature of the day can be reduced up to 4K. Campra et al. (2008) also reported a 0.3K average surface air temperature drop in the city with white roofs, compared with the rural area where white roofs were not adopted. Taleghani et al. (2014) compared the surface temperature of roofs with different albedo (0.37 in black and 0.91 in white), discovered that surface temperature above the white roof surface was 1.3K lower than the black roof surface. The decrease of surface temperature was also found in other studies (Chatzidimitriou & Yannas, 2015; Doulos et al., 2004; Niachou et al., 2008), which can result in a reduction of long-wave radiation from the surfaces. However, other studies proved that the albedo increase may also lead to an increase in mean radiant temperature. Yang et al. (2011) carried out field measurements to evaluate the effects of high-albedo pavement have on outdoor microclimate. It was found that mean radiant temperature was increased by up to 14K if the albedo of the pavement was increased by 0.4. Taleghani et al. (2014) also discovered a 2.9K increase of mean radiant temperature above roof surface when adopting a white roof rather than a black roof.

2.1.2.3 Building geometry

Another hot field of outdoor thermal comfort research is adopting building geometry to promote the urban local thermal environment at the pedestrian level. Among the numerous methods for environmental enhancement, the street canyon is the building geometry that received the most attention. According to the studies performed by Shashua-Bar and Hoffman (2000), about 70% of the city areas are consist of different street canyons. A vast number of studies have performed in-depth investigations on the street canyons' features and their impacts on the local thermal conditions and occupants' thermal perceptions, in which the aspect ratio and orientation of the canyons are the major research focuses. It was discovered that T_a in the street canyons with high aspect ratios is often lower than those with low aspect ratios (Bourbia & Boucheriba, 2010; Emmanuel et al., 2007; Giannopoulou et al., 2010). PET was also found to be lower in the high-aspect-ratio street canyons (Abreu-Harbich et al., 2014; Ali-Toudert & Mayer, 2007) because of less solar irradiance. Other studies focused on the direction of the street canyons reported that the north-south orientated street canyons showed better pedestrian-level microclimate than the east-west orientated ones (Toudert, 2005). Moreover, Jamei et al. (2016) stated that the determination of street canyon features should also rely on the local climate and required solar irradiance. The "lift-up" design is another building geometry that is believed to be advantageous in optimizing urban local thermal conditions and the occupants' thermal perceptions. The principle of the "lift-up" design is to create a pillar-supported stilt floor at ground level, which provides not only shelters that prevent occupants from direct solar irradiance, but also local wind amplification that is favorable for the residents living in the hot subtropical climate (Niu et al., 2015). The subsequent investigations were conducted to examine the effects of the "lift-up" design on the local wind and thermal environment as well as occupants' comfort conditions. Huang et al. (Huang et al., 2017; Huang et al., 2020) performed field studies in several sites underneath the lift-up building, confirming that the local thermal conditions and the occupants' thermal perceptions were significantly improved in the lift-up area due to its amplified wind and shading shelters.

2.2 Outdoor thermal comfort indices

2.2.1 SET*

2.2.1.1 Basis of SET*

SET* (standard effective temperature) was developed from the effective temperature (ET*), which is based on Pierce two-node model (Gagge, 1971) combined with human thermal regulation and heat transfer. The assessed environemnt can be substituted by the environment of a artificial room, where $T_{mr}=T_a$ and RH=50%. A. Gagge et al. (1986) proposed the new standard effective temperature (SET*) by enhancing the effective temperature, expanding the index availability in outdoor situations. SET* was an equivalent air temperature of an isothermal environment when mean radiant temperature equals to air temperature, RH=50% and v=0.15 ms^{-1}, in which a person wears standardized clothing and activity level experienced the same heat stress and has the same skin wittedness (ASHRAE, 2009).

The Pierce two-node model considered that body of the human can be separated into two isothermal parts, skin and core. Thermal regulation and heat transfer within the human body are constructed based on the model. In another word, the basic physiological parameters of the human body can all be obtained by calculating the corresponding deviations from the set points. The physiological indicators concerning sweat and blood flows can also be obtained according to these basic parameters.

For a description of the heat balance between the human and the ambient environment, Gagge (Gagge, 1971) originally proposed that

$$S=M-E+R+C-W \tag{2.1}$$

where M is the rate of heating or cooling by the body, measured by energy/time, M is the metabolic rate, E is the heat loss from evaporation, R is radiation heat flow, C is the convection heat flow and W denotes the work.

In a uniform environment, if the subject is not doing external work, i.e. W=0, Equation (2.1) can be written as:

$$S = M\left[\left(1 - 0.0023(44 - \emptyset_a P_a)\right)\right] - 2.2h_c(0.06 + 0.94w_{rsw})[P_{sk} - \emptyset_a P_a]F_{pcl} - (h_r + h_c)(T_{core} - T_{skin})F_{cl} \tag{2.2}$$

where $\emptyset_a$ is the relative humidity, P_a is the saturated vapor pressure for the dry-bulb temperature, h_r and h_c are respectively the radiation exchange coefficient and the convective heat transfer coefficient, P_{sk} is saturated vapor pressure, F_{cl} and F_{pcl} are the analogous factors, respectively. For an assessment of the heat transfer between the human body and the environment, these two parts are treated as two concentric shells, as illustrated in Figure 2.1.

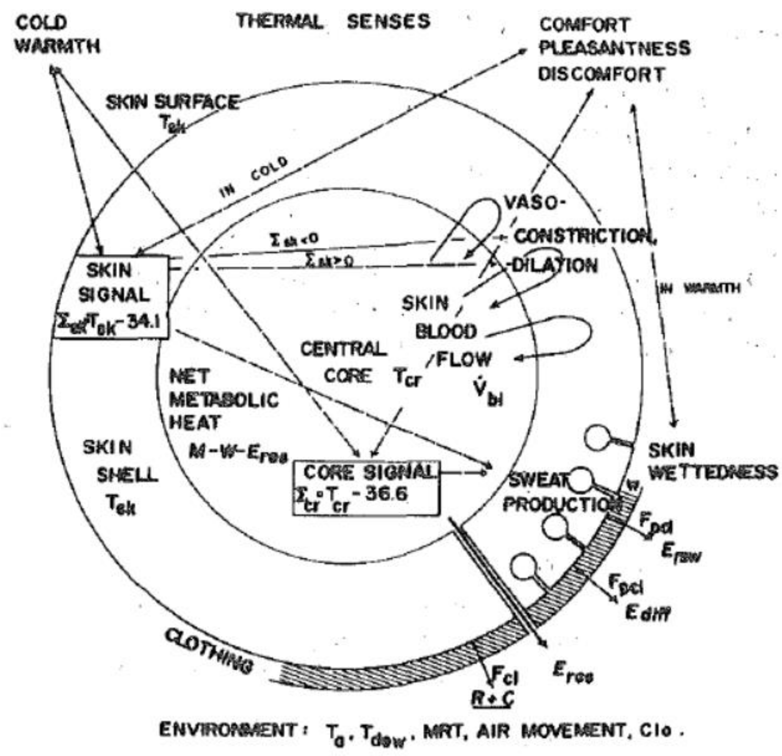

Figure 2.1 Concentric model of core and skin of human body and the environment (Gagge, 1971)

The heat exchange to the skin tissue is expressed by Equation (2.3):

$$S_{sk} = K_{min}(T_{cr} - T_{sk}) + c_b\dot{V}_b(T_{cr} - T_{sk}) - E_{sk} - R + C \quad (2.3)$$

where S_{sk} is the rate of heat storage, c_b is the specific heat of blood, V_b is the rate of skin blood flow and K_{min} is the minimum skin tissue heat conductance. The heat exchange to the core is expressed by Equation (2.4):

$$S_{cr} = (M - E_{res} - W) - K_{min}(T_{cr} - T_{sk}) + c_{b1}\dot{V_{b1}}(T_{cr} - T_{sk}) \quad (2.4)$$

where E_{res} is the respirational heat of vaporized moisture, whose relation was given by Fanger (1967) that:

$$E_{res} = 0.023M[44 - \emptyset_a P_a] \quad (2.5)$$

where $\emptyset_a$ is the relative humidity and P_a is the saturated vapor pressure for the dry bulb of air temperature of the environment. For a description of the controlling system in the human body, it is assumed that the signals from the skin and core are given by:

$$\sum_{sk} = T_{sk} - 34.1 \tag{2.6}$$

$$\sum_{cr} = T_{cr} - 36.6 \tag{2.7}$$

Other factors such as skin blood flow V_{b1} and heat exchange from sweating E_{rsw} are respectively represented by Equation (2.8) and (2.9).

$$\dot{V_{b1}} = (6.3 + 75\sum_{cr})/(1 - 0.5\sum_{sk}) \tag{2.8}$$

$$E_{rsw} = 0.7\dot{m_{rsw}}[2^{(T_{sk}-34.1)/3}] \tag{2.9}$$

where m_{rsw} is the rate of sweat production of the human body.

Finally, energy exchanges and temperatures of the human body model can be given by Equation (2.2) to (2.5). with supplemental equations of other factors not illustrated. And it is possible to integrate the skin and core temperature difference with the thermal neutrality conditions and the sweating effect to predict physiological energy and temperature factors by using Equation (2.6) to (2.9), which forms the calculation basis of the thermal indices ET* and SET*.

2.2.1.2 SET* applications in outdoor thermal comfort

SET* was employed by Lin et al. (2011) as an indicator evaluating the overall outdoor environmental conditions to assess the occupants' thermal perceptions and individual preferences in the outdoor environment. It is found that even though subjects' preferences upon T_a and sunlight diverged in different seasons for the same SET* exposure in the two seasons. Johansson et al. (2018) compared the occupants' subjective thermal perceptions and with SET* to evaluate the different local thermal conditions' effect on subjects' outdoor thermal comfort. The result indicated that the neutral value of SET* is above the theoretical neutral value, indicating people in the temperate climate zones can accept unacceptable thermal conditions. Nazarian et al. (2017) used SET* to describe the complex outdoor thermal conditions and developed the outdoor thermal comfort predicting methodology and its spatial variability in urban streets. The study focused on the performance of a thermal comfort model taking into account the flow patterns and the heat distribution of urban geometries, since SET* may change up to 10 °C due to the wind shelters. Zhou et al. (2013) adopted SET* to clarify the effect of piloti on thermal comfort in a humid subtropical city. The correlation between SET* and TSV was obtained, and the neutral SET* was about 24.8°C. Similar research on the enhancement of outdoor thermal comfort brought by the piloti was performed by Xi et al. (2012). Pickup and de Dear (2000) improved the SET* and proposed OUT_SET*, which is especially for the assessment of the outdoor environment. The new index resolves the limitation in the assumption $T_{mr}=T_a$, which may limit the application of SET* to be only in indoor environmental conditions.

2.2.2 PET

2.2.2.1 Basis of PET

PET is based on the thermal regulation and human body heat balance model Munich energy balance model for individuals (MEMI) (Höppe, 1994). It was proposed to take into account the thermo-physiological effects by Höppe (1993). According to the study performed by Mayer and Höppe (1987), PET has a similar definition to SET*, and is defined as the equivalent air temperature at which, in a typical indoor condition heat balance of the human body exists (work metabolism 80 W of light activity, and clothing of 0.9 clo). The assumptions of the artificial indoor environment include T_{mr}=Ta, Va=0.1 m/s and VP=12 hPa. To calculate PET, the thermal conditions of the body should be calculated with MEMI for a given combination of meteorological parameters. In addition, insertion of the calculated values for mean skin temperature and core temperature should be joined into the model MEMI and solving the equation system (Equation (2.10) to (2.12)) to obatin T_a. The output from the calculation equals PET.

It is necessary to cover all basic thermoregulatory processes for the purpose of predicting the physiological quantities of the human body. A great example is thermal regulation and human body heat balance model, Munich energy balance model for individuals (MEMI), on which PET calculation is based. The MEMI model is based on the energy balance equation of the human body, Equation (2.10), which is a detailed expression of the heat balance equation in Pierce two-node model:

$$M + W + R + C + E_D + E_{Re} + E_{Sw} + S = 0 \tag{2.10}$$

M: metabolic heat production; W: physical work; R: human body radiative heat flow, C: convective heat transfer; E_D: latent heat; E_{Re}: heat flows from respiratory; E_{Sw}: heat flows from sweat evaporation; S: storage of heat flow.

Some terms from Equation (2.11) are dependent on the ambient conditions and controlling system. For example, the E_{Sw} (physiological sweat rate) depends on the human core temperature. Therefore, another three parameters need to be added to solve Equation (2.11), including T_{cl} (mean clothing surface temperature), T_{sk} (mean skin temperature) and T_c (core temperature). In order to calculate these three quantities describing the heat flows from the body core to skin surface, F_{CS} and skin surface through the clothing layer to the clothing surface, F_{SC} in addition to Equation (2.11) are necessary. These two factors are represented respectively by:

$$F_{CS} = v_b \rho_b c_b (T_c - T_{sk}) \tag{2.11}$$

where v_b is the blood flow from the body core to the skin, ρ_b is the blood density and c_b is the specific heat.

$$F_{SC} = (1 - I_{clo})/(T_{sk} - T_{cl}) \tag{2.12}$$

where I_{clo} is the heat resistance of the clothing.

By means of joining Equation (2.10) to (2.12) and other thermo-physiological considerations proposed by Höppe (1984), it is possible to calculate the thermal state of the body, which is characterized by the heat flows, body temperatures and sweat rate, in any combinations of meteorological parameters and personal details. PET is an index derived from an artificial indoor room, but it is believed to apply to the assessments of the outdoor environment. With the help of Software RayMan proposed by Matzarakis et al. (2007), PET can be directly obtained by the inputs of geographic and time data, environmental data including air temperature, vapor pressure, RH, wind velocity, mean radiant temperature, etc., personal data of subject and the clothing and activity information.

2.2.2.2 PET applications in outdoor thermal comfort

PET is a widely used indicator of outdoor thermal conditions due to understandable output as well as the convenience in the computational calculation. Matzarakis et al. (1999) demonstrated the PET classes in the corresponding physiological stress in Greece, which was summarized according to the studies by Matzarakis and Mayer (1997), which was illustrated in Figure 2.2. The distribution of PET was performed by Svensson et al. (2003) with the help of GIS. Large variations in PET during a clear, calm day during average conditions in July were discovered, indicating that magnitude and spatial variations exist within the high, midlatitude, urban area during summer. Thermal conditions in Szeged were assessed by Gulyás et al. (2006) adopting PET as a thermal index, showing that PET differences amongst the selected research areas can be up to 15 to 20K. A significant difference was also found in the human comfort sensation between different sites. Ali-Toudert and Mayer (2006) adopted PET as an assessment index to evaluate human bio-meteorological conditions and analyzed aspect ratio and orientation’s effects on the thermal microclimate of the urban street canyons. It was revealed that aspect ratio and street orientation are strong dependents of the spatial distribution of PET at street level. Bouyer et al. (2007) adopted PET and wind tunnels and studied the thermal perceptions of human subjects in the stadium.

Alexandri and Jones (2008) demonstrated the PET simulations of green infrastructure's impact on the thermal environment of street canyons. Du et al. (2017) combined wind tunnel tests and on-site monitoring in a university campus to generate PET values in order to develop an integrated method to assess outdoor. Huang et al. (2017) investigated the regression qualities between PET and mean thermal sensation and found that PET showed great linear relation with subjects' mean thermal sensation vote. But the deviations in the regressions from different outdoor sites indicated the potential inaccuracy of PET when predicting thermal sensation. Fang et al. (2018) studied the sensitivities of personal details and physical factors on PET. It was found that relation between air velocity and PET was positive, while RH, I_{clo} and metabolism had insignificant effect on PET.

PMV	PET (°C)	Thermal perception	Grade of physiological stress
		Very cold	Extreme cold stress
–3.5	4		
		Cold	Strong cold stress
–2.5	8		
		Cool	Moderate cold stress
–1.5	13		
		Slightly cool	Slight cold stress
–0.5	18		
		Comfortable	No thermal stress
0.5	23		
		Slightly warm	Slight heat stress
1.5	29		
		Warm	Moderate heat stress
2.5	35		
		Hot	Strong heat stress
3.5	41		
		Very hot	Extreme heat stress

Figure 2.2 PET classes in the corresponding thermal perception and physiological stress grades (Matzarakis & Mayer, 1997).

2.2.3 UTCI

2.2.3.1 Basis of UTCI

In 2011, a new thermal index for outdoor thermal environments was announced by the International Society of Biometeorology called the Universal Thermal Climate Index (UTCI). The proposal of UTCI is to create an internationally accepted index that can be applied in the outdoor thermal environment in the major bio-meteorological situations (Jendritzky et al., 2012).

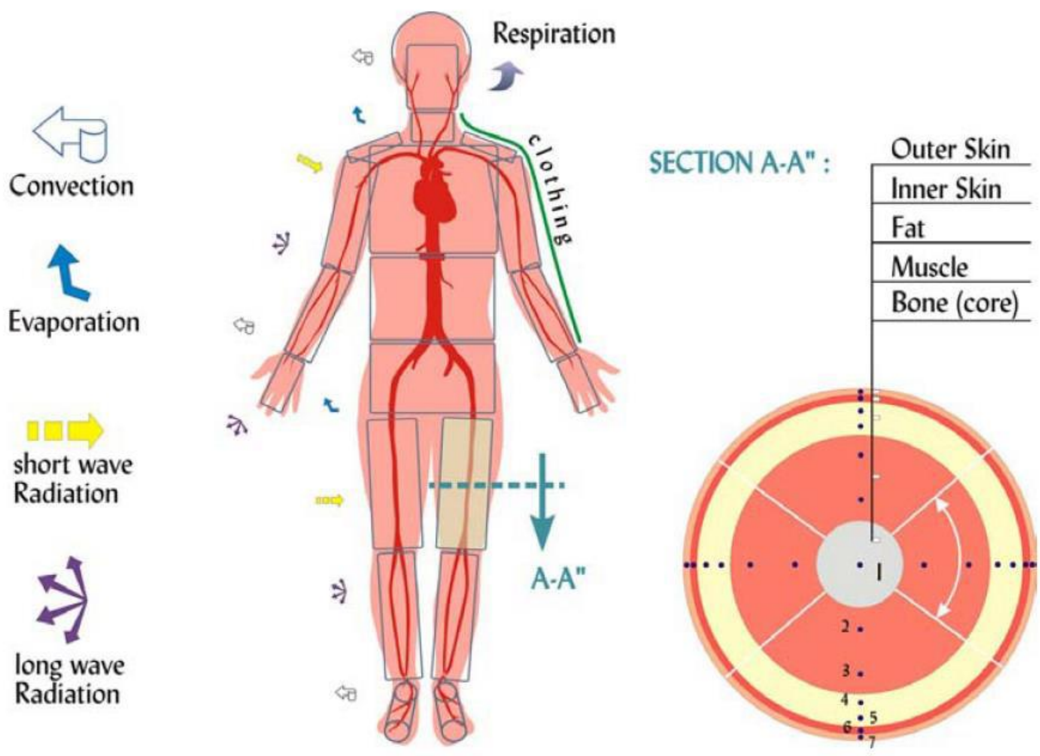

Figure 2.3 Passive system derived from the Fiala thermal comfort model (Fiala et al., 2012).

The Fiala multi-node model consists of the passive system (Figure 2.3) and the active system (Figure 2.4). 20 separate elements in sphere and cylinder were used to represent the human body. Each element was composed of five annular concentric tissue layers (Fiala et al., 2010). Equation (2.13) (Fiala, 1998) is used to calculate the heat transfer in each node of Fiala model in polar and spherical coordinates:

$$\rho c\frac{dT}{dt} = k\left(\frac{d^2T}{dr^2} + \frac{g}{r}\frac{dT}{dr}\right) + q_m + \rho_{bl}\omega_{bl}c_{bl}(T_{bla} - T) \qquad (2.13)$$

where ρ is the density of the tissue, c is the heat capacitance, k is the heat conductivity, T is the tissue temperature, g is a factor that indicates polar or spherical ordinates, ρ_{bl} is blood density, ω_{bl} is the perfusion rate of blood, c_{bl} is the blood heat capacitance, T_{bla} is blood temperature of arterial, t and r are time and radius, respectively.

Active System

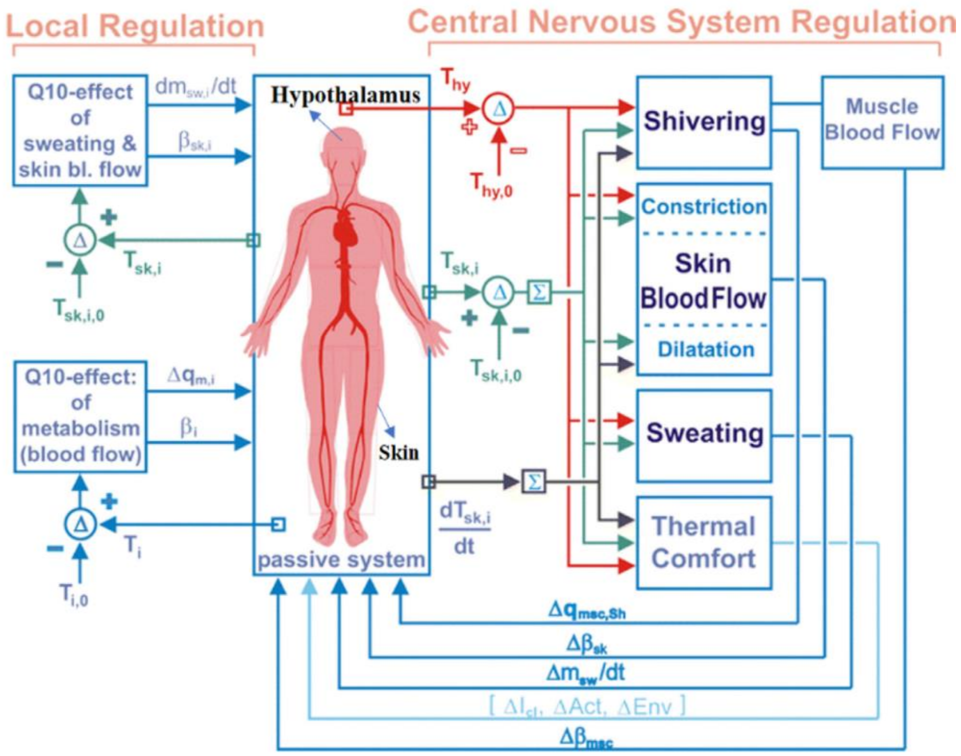

Figure 2.4 Active system derived from the Fiala thermal comfort model (Fiala et al., 2012).

Evaluation of dynamic thermal sensation (DTS), which considered the mean skin temperature and its change range, was included in the Fiala multi-node model to interpret the physiological parameters into the thermal sensation in both steady and transient environments:

$$DTS = 3\tanh\left(\frac{0.11\frac{dT^{-}_{skin,m}}{dt}+1.91\frac{dT^{+}_{skin,m}}{dt_{max}}e^{-0.681t}}{1+G} + m\left(T_{skin,m}-34.4\right)+G\right) \tag{2.13}$$

$$G = 7.94e^{\left(\frac{-0.902}{T_{hy}-36.6}+\frac{7.612}{T_{skin,m}-38.4}\right)} \tag{2.14}$$

where $T_{skin,m}$ is the mean skin temperature, T_{hy} is the head core temperature, m is a constant for different mean skin temperature, $\frac{dT^{+}_{skin,m}}{dt_{max}}$ is the maximum positive skin temperature change rate, and t is the elapsed time.

On the basis of "Fiala" model, UTCI was proposed and defined as the air temperature of the reference environment which produces the same strain index value. That is, the thermal stress of an actual environment presented by the combination of air temperature (Ta, °C), 10-m wind speed (V_{10}, ms^{-1}), vapor pressure (VP, hPa), and mean radiant temperature (T_{mr}, °C) can be represented by UTCI which introduces the same level of thermal stress under a combination of reference parameters. This reference environment was defined with RH=50%, V_a=0 and T_{mr}=T_a.

2.2.3.2 UTCI applications in outdoor thermal comfort

UTCI was adopted by worldwide researchers to examine the urban thermal microclimate under different building and landscape geometries and occupants' thermal comfort outdoors in different climate zones. Research conducted by Bröde et al. (2012) analyzed the thermal sensation predictions made by UTCI and compared them with actual TSV. It was shown that UTCI provided satisfactory predictions of TSV according to the environmental conditions, which can be appropriate for the evaluation of urban thermal comfort in the subtropical regions. Bröde et al. (2013) carried out field studies and bioclimatic surveys in the sub-tropical urban area of Curitiba, which also serves as evidence that adequate predictions of pedestrians' behavior and thermal sensation can be made by UTCI. Lam and Lau (2018) compared the subjects' thermal perceptions from two cities, Hong Kong and Melbourne, in different climate zones with similar UTCI ranges. The result indicated that Melbourne residents stated hot sensations when experiencing higher UTCI. It was recommended to develop different thermal sensation - UTCI scales for different climate zones in order to perform enhanced prediction of thermal comfort outdoors from different regions. Huang et al. (2017) relate thermal sensation votes with UTCI values of the occupant in two different outdoor building geometries, the underneath elevated building shaded area and the open sunlit area. Strong linear relations between occupants MTSV and UTCI were discovered. Other studies compared the thermal perception predicting accuracy or availability of UTCI with that of other thermal comfort indices. Lai, Guo, et al. (2014) conducted field measurements and subject surveys at a park in Tianjin, compared the thermal comfort predictions made by UTCI and PMV and found that UTCI satisfactorily predicted thermal comfort, while the PMV overestimated thermal comfort in the selected outdoor site. Fang et al. (2018) established regressions of MTSV with PET or UTCI in different metabolisms of the research subjects, discovered that differences exist in the neutral PET and UTCI within the metabolic rate range 1–2 MET (for PET) and 2.6 MET (for UTCI). Provençal et al. (2016) compared the sensitivities of UTCI, PET, HX (humidex) and WC (wind chill index) in different meteorological parameters. Compared with PET, UTCI was more sensitive to T_{mr}, slightly more sensitive to RH and significantly more sensitive to V_a.

2.3 transient state thermal comfort

Early thermal comfort investigations assumed that the research subjects stayed in the imaginary static indoor environment with no solar radiation, low air velocity and subjects maintaining thermal steady state. If the research subjects are exposed long enough, heat transfer between the ambient environment and themselves will finally stabilize and the thermal steady state is achieved. Nevertheless, the outdoor environment is usually not static and the variations of outdoor meteorological parameters can be much more intense compared with the indoor conditions. Therefore, the thermal steady state is almost impossible to reach in the outdoor area. In-depth studies focused on the transient state thermal perceptions are thus required for the better description of occupants' thermal comfort in the complex outdoor environment.

De Dear (2011) employed a psychophysiological phenomenon "alliesthesia" to separate human's thermal pleasant from thermal neutrality and acceptability under transient conditions. The external stimulus that decreases/increases the error of the regulated variable to its set-point will be perceived as pleasant (positive alliesthesia)/unpleasant (negative alliesthesia). The principle of alliesthesia opened a new territory of thermal comfort investigations. Parkinson and De Dear (2015) explained the basic theory of alliesthesia and carried out lab experiments to assess the alliethesia effect in the transient environment (Parkinson & de Dear, 2016, 2017; Parkinson et al., 2016). To sum up, occupants' thermal perception in the transient state is in intensive exploration since the understand of subjective thermal responses and perceptions in a complex, rapid changing environment will be helpful to better characterize human thermal comfort in realistic situations.

Climate chamber experiments were performed by Liu et al. (2014) in order to investigate the subjects' subjective responses and T_{skin} in the step-change transient process. It was discovered that subjects' TSVs are in great relation with the heat transfer from the outer skin, suggesting the skin heat transfer can be a good indicator to account for transient thermal perceptions. A similar methodology was employed by Xiong et al. (2016) to assess occupants' transient TSV and T_{skin} in step-change T_a. Results indicated that mean T_{skin} took over 45 minutes to achieve static. Mihara et al. (2019) studied different parameters' impacts on transient thermal sensation in the tropical areas. It was found that air velocity, tempareture and initial metabolism greatly influenced variations of transient thermal sensation, comfort and acceptability when entering air-conditioned indoor areas from outdoor areas. Lau et al. (2019) also discovered that occupants' short-term transient thermal experience had great impacts on participants' thermal sensation. Dahlan and Gital (2016) performed experiments aiming at the occupants' TSV and TCV in the transient process of transferring between outdoor corridors and the indoor office with air-conditioning. Environmental step-changes effects on the occupants' transient thermal sensation and thermal comfort in a hot and humid climate were examined thoroughly. The same method was adopted by Yu et al. (2015), yet the attention of the study was paid to find out the optimal T_a range in the temporarily occupied areas in winter. Cheung and Jim (2019) proposed the transient acceptable temperature range for the evaluation of 1-hour thermal acceptability, which was validated with the respondent survey conducted in Hong Kong. The 1-hour acceptable temperature range was recommended as standard for transient outdoor thermal comfort assessment. Zhang et al. (2020) developed a predicting model for occpant's mean thermal sensation vote during the process of moving outdoors. By including the additional parameter, the difference between initial and later metabolic rate, the model was considered to accurately predict occupants transient thermal comfort.

To build up comfortable and livable urban outdoor thermal environment, it is crucial to understand the occupants' thermal perceptions during the transitional exposure outdoors. The above-mentioned studies summarized the meteorological, physiological and personal parameters' impacts on occupants' thermal sensation and thermal comfort in transient state. Some models focused on participants' thermal comfort during specific transient state exposure were also developed. Yet, relevant studies that focus on the transient state thermal perceptions during outdoor short-term exposure (less than 15 minutes) and development of corresponding predicting models were little in the prior studies.

2.4 correlations to translate thermal comfort indices into thermal perceptions

Although the thermal comfort indices provide convenient access to evaluating the outdoor thermal environment, one of the limitations in the thermal comfort indices that adopt equivalent temperature as an output parameter is that occupants' thermal perceptions cannot be directly obtained. During the past two decades, an effort has been made among global researchers to interpret these thermal comfort indices into thermal perceptions by conducting field measurements and subject interviews, correlating subjects' thermal perceptions with the thermal comfort indices.

The mainstream regression method is linear regression fitting subjects' TSV with the corresponding thermal comfort indices. In most cases, the linear regression provides satisfactory fitting quality while correlating subjects' mean TSV with thermal comfort indices. (Hwang & Lin, 2007) collected 8077 sets of data from a field survey of five public places in Taiwan to investigate thermal comfort ranges, neutral temperatures, and preferred temperatures for the semi-outdoor and outdoor environment. Correlations between subjects' mean TSV and SET* were performed, showing a strong linear relation for both semi-outdoor environment (R^2=0.97) and outdoor environment (R^2=0.98) cases. Following studies that examined 1644 subjects in the outdoor environment in Taiwan (Lin et al., 2009; Lin et al., 2011) also observed the strong linear relations between MTSV and SET* (R^2=0.919 for hot season, R^2=0.945 for hot season)/PET (R^2=0.96 for hot season, R^2=0.89 for cool season). Results reported in other studies (Cohen et al., 2013; Elnabawi et al., 2016; Krüger et al., 2015; Lai, Guo, et al., 2014; Mahmoud, 2011; Salata et al., 2016) also supported this conclusion. Only a few studies performed a poor regression quality (Huang et al., 2016; Yahia & Johansson, 2013).

Although employing linear regression to fit MTSV with thermal comfort indices provides high-quality results, one single linear model with merely one independent variable (the adopted thermal comfort index) is insufficient to cover all environmental or climate conditions. Among a number of studies, it was discovered that the linear regressions equation and the corresponding neutral temperatures are different when comparing the data acquired from different weather, research sites and climate zones. A list of studies concerning the correlations between MTSV and thermal comfort indices is demonstrated in Table 2.3. The correlations between MTSV and PET performed by Yahia and Johansson (2013) were separated between hot (neutral PET=15.7℃) and cool (neutral PET=24.2℃) season, with about 0.5 unit difference in vertical ordinate. Huang et al. (2017) compared the linear equations obtained from different experimental sites, including one shaded site and one sunlit site, observed clear separations in the linear lines. The neutral temperatures are also distinct for the regressions using PET (21.0℃ in sunlit areas and 27.2℃ in shaded areas) and the regressions using UTCI (22.7℃ in sunlit areas and 28.5℃ in shaded areas). Various neutral temperatures in different seasons or climates were also reported by other studies (Hwang & Lin, 2007; W. Liu et al., 2016; Mahmoud, 2011). This indicates that merely a one-predictor linear model is not sufficient to predict human thermal perceptions in all environmental conditions. Different climate regions with different building or landscape designs form specific thermal conditions. It is believed that the outdoor thermal perceptions in different areas with different climates and building geometries should be assessed case by case and there is not such a uniform solution for all cases (Xie, 2020). This is also the essential motivation for researchers to continue enriching the outdoor thermal comfort database and developing models that allow a better prediction of human thermal perceptions.

Table 2.3 Summary of studies correlating MTSV with thermal comfort indices. Excerpts from Fang et al. (2019).

Reference	Region	Linear equation	R^2	Neutral temperature
(Hwang & Lin, 2007)	Taiwan	MTSV=0.087SET* - 2.248 (semi-outdoor)	0.970	25.8°C
		MTSV=0.116SET* - 3.156 (outdoor)	0.980	27.2°C
(Lin et al., 2009)	Taiwan	MTSV=0.199PET - 4.722 (cool season)	0.890	23.7°C
		MTSV=0.118PET - 3.025 (hot season)	0.960	25.6°C
(Lin et al., 2011)	Taiwan	MTSV=0.0739SET* - 2.0657 (cool season)	0.945	27.9°C
		MTSV=0.1302SET* - 3.8142 (hot season)	0.919	29.3°C
(Mahmoud, 2011)	Cairo, Egypt	MTSV=0.099PET - 3.009 (cool season)	0.348	30.4°C
		MTSV=0.206PET - 6.680 (hot season)	0.953	32.4°C
(Cohen et al., 2013)	Tel Aviv, Israel	MTSV=0.2146PET - 3.5737 (cool season)	0.963	16.7°C
		MTSV=0.3292PET - 5.9692 (hot season)	0.885	18.1°C
(Yahia & Johansson, 2013)	Damascus, Syria	MTSV=0.114PET - 2.755 (cool season)	0.600	24.2°C
		MTSV=0.060PET - 0.941 (hot season)	0.420	15.7°C
(Lai, Guo, et al., 2014)	Tianjin, China	MTSV=0.188PET - 1.73 (cool season)	0.752	9.2°C
		MTSV=0.101PET - 1.571 (hot season)	0.893	15.6°C
		MTSV=0.183UTCI - 0.392 (cool season)	0.946	21.4°C
		MTSV=0.13UTCI - 2.273 (hot season)	0.876	17.5°C
(Elnabawi et al., 2016)	Cairo, Egypt	MTSV=0.0881PET - 2.1411 (Cool season)	0.811	24.3°C
		MTSV=0.0998PET - 2.947 (Hot season)	0.830	29.5°C

(W. Liu et al., 2016)	Changsha, China	MTSV=0.131PET - 2.296 (Spring)	0.585	17.5°C
		MTSV=0.188PET - 4.386 (Summer)	0.778	23.3°C
		MTSV=0.112PET - 2.232 (Autumn)	0.521	19.9°C
		MTSV=0.163PET - 2.431 (Winter)	0.663	14.9°C
(Salata et al., 2016)	Rome, Italy	MTSV=0.118PET - 2.941 (cool season)	0.949	24.9°C
		MTSV=0.17PET - 4.575 (hot season)	0.847	26.9°C
(Huang et al., 2017)	Hong Kong	MTSV=0.1119PET - 2.3475 (shaded sites)	0.746	27.2°C
		MTSV=0.1026PET - 2.7924 (sunlit sites)	0.890	21.0°C
		MTSV=0.0972UTCI - 2.7737 (shaded sites)	0.719	28.5°C
		MTSV=0.1341UTCI - 3.0474 (sunlit sites)	0.772	22.7°C

2.5 Summary and research gaps

This chapter presents the literature review on studies about urban thermal microclimate, outdoor thermal comfort and the assessing indices, correlations between thermal perceptions and thermal comfort indices, and transient thermal comfort. Research gaps are summarized as follows from the review:

1) The areas underneath an elevated building provide wind amplification and shadings, which were believed to be beneficial for enhancing local microclimate and occupants' thermal comfort in these areas. However, a comprehensive investigation on the occupants' thermal perceptions and urban microclimate conditions in these areas were not presented, hindering the examination of the actual performance of the elevated building design and the development of appropriate models for accurate predictions of human thermal perceptions under these outdoor environmental conditions.
2) The outdoor exposure in a city is usually passive and last for a short period of time, the residents' thermal perceptions during the short-term exposure after entering outdoors from the indoor environment should be emphasized, especially in the hot

and humid region, where the sudden exposure from the air-conditioned building interior to a hot outdoor area can induce strong heat stress. Yet, existing studies rarely focused on the residents' thermal perceptions during the short-term transitional exposure after entry to the outdoor environment.

3) Numerous studies in the past years adopted a single thermal comfort index as a predictor to develop predicting models for the predictions of the subjects' thermal perceptions in different outdoor thermal conditions by regression analysis. The regressions showed acceptable fitting qualities, but the predicting accuracy remains questionable since the regressions and neutral temperature obtained from different regions, climate and research sites are obviously different. It is necessary to develop enhanced predicting models that adopt additional factors as predictors to improve the predicting accuracy.

Chapter 3 Methodologies

3.1 Field measurement and survey

3.1.1 Measurement parameters and instruments

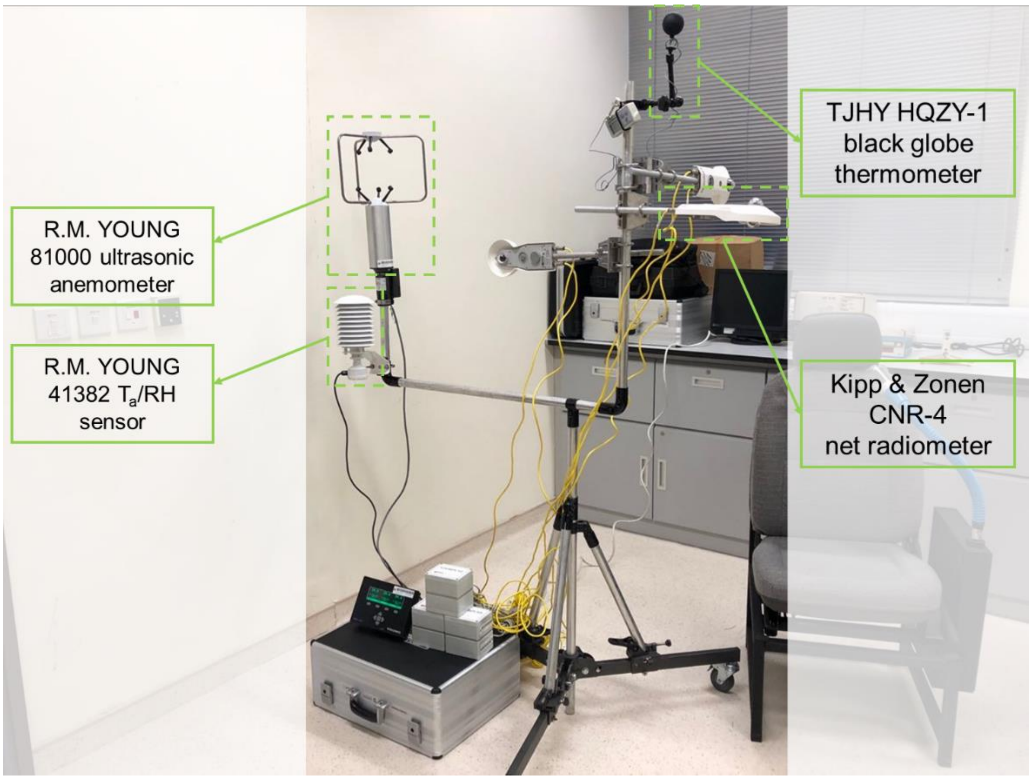

Figure 3.1 Mini weather station and the relevant instruments

In order to measure the relevant meteorological parameters that have impacts on human thermal comfort, i.e. T_a, RH, V_a and radiation, a portable weather station including mounting brackets, monitoring sensors and data-loggers demonstrated in Figure 3.1 was built. The measuring sensors can directly record the data of T_a, RH, V_a, T_g, short-wave solar radiation (Q_s) and long-wave solar radiation. Particularly, the measurement of directional long-wave and short-wave radiation utilized the combination of 3 sets of net radiometers. Each net radiometer can measure Q_l and Q_s

simultaneously from opposite directions. Thus, 6-direction short-wave and long-wave radiation can be simultaneously measured. Measuring instruments were all mounted at 1.5m above the ground level, which is about a pedestrian's chest height. The sensors were well-calibrated before each field experiment to reduce measurement error. The mentioned sensors' specifications are illustrated in Table 3.1. All of the measurement sensors used for field measurement are compliant with ISO standard 7726 (Standardization, 1998).

Table 3.1 Specifications of measurement sensors

Meteorological parameter	**Sensor**	**Measuring Range**	**Accuracy**
Air temperature (T_a)	R.M.YOUNG 41382	-50 ~ 50 (℃)	±0.3℃
Relative humidity (RH)		0 ~ 100 (%)	±1%
Wind velocity (V_a)	R.M.YOUNG 81000	0 ~ 40 (ms^{-1})	±0.05 ms^{-1}
Globe temperature (T_g)	TJHY HQZY-1	-40 ~ 60 (℃)	±0.3℃
Long-wave solar radiation (Q_l)	Kipp & Zonen CNR-4	-250 ~ 250 (Wm^{-2})	<10%
Short-wave solar radiation (Q_s)		0 ~ 2000 (Wm^{-2})	<5%

3.1.2 Questionnaire

The questionnaire comprises three main parts: subjective feelings, clothing/activity and personal detail. In the first section, 7 subjective feelings of the research subjects were collected, including TSV, TCV thermal acceptability vote (TAV), subjective perceptions on sunlight level, subjective perceptions on wind level, the emotion of the subject and ambient noise. The thermal sensation vote (TSV) scale was designed according to the ASHARE 7-point scale. The thermal comfort vote (TCV) scale employed a 5-point scale. The scales used to evaluate the above-mentioned respondent perceptions are shown in Figure 3.2.

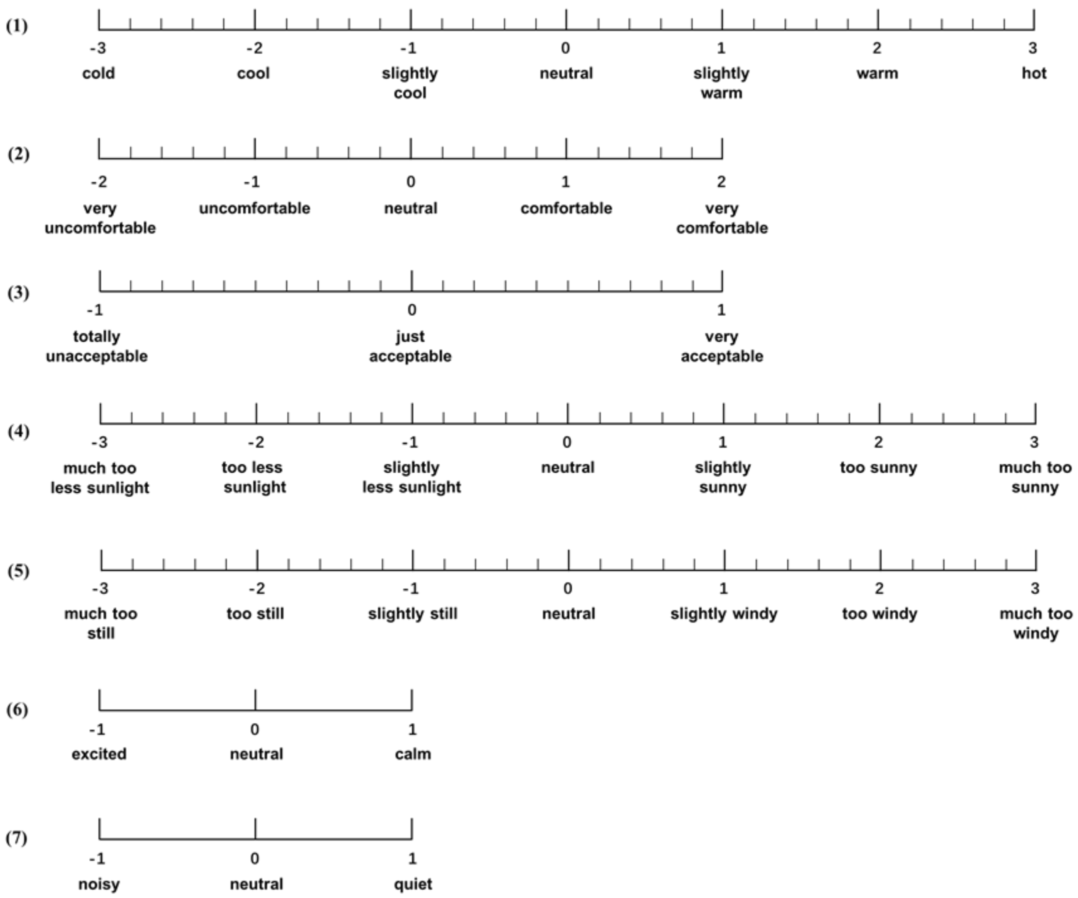

Figure 3.2 Scales for assessing respondent subjective thermal perceptions or other feelings to the ambient environment.
(1) thermal sensation vote (TSV); (2) thermal comfort vote (TCV); (3) thermal acceptability vote (TAV); (4) subjective perceptions on sunlight level; (5) subjective perceptions on wind level; (6) emotion of the subject; (7) ambient noise.

The second section of the questionnaire aims at collecting the subjects' clothing and activity conditions to obtain the clothing insulations in their corresponding clothes and the metabolic rate at their corresponding activity levels. During the experiments, subjects were not demanded to wear certain kinds of clothes, but they were required to conduct mild activities, including sitting, standing and slow walking. They were also asked to record their clothing conditions and the activities they had been conducting in the questionnaire during the experiment periods. Clothing and activity conditions can be quantitatively converted to I_{clo} and M according to ASHRAE standard 55 (Standard, 1992) and ISO standard 7730 (ISO, 2005), respectively.

The third section of the questionnaire collects the subject's personal details, including age, gender, height and weight, which are the necessary input parameters of the PET model. The personal details data will be further analyzed to find out if they are strong indicators of human thermal perceptions.

3.2 Indices for thermal comfort evaluation

Thermal comfort evaluation indices PET and UTCI were employed in this thesis to describe the thermal stress of the ambient environment. PET is defined as the equivalent temperature at which the heat balance of the human body can be maintained and the human's core and skin temperature equal in both the assessed environment and an imaginary typical indoor situation. According to MEMI, T_{core} and T_{skin} of human body can be obtained for any combination of meteorological parameters and human personal details. The equivalent T_a of an imaginary indoor situation, which equals PET, can be obtained by comparing T_{core} and T_{skin} values with the respective calculated values in MEMI. MEMI introduced four additional parameters concerning human personal information to calculate PET, i.e. including height, weight, age and gender. The introduction of additional parameters was based on the parameters' correlations with human sweat rate and basic metabolism, which affect human thermal regulation. In the thesis, PET was calculated using the software package Rayman 1.2 (Matzarakis et al., 2007). Air temperature, relative humidity and wind velocity were directly measured by the mini weather station. Mean radiant temperature was calculated from globe temperature or directional solar radiations. Subject's metabolic rate, clothing insulation were obtained by the conversion of their activity and clothing conditions. Subject's height, weight, age and gender were obtained directly from the survey.

UTCI was developed based on "Fiala" multi-node model (Fiala et al., 2012) and defined as the equivalent air temperature of the reference environment (RH=50%, V_a=0, T_{mr}=T_a) which produces the same thermal strain, represented by the combination of air temperature, wind velocity at 10m height, vapor pressure and mean radiant temperature. Deviation of UTCI from T_a depends on the actual values of T_a, T_{mr}, V_a and RH. To express the offset of UTCI to T_a, a six-degree polynomial function that requires four meteorological parameters (air temperature, wind velocity at 10m height, vapor pressure and mean radiant temperature) as input is used. In this thesis, BioKlima 2.6 software package was employed for the calculation of UTCI.

3.3 Mean radiant temperature calculation methods

Mean radiant temperature (T_{mr}) plays a key role in thermal comfort studies. The calculation of the above-mentioned thermal comfort indices relies very much on mean radiant temperature. Mean radiant temperature employed °C as a unit to convert the radiation fluxes into temperature, indicating the uniform temperature of an imaginary black body-radiating surrounding, which causes the same level of radiant heat exchange for the human body inside this hypothetical environment as the assessed environment (Fanger, 1970). In this thesis, T_{mr} was calculated by two methods according to ISO standard 7726 (Standardization, 1998), respectively from globe temperature as shown in Equation (3.1) and 6-direction radiation as shown in Equation (3.2).

$$T_{mr} = [\left(T_g + 273.15\right)^{4} + \frac{1.10 \times 10^8 \times {V_a}^{0.6} \times \left(T_g - T_a\right)}{\varepsilon D^{0.4}}]^{1/4} - 273.15 \tag{3.1}$$

$$T_{mr} = (\frac{\sum F_i \times (\alpha_s Q_s + \alpha_l Q_l)}{\alpha_s \sigma})^{1/4} - 273.15 \tag{3.2}$$

In this study, the diameter of the black globe was 40mm. The emissivity (ε) of the globe was assumed as 0.95 for a normal black globe sensor. σ is Stefan-Boltzmann constant and equals $5.67 \cdot 10^{-8}$ ($Wm^{-2}k^{-4}$). α_s and α_l are respectively the short-wave and long-wave radiation absorption coefficients of normal clothing subjects, the value of which can be set to 0.7 and 0.97. F_i represents the angular factor between subjects and the ambient environment. The selection of F_i depends on the activity that the occupants had been conducting during the experiment. For a standing or walking subject, F_i=0.06

in the two vertical directions and F_i=0.22 in the four horizontal directions. For a sitting subject, F_i=0.167 in all 6 directions.

3.4 Statistical methods

3.4.1 Ridit analysis

In order to statistically determine human thermal perceptions differences in different experimental sites, Ridit analysis, i.e. relative to an identified distribution unit analysis (Bross, 1958) was employed in this study. Discrete categorical variables are converted to continuous variables by the Ridit analysis to obtain the "Ridit values". Hypothesis tests like t-test are employed to compare two sets of Ridit values. The demonstration of Ridit analysis can either be comparing the confidence intervals of different average Ridit values or observing the significance level of the t-test. Both methods are equivalent statistically. To illustrate the difference more explicitly, the former method was employed. Confidence intervals of two sets of average Ridit values were calculated and compared at the significance level of 0.05. If no overlap is observed between the two confidence intervals, the original categorical variables can be regarded as significantly different at the 95% confidence level. In this study, IBM SPSS Statistics 22.0 was employed to calculate Ridit values.

3.4.2 ANOVA test

One-way ANOVA was performed in Chapter 5 to compare the research subjects' thermal perceptions between the selected experimental areas. The ANOVA tests were conducted by IBM SPSS Statistics 22.0.

3.4.3 Stepwise regression

Stepwise regression was adopted in the thesis to filter the potential predictors in the development of TS and TCV predicting models. The stepwise regression uses a combination of forward selection and reverse elimination to automatically select the right independent variables, thereby determining the effect of independent variables on dependent variables. The method was used in several studies conducted by Lam et al. (1997), Amiri et al. (2015) and Lin et al. (2021) to predict building performance.

IBM SPSS Statistics 22.0 was adopted for stepwise regression and the development of the TSV and TCV predicting models. The entry significant level was set to 0.01 and the removal significant level was set to 0.05. This indicates that the predictor will be included by the model if the potential predictor's probability of the maximum F value is less than 0.01, while it will be removed from the model if the probability exceeds 0.05. The predictors with F value between 0.01 and 0.05 will stay in the model.

Chapter 4 Thermal perceptions after 15-min outdoor exposure

This chapter presents an investigation on research subjects' thermal perceptions, including thermal comfort and thermal sensation conditions after a 15-min exposure in several outdoor sites located in a university campus. The experiments were conducted in 23 days from Mar-2016 to Dec-2016. In total, 1,107 questionnaires including 556 male subjects and 551 female subjects were recorded in this experiment. The research subjects were all students and staff aging from 15 years to 63 years, averaging 25 years.

4.1 Experimental sites

The on-site thermal comfort experiments, which include field measurements and questionnaire surveys were performed in a university campus in Hong Kong, which is located in the humid subtropical climate zone (Cwa) according to Köppen-Geiger climate classification (KOPPEN, 1936). Figure 4.1 demonstrates the specific features and locations and of the field experimental sites.

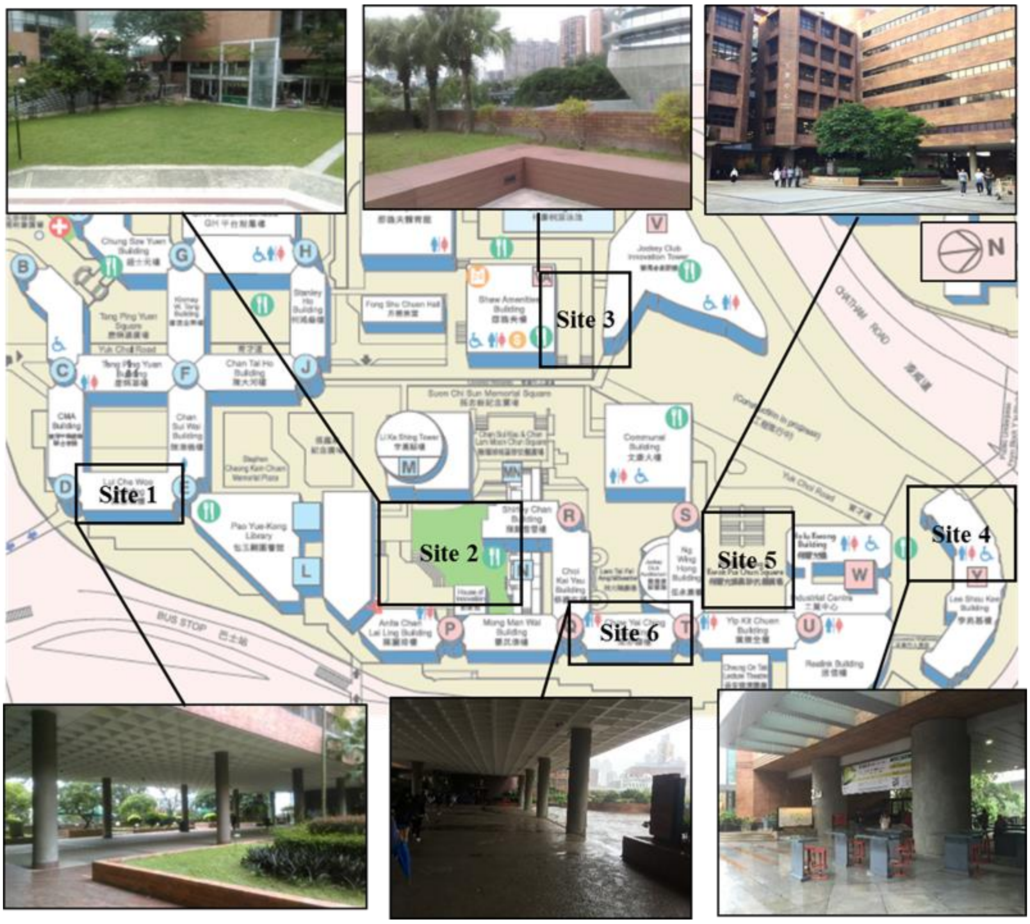

Figure 4.1 Features and locations of the field experiment sites.
(Sunlit sites: site 2, 3, 5 on the upper figure; shaded sites: site 1, 4, 6 on the lower figure)

The three “sunlit” sites, which receive direct irradiance from the sun and reflected irradiance from the surrounding façade and ground at daytime are site 2, site 3 and site 5. Site 2 is a wide-open sward at the underground level, encircled by high buildings in all directions. Site 3 is an east-west orientated street canyon, the south and the north of which are blocked by two high-rise buildings. Site 5 is a one-side-open public square. Building blocks stand in the east, south and north directions of the square.

The three “shaded” sites, which are sheltered and receive only reflected solar irradiance are site 1, site 4 and site 6. Site 1 is a north-south orientated ground-level corridor connecting two buildings underneath the building lift-up area. The surrounding of which is hardly sheltered, resulting in a visually bright and wide-open characteristic. Site 4 is a resting area at the ground level beneath a high-rise building. Similar to site 1, site 6 is also a north-south orientated connecting corridor underneath a lift-up building, but the building density around site 6 is much higher than site 1.

4.2 Experimental procedure

The field experiments were carried out during summer, fall and winter during 2016 in Hong Kong. Meteorological monitoring and subject surveys were conducted simultaneously in the above-mentioned six sites on a university campus. The mini weather station illustrated in Figure 4.2 was used to collect T_a, RH, V_a and directional short-wave and long-wave solar radiation data. The subjects were required to finish questionnaires to collect their personal information and conditions concerning activity and clothing during the field experiments.

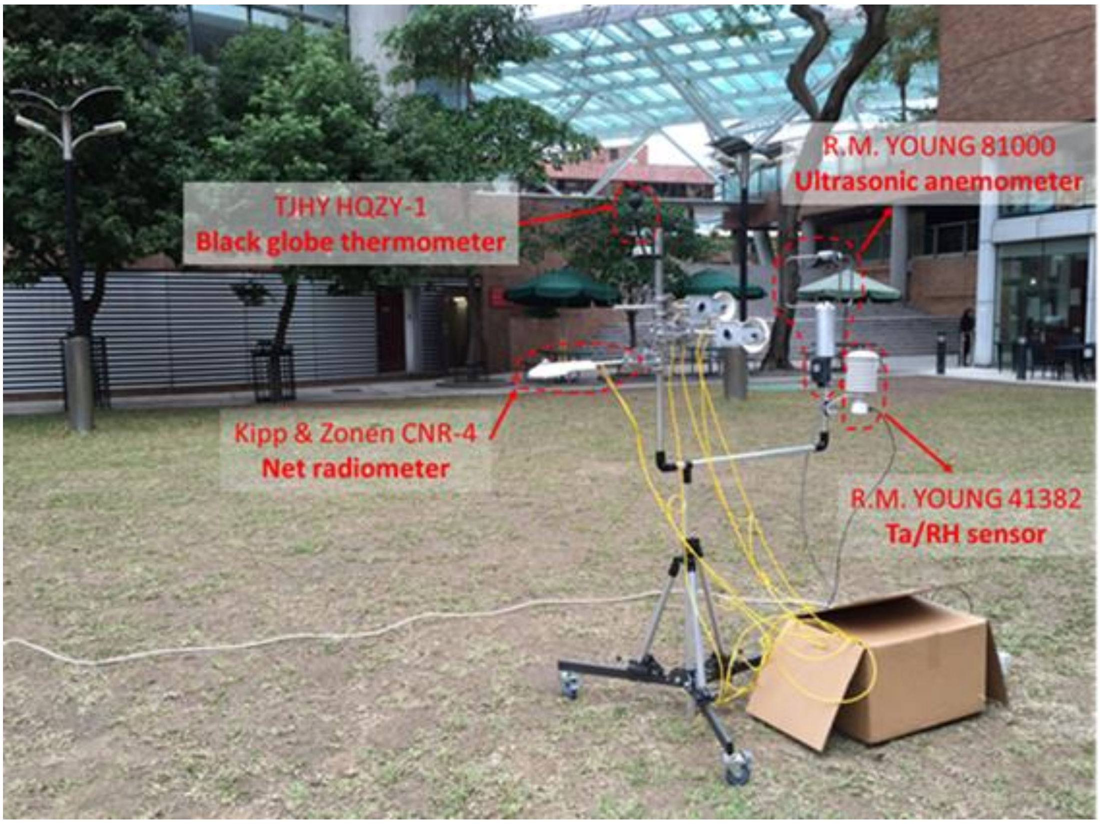

Figure 4.2 Mini weather station adopted in the field experiments.

The research subjects were mostly recruited by emails or campus advertisements. They were paid in cash as an incentive of attendance. This encourages research subjects to treat the survey with earnestness and concentration, which can be helpful in improving the precision in recording their actual thermal perceptions. The basic procedure of the field study is to expose the research subjects to three selected experimental sites in turn. The exposure time of each site is 15 minutes. During the exposure, subjects were only allowed to sit, stand and slowly walk, i.e. conducting mild activities. Subjects were asked to fill in the questionnaires immediately after the 15-minute exposure in each of the selected sites. Then they were told to slowly walk to the next experimental site and rest for 10 minutes before another 15-minute exposure. This helped reduce the discrepancy in subjective responses due to the vibration of metabolism caused by walking from one site to another. The full experimental procedure timeline is illustrated in Figure 4.2.

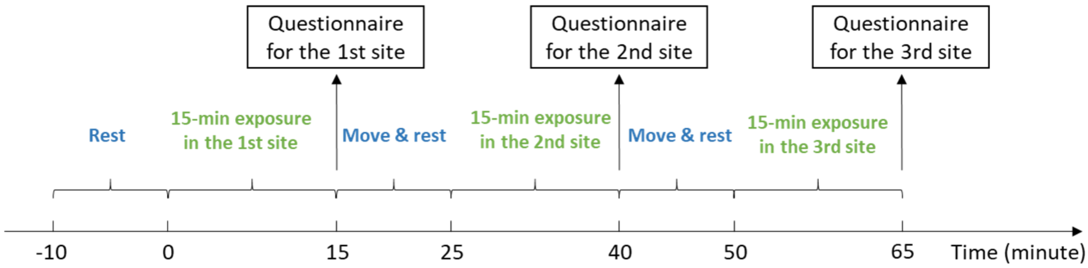

Figure 4.3 Timeline of the experimental procedure

4.3 Meteorological conditions during experiments

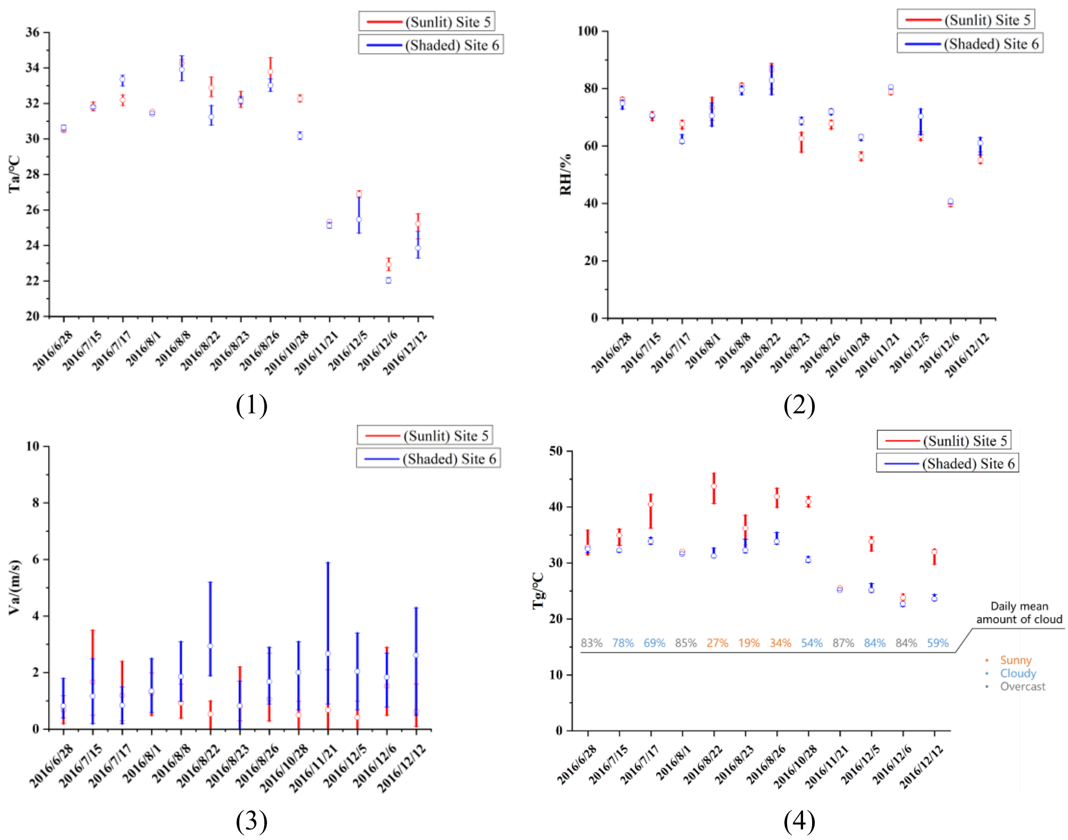

Figure 4.4 Meteorological parameters comparisons between the shaded and the sunlit sites. (1) T_a, (2) RH, (3) wind speed, (4) T_g.

Vertical bars denote the max/min values of the corresponding parameters during the field experiment recording periods. Circles denote the mean values.

Table 4.1 Corresponding maximum (Max), minimum (Min) and average (Avg) values of the four meteorological parameters in the two sites during experiment periods

	T_a (°C)						**RH (%)**					
	Site 5 (Sunlit)			**Site 6 (Shaded)**			**Site 5 (Sunlit)**			**Site 6 (Shaded)**		
Date	Max	Min	**Avg**	Max	Min	**Avg**	Max	Min	**Avg**	Max	Min	**Avg**
6/28	30.6	30.4	**30.5**	30.8	30.5	**30.7**	77	75	**76**	76	73	**75**
7/15	32.1	31.6	**31.8**	31.9	31.7	**31.8**	72	69	**71**	71	70	**71**
7/17	32.5	31.9	**32.2**	33.6	33.0	**33.5**	69	66	**68**	64	61	**62**
8/1	31.6	31.5	**31.5**	31.5	31.4	**31.4**	77	69	**74**	75	67	**71**
8/8	34.5	34.0	**34.3**	34.7	33.3	**33.8**	82	80	**81**	75	67	**71**
8/22	33.5	32.4	**32.8**	31.9	30.8	**31.1**	88	80	**87**	88	78	**83**
8/23	32.7	31.8	**32.3**	32.4	32.0	**32.1**	64	58	**63**	58	54	**57**
8/26	34.6	33.1	**33.7**	33.4	32.7	**33.0**	69	66	**68**	73	71	**72**
10/28	32.1	32.5	**32.2**	30.4	30.0	**30.2**	70	67	**69**	64	62	**63**
11/21	25.4	25.3	**25.4**	25.3	25.0	**25.1**	80	78	**79**	81	80	**81**
12/5	27.1	26.7	**26.9**	26.7	24.7	**25.1**	65	62	**64**	73	64	**70**
12/6	23.3	22.6	**22.9**	22.2	21.9	**22.0**	41	39	**40**	41	40	**41**
12/12	25.8	24.4	**25.4**	24.8	23.3	**23.6**	58	54	**55**	63	57	**61**

	V_a (ms^{-1})						**T_g (°C)**					
	Site 5 (Sunlit)			**Site 6 (Shaded)**			**Site 5 (Sunlit)**			**Site 6 (Shaded)**		
Date	Max	Min	**Avg**	Max	Min	**Avg**	Max	Min	**Avg**	Max	Min	**Avg**
6/28	1.2	0.2	**0.7**	1.8	0.4	**0.8**	35.9	31.5	**32.9**	32.8	31.9	**32.6**
7/15	3.5	0.5	**1.7**	2.5	0.2	**1.2**	36.1	33.2	**35.0**	32.5	32.0	**32.3**
7/17	2.4	0.3	**1.2**	1.5	0.2	**0.9**	42.3	36.3	**40.6**	34.6	33.4	**33.9**
8/1	2.0	0.5	**1.3**	2.5	0.6	**1.4**	32.2	32.0	**32.1**	31.7	31.6	**31.7**
8/8	1.6	0.4	**0.9**	3.1	1.0	**1.8**	-	-	-	-	-	-
8/22	1.0	0.0	**0.5**	5.2	1.9	**2.9**	46.1	40.7	**43.8**	32.7	31.0	**31.3**
8/23	2.2	0.3	**0.7**	1.0	0.0	**0.5**	38.6	33.3	**36.3**	34.3	31.9	**32.2**
8/26	2.7	0.3	**1.1**	2.9	0.9	**1.7**	43.4	40.0	**42.0**	35.5	33.4	**33.9**
10/28	1.7	0.0	**0.8**	3.1	0.7	**2.0**	41.9	40.1	**41.0**	31.2	30.2	**30.5**
11/21	2.1	0.0	**0.7**	5.9	0.9	**2.7**	25.7	25.4	**25.6**	25.3	25.1	**25.2**
12/6	1.0	0.0	**0.4**	3.4	0.7	**2.1**	34.7	32.2	**33.9**	26.4	24.8	**25.2**
12/6	2.9	0.5	**1.5**	2.7	0.8	**1.8**	24.5	23.4	**23.8**	23.0	22.3	**22.8**
12/12	1.6	0.1	**0.6**	4.3	0.5	**2.6**	32.5	29.8	**32.0**	24.4	23.3	**23.6**

The pairwise meteorological parameters comparisons between a sunlit area site 5 and a shaded area site 6 are demonstrated in Figure 4.4. The experiments were conducted in 13 days during the daytime. The maximum, minimum and average values of the corresponding meteorological parameters during the experiment periods are summarized in Table 4.1. It can be found that the T_a and RH differences between the selected areas are subtle during the field experiment. Only around 0~2K difference in air temperature and 2~10% difference in relative humidity were observed. Mean T_a in the open sites is about 2K higher, presumably due to the instrumental error caused by solar radiation. RH difference between the sunlit and the open sites is below 7%. Generally, the differences in both T_a and RH between the two areas are subtle, almost negligible in all of the seasons.

More obvious differences in V_a and solar irradiance between the two selected sites can be observed compared with the subtle difference in Ta and RH. Maximum V_a in site 5 (sunlit) can exceed 3.0 ms^{-1} and maximum V_a in site 6 (shaded) is over 5.0 ms^{-1}. It can be inferred that wind flows in the sunlit sites are in general stronger than the open sites. According to observations in the field measurements with Hong Kong Observatory daily mean amount of cloud data, the measurement days' weather conditions, i.e. sunny, cloudy or overcast were acquired. It can be observed that on overcast days, T_g in the two areas is almost the same. However, on sunny and cloudy days, T_g in the open sites is significantly over those in the shaded sites.

4.4 Thermal perceptions comparisons

4.4.1 Overall comparison

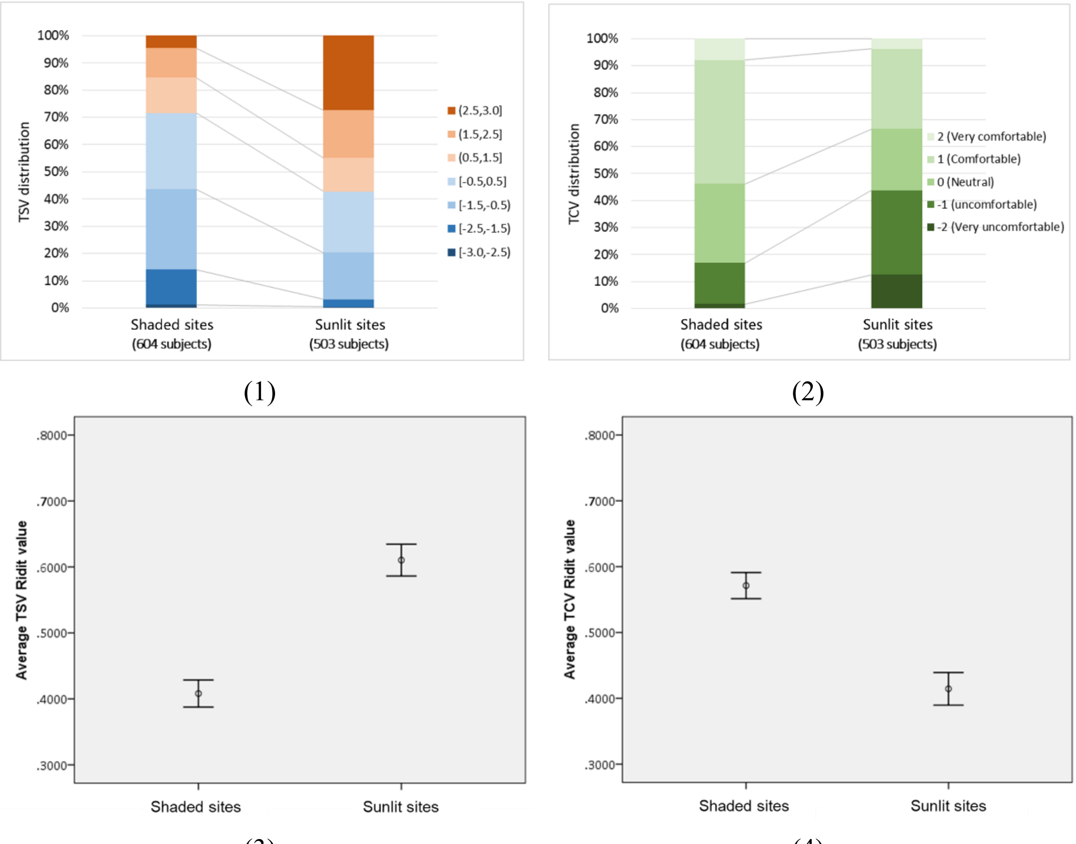

Figure 4.5 TCV and TSV distributions between sunlit sites and shaded sites in all weather conditions.

(1) TSV distributions, (2) TCV distributions, (3) Average TSV Ridit confidence intervals, (4) Average TCV Ridit confidence intervals.

TSV and TCV distributions between the shaded areas and the sunlit areas in all weather conditions are shown in Figure 4.5. It is observed that in the shaded areas 71% of the research subjects hold the thermal sensation of neutral, cool or cold, while over 80% of the research subjects found the ambient environment to be neutral or comfortable. In the sunlit areas, the percentage of research subjects feeling not warm or hot drops to 42% and the percentage of research subjects feeling not uncomfortable is only 43%.

It can be inferred that the research subjects in the shaded sites generally feel cooler and more comfortable than in the sunlit sites. The Ridit confidence intervals comparisons shown in Figure 4.5 (3) and (4) also serve as evidence that TSV and TCV of the research subjects are significantly distinct between the two sites with different building morphologies.

Statistics of research subjects' TSV and TCV frequency in each thermal perception range were demonstrated in Table 4.2.

Table 4.2 Summary of research subjects' TSV and TCV

Index	**Range**	**Frequency in cold weather (T_a<26°C)**		**Frequency in hot weather (T_a≥26°C)**		**Total**
		Shaded	**Sunlit**	**Shaded**	**Sunlit**	
TSV	(2.5, 3.0]	3	9	25	129	166
	(1.5, 2.5]	7	21	58	67	153
	(0.5, 1.5]	26	35	53	27	141
	[-0.5, 0.5]	72	99	97	14	282
	[-1.5, -0.5)	102	68	76	18	264
	[-2.5, -1.5)	57	13	21	1	92
	[-3.0, -2.5)	7	2	0	0	9
	Total	**274**	**247**	**330**	**256**	**1,107**
TCV	2	31	16	17	3	67
	1	122	117	155	32	426
	0	74	74	103	41	292
	-1	45	31	47	126	249
	-2	2	9	8	54	73
	Total	**274**	**247**	**330**	**256**	**1,107**

4.4.2 TSV comparisons in hot and cold weathers

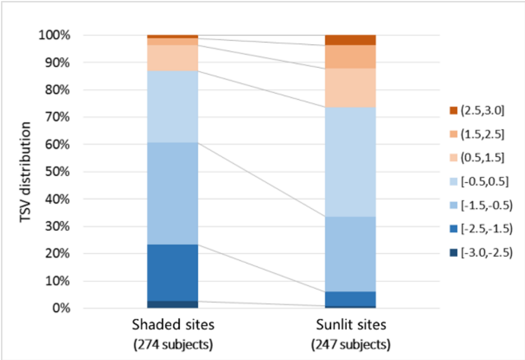

(1)

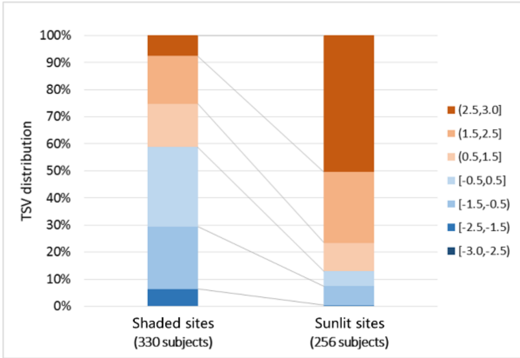

(2)

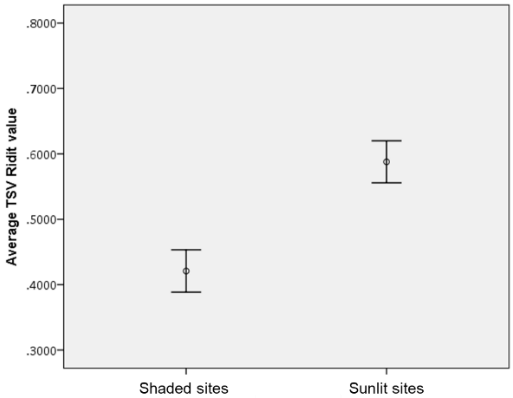

(3)

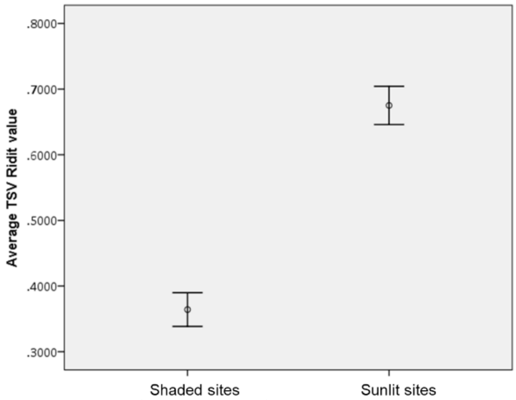

(4)

Figure 4.6 TSV distributions between sunlit sites and shaded sites in different weather. (1) Cold weather TSV distributions, (2) Hot weather TSV distributions, (3) Cold weather average TSV Ridit confidence intervals, (4) Hot weather average TSV Ridit confidence intervals.

TSV distributions between the shaded areas and the sunlit areas in hot or cold weather conditions are shown in Figure 4.6. The weather conditions were divided according to the average air temperature (around 25-26°C) during working hours (9:00 - 17:00) in Hong Kong. Experiment periods with average T_a lower than 26°C were considered as cold weather conditions, while those with average T_a equals or higher than 26°C were hot weather conditions. Subjective TSV was divided into 7 ranges, which were represented by different colors in the bar charts.

It can be observed in Figure 4.6 (1) and (3) that in the cold weather, research subjects with cold or cool perceptions are higher in percentage in the shaded sites compared with the sunlit sites. TSV Ridit confidence intervals of the two selected sites do not overlap, indicating in the cold weather, research subjects in the shaded sites perceive significantly colder compared with the sunlit sites. It can also be observed in Figure 4.6 (2) and (4) that in the hot weather, research subjects with cold or cool perceptions are higher in percentage in the shaded sites compared with the sunlit sites. Ridit analysis also suggests that in the hot weather, research subjects in the sunlit sites felt significantly hotter compared with the shaded sites. In general, no matter in hot or cold weather, research subjects' thermal sensations towards the ambient environment were significantly different between the shaded sites and the sunlit sites.

4.4.3 TCV comparisons in hot and cold weathers

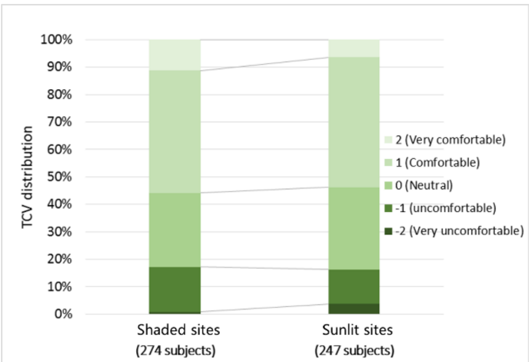

(1)

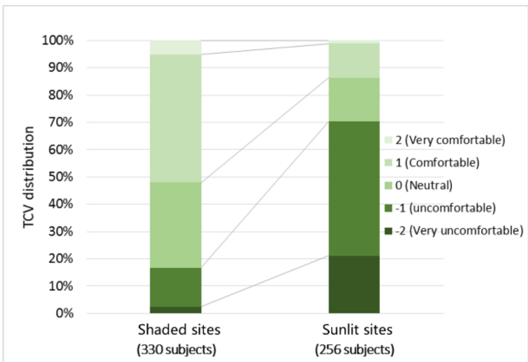

(2)

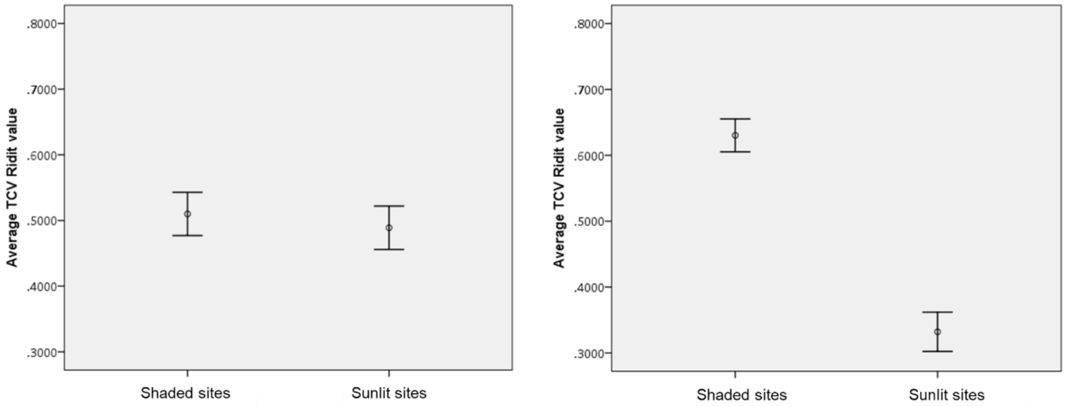

(3) (4)

Figure 4.7 TCV distributions between sunlit sites and shaded sites in different weather. (1) Cold weather TCV distributions, (2) Hot weather TCV distributions, (3) Cold weather average TCV Ridit confidence intervals, (4) Hot weather average TCV Ridit confidence intervals.

TCV distributions between the shaded areas and the sunlit areas in hot or cold weather conditions are shown in Figure 4.7. TCV is expressed by five levels from -2 to 2, indicating very uncomfortable, uncomfortable, neutral, comfortable, very comfortable, respectively. It can be seen in Figure 4.7 (1) and (3) that in the cold weather, around 89% of the research subjects perceived neutral, comfortable or very comfortable in TCV. The former section has demonstrated that the subjects are significantly hotter in the sunlit sites in the cold weather. However, subjects' TCV distributions are almost the same between the shaded sites and the sunlit sites, which indicates that subjects can accept both sites in terms of thermal comfort in the cold weather. The overlap of Ridit confidence intervals in TCV also suggests that the difference in subjects' TCV between the shaded sites and the sunlit sites is not significant. Unlike the results in the cold weather, in the hot weather, the percentage of subjects that feel uncomfortable in the sunlit sites is obviously much higher than in the shaded sites as shown in Figure 4.7 (2). Even though 41% of the subjects feel hot or warm in the shaded sites in hot weather, only 18% of them feel uncomfortable. This indicates that during hot seasons, the shaded sites are better accepted in terms of thermal comfort compared with the sunlit sites. This conclusion is also proved by the Ridit comparisons in Figure 4.7 (4), where no overlap was found between the two confidence intervals.

It should be noted that the field meteorological measurement did not cover all the extremely cold weather in Hong Kong due to the limited experiment time. The finding s arose from the TSV and TCV comparison in the cold weather may not be appropriate to evaluate the occupants' thermal perceptions in extremely cold weather. In this study, minimum air temperature that measured during the experimental periods is around 15℃. However, the periods that air temperature below 15℃ in Hong Kong only account for 5% of all periods during work hours (9:00-17:00). Therefore, in most situations, the conclusions made in this section are available in terms of occupants' thermal perceptions evaluation.

4.5 Sunlight and wind perceptions comparisons

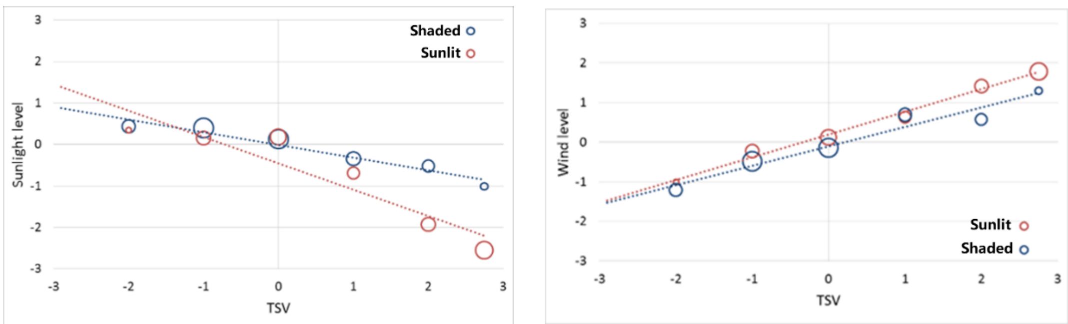

(1) (2)

Figure 4.8 Regressions between subjective sunlight/wind level and TSV.
(1) subjective sunlight level versus TSV; (2) subjective wind level versus TSV.

Figure 4.8 demonstrates the regressions between subjective sunlight/wind level and TSV. Subjective radiation/wind level is calculated according to the 7 TSV ranges, -3 ~ -2.5, -2.5 ~ -1.5, -1.5 ~ -0.5, -0.5 ~ 0.5, 0.5 ~1.5, 1.5 ~ 2.5 and 2.5 ~ 3. The diameter of the bubble represents the corresponding sample size. It can be inferred from Figure 4.8 that subjects' TSV is closely related to their perceptions of sunlight and wind level. It is found that subjective sunlight level and TSV are in negative relation, while the relation between subjects' wind level perceptions and their TSV is positive. It can be concluded that sunlight and wind have opposite impacts on the subjects' TSV in the selected experimental areas with a hot and humid climate. Subjective wind levels in the sunlit and the shaded sites are similar in terms of variation trends according to Figure 4.8 (2). However, in the hot weather where subjects' TSV is above 0, subjective sunlight level in the sunlit sites decreases dramatically compared with that in the shaded sites, the drop of which is relatively mild. This means subjective sunlight level affects occupants' TSV more in the sunlit area, especially in hot conditions, while subjective wind level affects the subjects' TSV equally in both sites. In terms of factors that affect their thermal sensation, subjects are more sensitive to the sunlight level rather than the wind level.

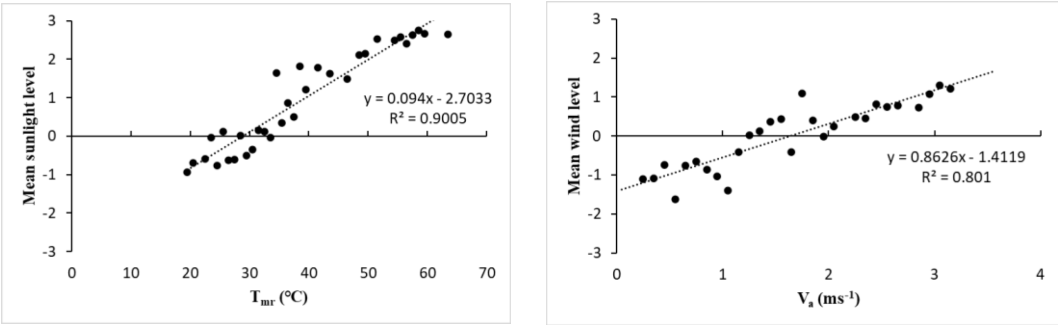

(1) (2)

Figure 4.9 Regressions between subjective sunlight/wind level and T_{mr}/V_a.

(1) Mean sunlight level versus T_{mr}; (2) Mean wind level versus V_a.

Figure 4.9 illustrates the regression between mean sunlight level (average sunlight level per 1K T_{mr} range) v.s. T_{mr} and the regression between mean wind level (average wind level per 0.1ms^{-1} V_a range) and V_a. It appears that good linear relations are shown between both correlations, with high R^2 values exceeding 0.8 in both correlations. Thus, the perceived sunlight level and wind level can be predicted by inputting mean radiation temperature or air velocity to the linear fitting formulae.

4.6 Comparisons of thermal comfort models

4.6.1 Correlating MTSV with PET/UTCI

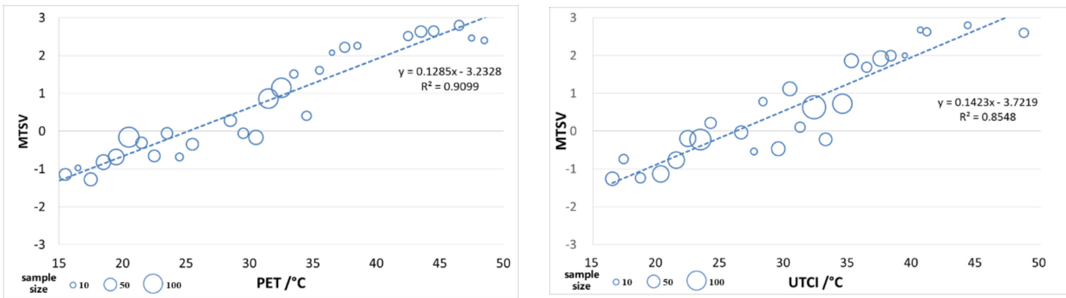

(1) (2)

Figure 4.10 Regressions between MTSV and PET/UTCI.

(1) MTSV v.s. PET; (2) MTSV v.s. UTCI.

Table 4.3 MTSV in the corresponding PET or UTCI ranges

PET/UTCI range (K)	MTSV in the corresponding PET range				MTSV in the corresponding UTCI range			
	N	**MTSV±SD**	**Max**	**Min**	**N**	**MTSV±SD**	**Max**	**Min**
[14,15]	21	-0.97±0.91	1.0	-2.8	0	-	-	-
(15,16]	40	-1.15±0.76	0.0	-3.0	0	-	-	-
(16,17]	9	-0.98±0.87	0.0	-2.2	44	-1.25±0.68	1.0	-2.4
(17,18]	47	-1.28±1.02	2.5	-3.0	20	-0.73±0.88	0.0	-3.0
(18,19]	59	-0.82±0.92	1.0	-2.5	24	-1.24±0.86	0.4	-3.0
(19,20]	65	-0.68±1.01	2.8	-2.6	24	-	-	-
(20,21]	111	-0.16±0.88	3.0	-2.0	40	-1.10±1.03	2.5	-3.0
(21,22]	33	-0.31±0.88	1.0	-2.2	64	-0.78±0.93	2.8	-2.6
(22,23]	39	-0.65±0.94	1.6	-2.2	62	-0.17±0.94	3.0	-2.0
(23,24]	34	-0.06±1.10	2.6	-1.6	105	-0.22±0.84	2.1	-2.3
(24,25]	17	-0.68±1.23	2.6	-2.4	31	0.22±0.88	1.6	-2.2
(25,26]	42	-0.35±0.91	2.0	-2.0	0	-	-	-
(26,27]	0	-	-	-	42	-0.03±1.24	2.6	-2.4
(27,28]	0	-	-	-	21	-0.5±1.26	3.0	-1.6
(28,29]	40	0.28±1.25	3.0	-1.9	6	0.80±0.51	2.0	-1.0
(29,30]	31	-0.06±1.14	3.0	-2.0	45	-0.47±0.93	2.0	-2.0
(30,31]	58	-0.16±1.16	2.4	-2.0	48	1.12±1.49	3.0	-2.3
(31,32]	103	0.86±1.35	3.0	-2.3	25	0.10±1.03	2.0	-2.0
(32,33]	107	1.15±1.33	3.0	-1.2	129	0.63±1.43	3.0	-2.0
(33,34]	20	1.51±1.07	3.0	-1.8	40	-0.19±1.14	3.0	-2.0
(34,35]	24	0.40±1.36	3.0	-2.0	90	0.74±1.33	3.0	-2.0
(35,36]	17	1.61±1.19	3.0	-0.4	47	1.87±1.15	3.0	-1.0
(36,37]	8	2.08±1.21	3.0	-1.0	25	1.69±1.08	3.0	-0.4
(37,38]	26	2.22±0.93	3.0	-1.8	64	1.77±1.39	3.0	-2.0
(38,39]	15	2.26±0.86	3.0	0.7	30	2.00±0.49	3.0	1.5
(39,40]	0	-	-	-	6	2.00±1.01	3.0	0.8
(40,41]	0	-	-	-	35	2.63±0.32	3.0	2.0
(41,42]	0	-	-	-	15	2.63±0.16	3.0	2.4
(42,43]	23	2.51±0.61	3.0	0.8	0	-	-	-
(43,44]	37	2.64±0.52	3.0	1.0	0	-	-	-
(44,45]	33	2.65±0.50	3.0	1.0	11	2.80±0.31	3.0	2.0
(45,46]	0	-	-	-	0	-	-	-
(46,47]	26	2.80±0.29	3.0	2.0	0	-	-	-
(47,48]	10	2.46±0.21	3.0	2.4	0	-	-	-
(48,49]	12	2.40±0.34	3.0	2.0	20	2.60±0.58	3.0	1.0
Total	**1107**	-	-	-	**1107**	-	-	-

Linear regression of MTSV with the thermal comfort indices PET and UTCI are illustrated in Figure 4.10. The bubble size denotes the sample size in the corresponding thermal comfort index range. MTSV was calculated in 1 K PET or UTCI range. The employment of average thermal sensation vote instead of TSV raw data is able to equalize the fitting contribution of regression data from different PET or UTCI range. Detailed statistics of MTSV, including the corresponding sample size, standard deviation, maximum, minimum values by PET or UTCI range are listed in Table 4.3. It appears that MTSV is in strong linear relation with the two selected thermal comfort indices while adopting linear regression. Fitting equations for PET and UTCI are shown in Equation (4.1) and (4.2), respectively. Both fitting results show high R^2 values (0.91 for PET, 0.85 for UTCI), indicating satisfactory qualities. Neutral PET and UTCI, which were obtained by calculating the corresponding thermal comfort index when MTSV=0, are 24.7°C and 26.2°C, respectively.

$$MTSV=0.1285PET-3.2328\ (R^2=0.9099) \tag{4.1}$$

$$MTSV=0.1423UTCI-3.7219\ (R^2=0.8548) \tag{4.2}$$

4.6.2 MTSV regressions with PET/UTCI in different experimental sites

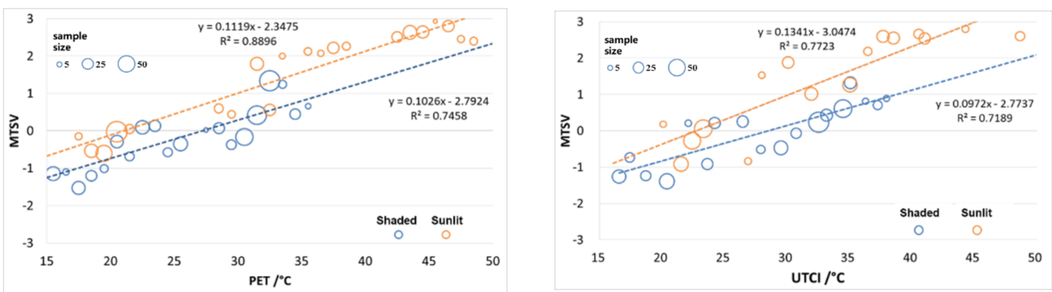

(1) (2)

Figure 4.11 Corresponding MTSV regressions with PET/UTCI in the shaded (blue) and the sunlit (orange) sites.

(1) MTSV v.s. PET; (2) MTSV v.s. UTCI.

In section 4.4, it was shown that subjects perceived differently in terms of TSV and TCV in the two different building morphologies. This section further examined this distinction by respectively fitting MTSV with PET/UTCI employing linear regression from the two selected sites. Figure 4.11 presents the results of the regressions. Obvious separations in both fitting lines, which respectively denote data from the shaded (blue) and the sunlit (orange) sites can be found, no matter for PET or UTCI regressions. The fitting line slopes are 0.1026 (shaded sites), 0.1119 (sunlit sites) for PET and 0.0972 (shaded sites), 0.1341 (sunlit sites), respectively. The higher slope of the fitting line for the sunlit sites indicates that occupants are more sensitive to the variation of thermal stress in the sunlit sites rather than the shaded sites. It can also be observed that neutral PET and neutral UTCI are separated while splitting the data into two groups and conducting respective linear regressions. Neutral PETs are 21.0 ºC (sunlit sites) and 27.2ºC (shaded sites) and neutral UTCI are 22.7ºC (sunlit sites) and 28.5 ºC (shaded sites), respectively. Within the same PET or UTCI range, the occupants in the sunlit sites report higher MTSV compared with those in the shaded sites.

The apparent fitting lines separations are likely caused by the limited predicting factors, i.e. the independent variables that account for the description of the complex outdoor environment adopted to predict subjects' MTSV. Certain extra impacts of extra factors on the occupants' thermal sensations including may be underestimated or ignored, including subjective expectations, preferences, emotional factors or other thermal perceptional factors that may influence the actual TSV. These separations reveal that the linear regression with merely one independent variable, i.e. PET or UTCI, cannot precisely describe the relationship between occupants' TSV and the thermal conditions in the outdoor environment. Therefore, it is not appropriate to adopt the one-predictor linear regression model to fit MTSV with the two selected thermal comfort indices. Further investigations on extra factors that have impacts on the research subjects' thermal perceptions need to be conducted to develop more accurate thermal perception predicting models for the evaluation of occupants' thermal sensation and thermal comfort in the urban outdoor environment.

4.7 Summary

This chapter presents the analysis of the respondent thermal perceptions after a 15-min exposure in different outdoor sites. The results can be summarized as follows:

(1) Major differences in meteorological parameters between the shaded sites and the sunlit sites were discovered according to the simultaneous field meteorological monitoring and subject surveys, among which solar irradiance and wind velocity showed the most significant difference.

(2) The comparisons of TSV and TCV distributions together with Ridit analyses proved that a significant difference of occupants' thermal sensation and thermal comfort conditions exists between the shaded and the sunlit areas. When staying in the shaded areas, subjects feel significantly cooler and more comfortable in hot weather conditions, without extra uncomfortable responses in cold weather

conditions. This would make the shaded area a more favorable and appealing place for occupants to enjoy outdoor activities.

(3) It is revealed that respondent thermal perceptions, which can be predicted by inputting mean radiation temperature or wind velocity, are closely related to the subjects’ perceptions of solar radiation and wind speed. Restricting radiation and amplifying wind flow can be effective approaches to a more comfortable thermal state, especially in the hot climate.

(4) Linear regressions between MTSV and PET/UTCI were carried out according to the data acquired from field studies conducted in the shaded and the sunlit areas. Although MTSV fitted well respectively with the two indices in linear regressions, there exist separations of the two individual regression lines for the shaded and the sunlit area, revealing that pedestrians’ actual thermal sensation and thermal comfort are not well predicted by the two models. Extra considerations on the factors affecting human’s expectations on neutral states should be taken into account for thermal comfort assessing indices to present better predictions of subjects’ thermal perceptions.

Chapter 5 Thermal perceptions during 10-min outdoor exposure

This chapter presents an investigation on research subjects' thermal perceptions, including thermal comfort, thermal sensation and thermal acceptability conditions during a 10-min exposure in two outdoor sites located at a university campus. The experiments were conducted in 14 days from Feb-2018 to Oct-2018. 197 research subjects (93 male subjects, 104 female subjects) participated in the repeat experiments and each of them submitted 6 copies of questionnaires concerning their thermal perceptions. Thus, a total number of 1,182 questionnaires were collected in this experiment. A large proportion of the survey subjects were students and staff aging from 19 years to 61 years, averaging 23 years.

5.1 Experimental sites

The two experimental sites in this chapter are located near the Y Block on a university campus in Hong Kong, features of which are shown in Figure 5.1. Site 1 is a shaded site underneath a lift-up building morphology. The northeast and southwest sides of this area are open and the other two sides are blocked by the surrounding buildings. During experimental periods, occupants in site 1 are only exposed to reflected solar irradiance and sheltered from direct solar irradiance. This makes the area relatively dark even during the daytime. Site 2 is a wide-open bright square that received direct solar irradiance during experimental periods. Strong wind is often observed in site 2 due to the surrounding "lift-up" designs that allow pedestrian-level wind to penetrate the surrounding buildings. The two experimental areas are so close to each other that only a few seconds are needed to transfer to the other site from one site. Average air temperatures are 22.8℃ and 29.9℃ respectively during cool period (February to April) and hot periods (August to October). Average air velocities are 1.0 m/s and 1.1 m/s respectively in the shaded site and the sunlit site. Air temperature (<0.2K in difference) and relative humidity (<2% in difference) in the two sites are almost the same according to the preliminary measurements.

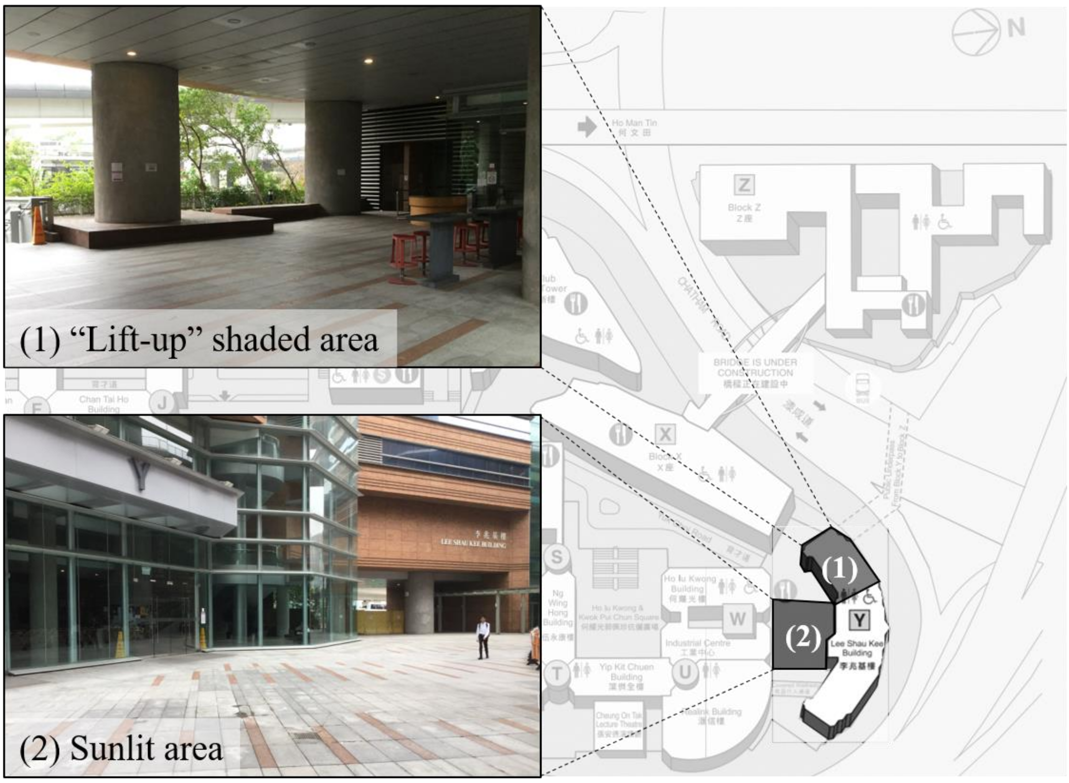

Figure 5.1 Two experimental sites in this chapter.

5.2 Experimental procedure

To reduce the historical activities effects on the subjects' metabolic rate before the experiments, breaks are needed in advance to help the research subjects recover from previous experiences. They were asked to stay in an indoor area on the ground floor of the Y Block nearby, which is air-conditioned with low V_a (< 0.1 ms^{-1}) and Q_s (< 10 Wm^{-2}). Subjects were required to take a 10-minute rest by sitting still on a couch after arriving at the spot for experimental preparation. They were then needed to finish one questionnaire for the collection of their subjective responses in the air-conditioned indoor area. Next, the subjects need to transfer to site 1 by slowly walking from the indoor site, experiencing the ambient environment in site 1 for 10 minutes. During the exposure, only light activities were permitted, i.e. sitting, standing or walking, whose corresponding metabolic rates are under 2 MET. 3 copies of questionnaires were needed to fill in, respectively at the 0th minute (upon arrival in the outdoor sites), the 5th minute and the 10th minute after reaching the experimental site to record their subjective responses during the short-term exposure in the shaded area. After the exposure in the first outdoor site, they slowly walk back to the initial indoor area and rest as usual for 10 minutes to recover. They were then required to replicate the experimental procedure again in site 2, including slowly transferring, mild activities limitation, filling in the 3 0-minute, 5-minute and 10-minute questionnaires to collect the occupants' thermal perceptions during the short-term exposure in the sunlit area. The weather station was set up near the research subjects during the experiment and used to monitor meteorological parameters simultaneously in both the indoor and the outdoor areas. The detailed experimental procedure timeline of a complete field experiment is illustrated in Figure 5.2.

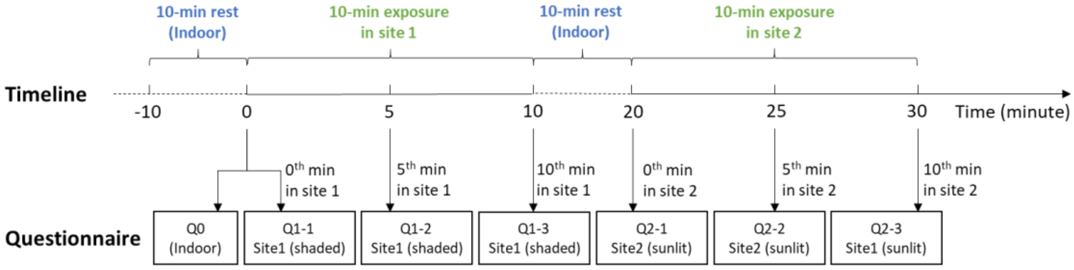

Figure 5.2 Experimental procedure timeline.

5.3 Subjects' thermal perceptions during short-term exposure

5.3.1 Comparisons according to sites

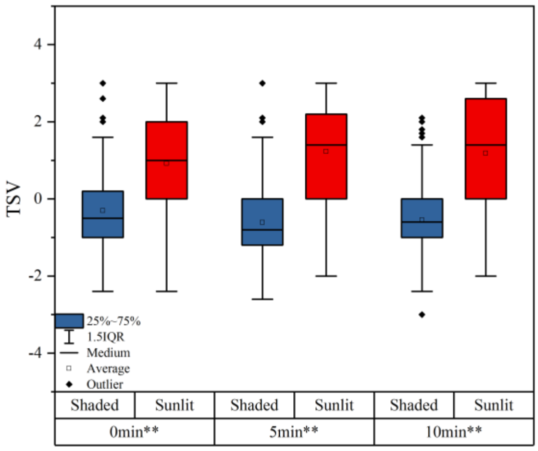

(1)

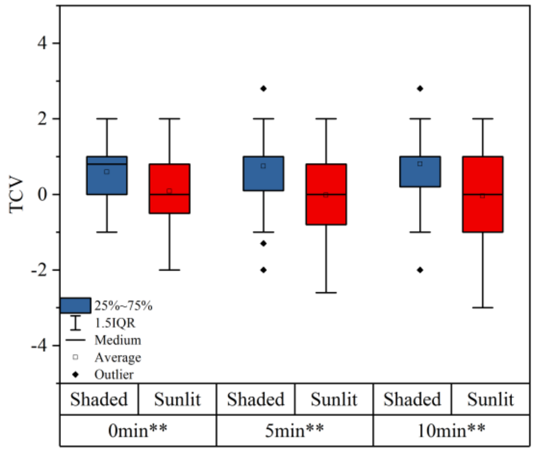

(2)

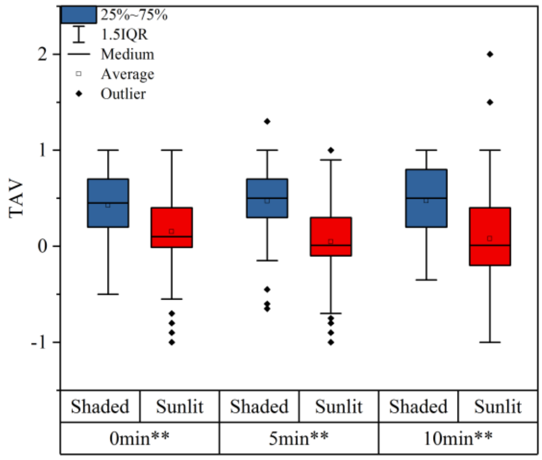

(3)

Figure 5.3 Thermal perceptions between site 1 (sunlit, red) and site 2 (shaded, blue) at the 0-minute, 5-minute and 10-minute of outdoor exposure.

(1) TSV; (2) TCV; (3) TAV. The symbol ** represents a significant (p<0.01 in ANOVA)

difference.

Figure 5.3 demonstrates the occupants' thermal perceptions (TSV, TCV and TAV) during the outdoor short-term exposure in the two selected outdoor sites. It can be observed that in all of the three exposure periods, occupants' mean TSV values in site 2 (shaded) were ranged from -0.3 to -0.6, while the TSV values in site 1 (sunlit) were ranged from 0.9 ~ 1.2. The average difference in mean TSV is 1.6 units, suggesting a colder subjective sensation in the shaded site during the short-term exposure. Likewise, occupants' mean thermal comfort vote (around 0.7 difference) and thermal acceptability vote (around 0.4 difference) were higher in site 2 (shaded) for all of the three experimental periods. This indicates that compared with the sunlit site, the "lift-up" shaded site was more comfortable and acceptable during the short-term outdoor exposure. ANOVA tests also serve as evidence that all of the pairwise comparisons between the two sites show significant differences at the 0.01 significance level.

5.3.2 Comparisons according to seasons

Figure 5.4 illustrates the comparisons of occupants' average TSV, TCV and TAV classified by the experimental sites and seasons. Experimental data were divided into two groups: summer (Aug. ~ Oct.) and winter (Feb. ~ Apr.).

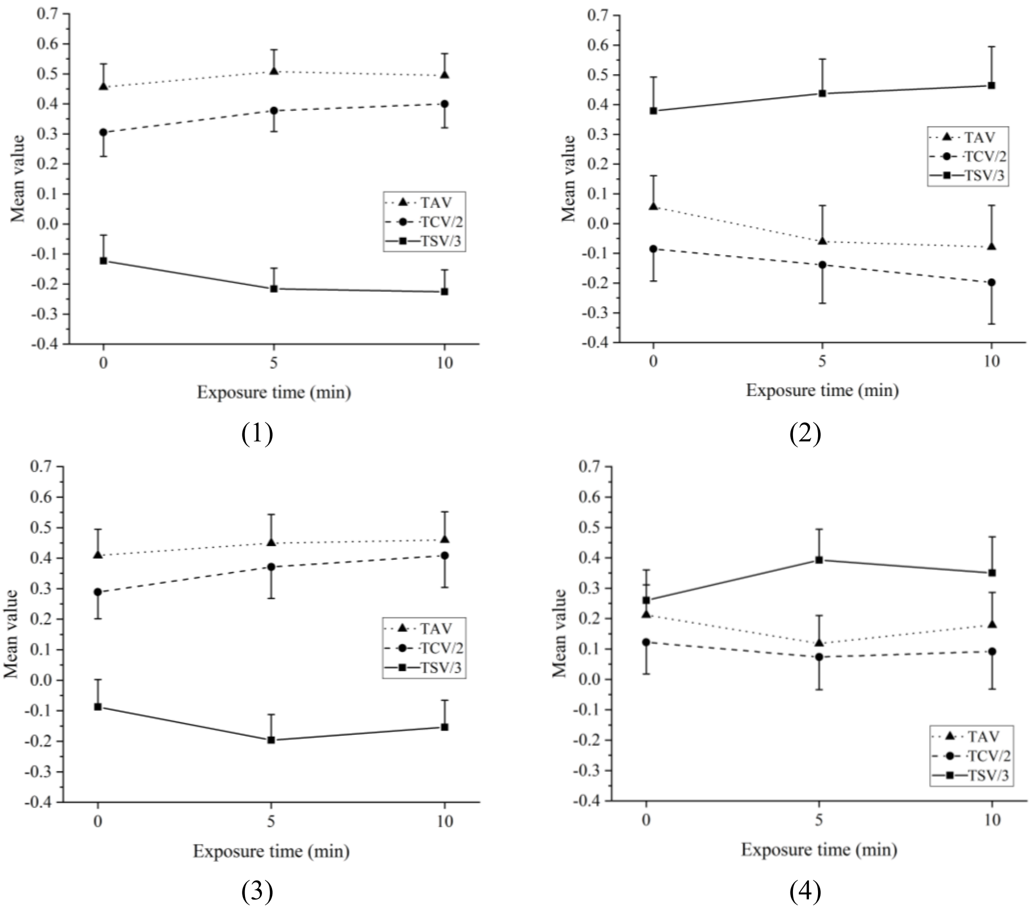

Figure 5.4 Thermal perceptions comparisons by season and site at the 0-minute, 5-minute and 10-minute of outdoor exposure.
(1) site 2 (shaded) in summer; (2) site 1 (sunlit) in summer; (3) site 2 (shaded) in winter; (4) site 1 (sunlit) in winter. Vertical bars indicate ±SD. Thermal sensation vote and thermal comfort vote were respectively divided by 3 and 2 to unify the y-axis.

According to the variations of thermal perception over time as illustrated in Figure 5.4 (1) and Figure 5.4 (2), occupants' mean TSV, TCV and TAV in different seasons in site 2 (shaded site) are similar due to the fact the research subjects were prevented from direct solar radiation by the "lift-up" building morphology. Even though T_a is generally higher in summer, the average thermal perceptions in the shaded site did not show much difference compared with the results in winter. Nevertheless, in the sunlit site, occupants' mean TSV, TCV and TAV are distinct between summer and winter, as shown in Figure 5.4 (2) and Figure 5.4 (4). Occupants' changing rate of TSV, TCV and TAV during the first 5 minutes is higher than the changing rate in the last 5 minutes during the 10-minute exposure. This is because physiological conditions of the occupants gradually reach steady and both internal effort for thermal regulations and heat transfer between human and the ambient environment become weaker as exposure time increases. It can be observed that occupants in site 1 (sunlit site) generally felt hotter no matter for the 0th minute (0.35 unit of TSV difference), the 5th minute (0.13 unit of TSV difference) or the 10th minute (0.34 unit of TSV difference). It is also reported that the subjects are less comfortable (0.41 unit, 0.43 unit and 0.58 unit of TCV difference respectively at the 0th minute,5th minute and 10th minute of exposure) and less acceptable (0.16 unit, 0.18 unit and 0.26 unit of TAV difference at the 0th minute,5th minute and 10th minute of exposure). In the sunlit area, the occupants' thermal comfort and thermal acceptability conditions are aggravated in summer, which suggests that adopting such a building design that exposes occupants to direct solar irradiance during short-term exposure can introduce additional unpleasant thermal perceptions in hot weather.

5.4 Correlations between thermal perceptions and environmental differences

One of the main causes that induce variations in the occupants' thermal perceptions is the environmental changes. During the process of transferring to the outdoor site from the indoor site, the intensive environmental changes between indoor and outdoor areas will lead to a significant difference in thermal responses (Dahlan & Gital, 2016; Yu et al., 2015). Therefore, the indoor-outdoor environmental difference acts as a crucial factor that accounts for subjective thermal perceptions variations during the short periods of outdoor exposure.

To find out the relations between subjective thermal perceptions and the environmental difference between the indoor and the outdoor sites, two thermal comfort indices, PET and UTCI were employed to describe the occupants' thermal stress during the outdoor exposure. Average values of TSV, TCV and TAV at the 0^{th} minute, the 5^{th} minute and the 10^{th} minute (denoted by TSV_{xmin}, TCV_{xmin} and TAV_{xmin}, respectively) were calculated respectively at 1 K intervals. The thermal perception average values were correlated with the PET or UTCI differences between the outdoor area and the indoor area ($\triangle PET_{xmin\text{-}I}$ or $\triangle UTCI_{xmin\text{-}I}$), which was calculated using the PET or UTCI values at the xth minute outdoors (x=0, 5 or 10) less the PET or UTCI values of the indoor area. Linear regression was employed to fit TSV and second-order polynomial regression was adopted for TCV and TAV regressions. Figure 5.5 and Figure 5.6 illustrate the results of the $\triangle PET_{xmin\text{-}I}$ and $\triangle UTCI_{xmin\text{-}I}$ correlations, respectively. The corresponding data used for fitting, including mean values, standard deviations (SD), maximum and minimum values of the thermal perceptions, were listed from Table 5.1 to Table 5.6.

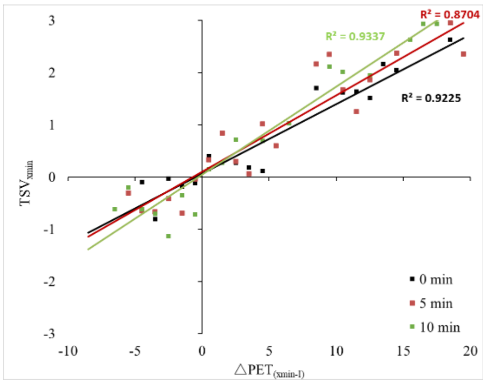

(1)

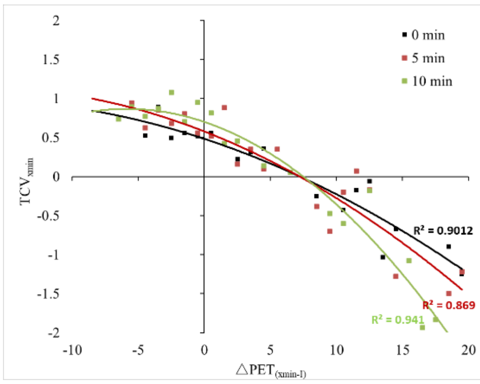

(2)

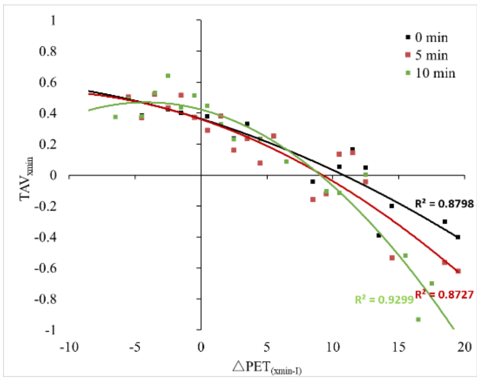

(3)

Figure 5.5 Correlations between average TSV, TCV and TAV at the xth minute of outdoor exposure and indoor-outdoor PET differences at the xth minute of outdoor exposure (x=0, 5 or 10).

(1) TSV_{xmin} versus $\triangle PET_{xmin\text{-}I}$; (2) TCV_{xmin} versus $\triangle PET_{xmin\text{-}I}$; (3) TAV_{xmin} versus $\triangle PET_{xmin\text{-}I}$.

Table 5.1 Statistics of TSV in the corresponding PET ranges

△PET Range (K)	Corresponding mean TSV at the 0th minute			Corresponding mean TSV at the 5th minute			Corresponding mean TSV at the 10th minute		
	N	Mean±SD	[Min,Max]	N	Mean±SD	[Min,Max]	N	Mean±SD	[Min,Max]
[-7,-6]	0	-	-	0	-	-	8	-0.61±0.54	[-1.2,0.4]
(-6,-5]	0	-	-	9	-0.30±0.73	[-1.4,1.6]	27	-0.21±1.05	[-2.0,2.0]
(-5,-4]	40	-0.09±1.07	[-2.4,2.0]	20	-0.65±1.05	[-2.6,2.0]	28	-0.61±1.16	[-3.0,1.8]
(-4,-3]	54	-0.80±0.82	[-2.0,1.4]	58	-0.66±0.83	[-2.0,1.0]	43	-0.70±0.94	[-2.0,2.0]
(-3,-2]	31	-0.03±1.13	[-2.0,3.0]	38	-0.41±1.10	[-2.0,3.0]	10	-1.13±0.78	[-2.4,0.0]
(-2,-1]	49	-0.19±0.89	[-1.6,2.6]	32	-0.69±0.92	[-2.2,2.0]	59	-0.35±0.93	[-2.0,2.1]
(-1,0]	50	-0.12±1.02	[-2.4,2.1]	54	-0.04±1.14	[-2.2,2.8]	44	-0.72±0.91	[-2.2,1.8]
(0,1]	27	0.40±1.23	[-2.0,3.0]	19	0.33±1.23	[-2.4,2.6]	7	0.15±1.63	[-2.4,3.0]
(1,2]	0	-	-	12	0.84±0.95	[-0.6,2.0]	22	0.27±0.92	[-1.0,2.0]
(2,3]	16	0.28±1.16	[-1.7,2.7]	11	0.30±0.84	[-1.0,2.1]	12	0.72±1.27	[-1.0,3.0]
(3,4]	11	0.18±1.14	[-1.4,1.8]	25	0.07±1.22	[-1.8,2.0]	0	-	-
(4,5]	26	0.11±1.22	[-2.4,2.2]	14	1.01±1.38	[-2.0,2.6]	33	0.69±1.26	[-2.0,2.0]
(5,6]	0	-	-	12	0.60±0.68	[-2.0,2.6]	0	-	-
(6,7]	0	-	-	0	-	-	13	1.02±1.49	[-2.0,3.0]

(7,8]	0	-	-	0	-	-	0	-	-
(8,9]	30	1.70±0.75	[0.0,3.0]	25	2.17±0.51	[1.0,3.0]	0	-	-
(9,10]	0	-	-	9	2.35±0.38	[0.0,0.0]	36	2.11±0.81	[0.0,3.0]
(10,11]	7	1.62±0.54	[1.0,2.8]	7	1.67±0.50	[1.0,3.0]	7	2.01±0.69	[0.8,2.8]
(11,12]	14	1.64±0.66	[0.8,2.7]	10	1.25±0.96	[-0.1,3.0]	0	-	-
(12,13]	16	1.51±0.78	[0.2,2.6]	21	1.86±0.79	[0.0,2.8]	23	1.95±0.86	[-0.8,3.0]
(13,14]	6	2.17±0.79	[0.0,3.0]	0	-	-	0	-	-
(14,15]	4	2.05±0.64	[1.2,3.0]	5	2.37±0.50	[1.8,3.0]	0	-	-
(15,16]	0	-	-	0	-	-	13	2.62±0.36	[2.0,3.0]
(16,17]	0	-	-	0	-	-	6	2.93±0.06	[2.6,3.0]
(17,18]	0	-	-	0	-	-	3	2.93±0.06	[2.8,3.0]
(18,19]	7	2.63±0.35	[2.0,3.0]	8	2.95±0.05	[2.8,3.0]	0	-	-
(19,20]	6	2.37±0.17	[2.0,2.6]	5	2.36±0.61	[1.0,3.0]	0	-	-
Total	**394**	**-**	**-**	**394**	**-**	**-**	**394**	**-**	**-**

Table 5.2 Statistics of TCV in the corresponding PET ranges

△PET Range (K)	**Corresponding mean TCV at the 0th minute**			**Corresponding mean TCV at the 5th minute**			**Corresponding mean TCV at the 10th minute**		
	N	**Mean±SD**	**[Min,Max]**	**N**	**Mean±SD**	**[Min,Max]**	**N**	**Mean±SD**	**[Min,Max]**
[-7,-6]	0	-	-	0	-	-	8	0.74±0.22	[0.0,1.0]
(-6,-5]	0	-	-	9	0.94±0.56	[0.0,2.0]	27	0.89±0.90	[-1.0,2.0]
(-5,-4]	40	0.53±0.66	[-1.0,1.5]	20	0.62±1.01	[-2.0,2.0]	28	0.77±0.97	[-2.0,2.0]
(-4,-3]	54	0.89±0.69	[-1.0,2.0]	58	0.85±0.67	[-0.5,2.0]	43	0.87±0.75	[-1.0,2.0]
(-3,-2]	31	0.49±0.68	[-1.0,2.0]	38	0.68±0.65	[-1.0,2.0]	10	1.08±0.23	[0.7,1.6]
(-2,-1]	49	0.56±0.55	[-1.0,1.4]	32	0.80±0.66	[-1.3,2.0]	59	0.70±0.73	[-1.0,2.0]
(-1,0]	50	0.52±0.68	[-1.0,2.0]	54	0.56±0.75	[-1.0,2.0]	44	0.95±0.62	[-0.2,2.0]
(0,1]	27	0.56±0.67	[-1.0,1.7]	19	0.52±0.81	[-1.0,2.0]	7	0.81±0.78	[-1.0,2.0]
(1,2]	0	-	-	12	0.88±0.70	[-0.3,2.0]	22	0.43±0.71	[-1.0,1.2]
(2,3]	16	0.22±0.70	[-1.1,2.0]	11	0.16±0.38	[-0.6,2.0]	12	0.46±0.53	[-0.5,1.2]
(3,4]	11	0.31±0.81	[-1.0,1.3]	25	0.35±0.60	[-1.0,1.3]	0	-	-
(4,5]	26	0.35±0.71	[-1.0,2.0]	14	0.10±0.90	[-1.1,2.0]	33	0.14±0.97	[-2.0,2.0]
(5,6]	0	-	-	12	0.35±0.67	[-1.1,1.5]	0	-	-
(6,7]	0	-	-	0	-	-	13	0.05±1.25	[-2.0,2.0]
(7,8]	0	-	-	0	-	-	0	-	-
(8,9]	30	-0.25±0.65	[-2.0,1.0]	25	-0.38±0.75	[-2.0,1.5]	0	-	-
(9,10]	0	-	-	9	-0.70±0.28	[0.0,0.0]	36	-0.48±0.81	[-2.0,1.2]
(10,11]	7	-0.43±0.57	[-1.0,0.4]	7	-0.20±0.16	[-1.0,0.0]	7	-0.60±0.33	[-1.1,-0.1]
(11,12]	14	-0.18±0.91	[-2.0,2.0]	10	0.07±0.62	[-1.0,1.0]	0	-	-
(12,13]	16	-0.06±0.65	[-1.0,1.0]	21	-0.17±0.91	[-1.8,1.3]	23	-0.18±1.00	[-2.0,2.0]
(13,14]	6	-1.03±0.68	[-2.0,0.0]	0	-	-	0	-	-
(14,15]	4	-0.68±0.29	[-1.0,-0.2]	5	-1.28±0.41	[-2.0,-0.8]	0	-	-
(15,16]	0	-	-	0	-	-	13	-1.08±0.81	[-2.0,0.1]
(16,17]	0	-	-	0	-	-	6	-1.93±0.06	[-2.0,-1.6]
(17,18]	0	-	-	0	-	-	3	-1.83±0.14	[-2.0,-1.5]

(18,19]	7	-0.90±0.56	[-2.0,0.0]	8	-1.50±0.50	[-2.0,-1.0]	0	-	-
(19,20]	6	-1.25±0.20	[-2.0,-1.0]	5	-1.22±0.61	[-2.0,-0.3]	0	-	-
Total	**394**	-	-	**394**	-	-	**394**	-	-

Table 5.3 Statistics of TAV in the corresponding PET ranges

△PET Range (K)	**Corresponding mean TAV at the 0th minute**			**Corresponding mean TAV at the 5th minute**			**Corresponding mean TAV at the 10th minute**		
	N	**Mean±SD**	**[Min,Max]**	**N**	**Mean±SD**	**[Min,Max]**	**N**	**Mean±SD**	**[Min,Max]**
[-7,-6]	0	-	-	0	-	-	8	0.38±0.19	[0.1,0.7]
(-6,-5]	0	-	-	9	0.50±0.30	[-0.1,1.0]	27	0.49±0.39	[-0.4,1.0]
(-5,-4]	40	0.38±0.30	[-0.1,0.9]	20	0.37±0.37	[-0.5,1.0]	28	0.38±0.38	[-0.3,1.0]
(-4,-3]	54	0.53±0.31	[0.0,1.0]	58	0.52±0.33	[-0.2,1.0]	43	0.53±0.35	[-0.1,1.0]
(-3,-2]	31	0.43±0.36	[-0.4,1.0]	38	0.43±0.30	[-0.1,1.0]	10	0.64±0.17	[0.4,1.0]
(-2,-1]	49	0.40±0.33	[-0.5,1.0]	32	0.52±0.39	[-0.7,1.0]	59	0.44±0.32	[-0.1,1.0]
(-1,0]	50	0.38±0.32	[-0.2,1.0]	54	0.37±0.33	[-0.3,1.0]	44	0.51±0.28	[0.0,1.0]
(0,1]	27	0.38±0.43	[-1.0,1.0]	19	0.29±0.39	[-0.3,1.0]	7	0.45±0.33	[-0.1,1.0]
(1,2]	0	-	-	12	0.38±0.35	[0.0,1.0]	22	0.33±0.38	[-0.1,1.0]
(2,3]	16	0.24±0.21	[0.0,1.0]	11	0.16±0.11	[0.0,1.0]	12	0.23±0.20	[0.0,0.6]
(3,4]	11	0.33±0.41	[-0.4,1.0]	25	0.24±0.22	[0.0,0.5]	0	-	-
(4,5]	26	0.23±0.31	[-0.3,1.0]	14	0.08±0.28	[-0.4,1.0]	33	0.23±0.39	[-0.8,1.0]
(5,6]	0	-	-	12	0.25±0.30	[-0.4,0.6]	0	-	-
(6,7]	0	-	-	0	-	-	13	0.09±0.61	[-0.8,1.0]
(7,8]	0	-	-	0	-	-	0	-	-
(8,9]	30	-0.04±0.34	[-0.8,0.6]	25	-0.16±0.30	[-1.0,0.3]	0	-	-
(9,10]	0	-	-	9	-0.12±0.13	[0.0,0.0]	36	-0.10±0.35	[-1.0,0.7]
(10,11]	7	0.05±0.16	[-0.3,0.3]	7	0.14±0.12	[-0.3,0.3]	7	-0.11±0.13	[-0.3,0.1]
(11,12]	14	0.17±0.33	[-0.4,0.9]	10	0.14±0.33	[-0.6,0.8]	0	-	-
(12,13]	16	0.05±0.24	[-0.4,0.6]	21	-0.04±0.40	[-0.8,0.7]	23	0.00±0.36	[-0.8,0.9]
(13,14]	6	-0.39±0.30	[-0.9,0.0]	0	-	-	0	-	-
(14,15]	4	-0.20±0.22	[-0.5,0.1]	5	-0.54±0.33	[-0.9,0.0]	0	-	-
(15,16]	0	-	-	0	-	-	13	-0.52±0.35	[-1.0,0.0]
(16,17]	0	-	-	0	-	-	6	-0.93±0.06	[-1.0,-0.7]
(17,18]	0	-	-	0	-	-	3	-0.70±0.26	[-1.0,-0.2]
(18,19]	7	-0.30±0.50	[-0.8,0.7]	8	-0.57±0.37	[-1.0,0.0]	0	-	-
(19,20]	6	-0.40±0.05	[-0.7,-0.3]	5	-0.62±0.25	[-1.0,-0.3]	0	-	-
Total	**394**	-	-	**394**	-	-	**394**	-	-

It can be seen from Figure 5.5 (1) that PET differences between the outdoor site and the indoor area ranged from -7K to 20K. There is a strong positive linear relation between TSV_{xmin} and the indoor-outdoor PET differences. The occupants felt warm or hot during the 10-minute outdoor exposure if the outdoor site was hotter than the indoor site in terms of PET ($\triangle PET_{xmin\text{-}I}$ >0) and vice versa. R^2 values of the correlations are 0.92, 0.87 and 0.93, respectively for the experimental data at the 0^{th}, 5^{th} and 10^{th} minute of exposure, indicating high fitting qualities.

It can be observed from Figure 5.5 (2) and (3) that the second-order regressions between TCV_{xmin}/TAV_{xmin} and $\triangle PET_{xmin\text{-}I}$ are also of great fitting qualities (R^2=0.90, 0.87 and 0.94, respectively for the 0^{th}, 5^{th} and 10^{th} minute in TCV regressions; R^2=0.88, 0.87 and 0.93, respectively for the 0^{th}, 5^{th} and 10^{th} minute in TAV regressions). the research subjects' average TCV and TAV values are around 0.7 and 0.4, respectively. When $\triangle PET_{xmin\text{-}I}$ is under 3K, subjects' mean TCV and TAV values do not show obvious variations. The occupants have the highest level of thermal comfort and thermal acceptability during the 10-minute outdoor exposure if $\triangle PET_{xmin\text{-}I}$ is below 3K. When $\triangle PET_{xmin\text{-}I}$ exceeds 3K and keeps increasing, occupants' TCV and TAV values decrease rapidly. Mean TCV and TAV at the 10^{th} minute of exposure are under those at the 0^{th} and the 5^{th} minute in the same $\triangle$PET range when $\triangle PET_{xmin\text{-}I}$ is higher than 10K, indicating that the outdoor site felt less comfortable and acceptable at the 10^{th} minute compared with the 0^{th} and 5^{th} minute in the cases that the outdoor environment was significantly hotter than the indoor area.

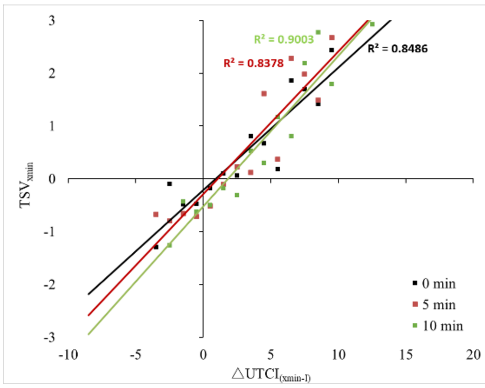

(1)

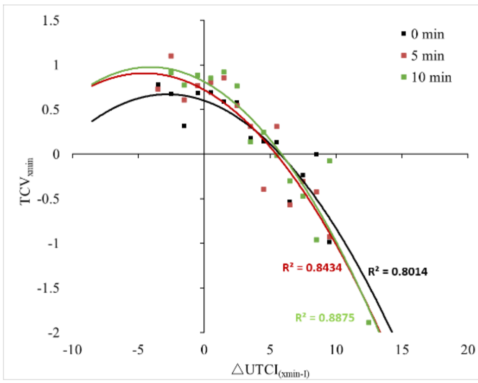

(2)

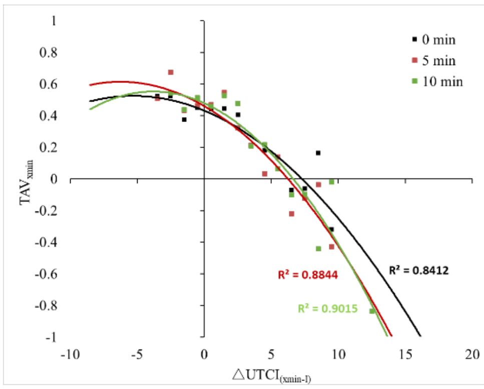

(3)

Figure 5.6 Correlations between average TSV, TCV and TAV at the xth minute of outdoor exposure and indoor-outdoor UTCI differences at the xth minute of outdoor exposure (x=0, 5 or 10).

(1) TSV_{xmin} v.s. $\Delta UTCI_{xmin-I}$; (2) TCV_{xmin} v.s. $\Delta UTCI_{xmin-I}$; (3) TAV_{xmin} v.s. $\Delta UTCI_{xmin-I}$.

Table 5.4 Statistics of TSV in the corresponding UTCI ranges

ΔUTCI Range	**Corresponding mean TSV at the 0th minute**			**Corresponding mean TSV at the 5th minute**			**Corresponding mean TSV at the 10th minute**		
(K)	**N**	**Mean±SD**	**[Min,Max]**	**N**	**Mean±SD**	**[Min,Max]**	**N**	**Mean±SD**	**[Min,Max]**
(-4,-3]	13	-1.29±0.61	[-2.0,1.4]	19	-0.68±0.78	[-2.0,1.0]	0	-	-
(-3,-2]	4	-0.10±0.50	[-0.6,0.4]	6	-0.80±0.20	[-1.0,-0.6]	14	-1.26±0.55	[-2.0,-0.4]
(-2,-1]	15	-0.48±1.27	[-2.4,2.0]	35	-0.66±1.21	[-2.0,2.0]	59	-0.43±1.11	[-3.0,2.0]
(-1,0]	74	-0.47±0.91	[-2.4,2.0]	56	-0.72±0.83	[-2.6,1.6]	55	-0.63±0.99	[-2.4,2.0]
(0,1]	64	-0.18±1.09	[-2.0,3.0]	32	-0.51±1.03	[-2.4,3.0]	48	-0.50±0.91	[-2.4,1.7]
(1,2]	21	0.10±0.80	[-2.0,2.0]	29	-0.11±1.06	[-2.0,2.8]	13	-0.18±1.22	[-1.6,3.0]
(2,3]	65	0.06±1.02	[-1.8,3.0]	44	0.23±1.11	[-1.8,2.6]	42	-0.30±1.22	[-2.0,3.0]
(3,4]	10	0.80±0.80	[0.0,2.1]	35	0.12±1.03	[-1.0,2.1]	19	0.53±0.97	[-1.0,3.0]
(4,5]	13	0.67±0.85	[-1.0,2.2]	21	1.62±0.62	[0.4,2.6]	23	0.30±0.99	[-2.0,2.1]
(5,6]	25	0.19±1.36	[-2.4,2.7]	46	0.37±1.34	[-2.0,2.6]	43	1.17±1.43	[-2.0,3.0]
(6,7]	18	1.87±0.80	[0.0,3.0]	11	2.28±0.56	[1.0,3.0]	3	0.80±1.14	[-0.8,1.8]
(7,8]	26	1.70±0.66	[0.2,3.0]	21	1.98±0.64	[-0.1,3.0]	41	2.19±0.77	[0.0,3.0]

(8,9]	25	1.42±0.76	[0.0,2.7]	27	1.49±0.86	[0.0,3.0]	13	2.78±0.31	[2.0,3.0]
(9,10]	21	2.44±0.47	[1.2,3.0]	12	2.67±0.48	[1.0,3.0]	13	1.80±0.65	[0.9,2.8]
(10,11]	0	-	-	0	-	-	0	-	-
(11,12]	0	-	-	0	-	-	0	-	-
(12,13]	0	-	-	0	-	-	8	2.93±0.14	[2.6,3.0]
Total	**394**	-	-	**394**	-	-	**394**	-	-

Table 5.5 Statistics of TCV in the corresponding UTCI ranges

△UTCI Range	**Corresponding mean TCV at the 0th minute**			**Corresponding mean TCV at the 5th minute**			**Corresponding mean TCV at the 10th minute**		
(K)	**N**	**Mean±SD**	**[Min,Max]**	**N**	**Mean±SD**	**[Min,Max]**	**N**	**Mean±SD**	**[Min,Max]**
(-4,-3]	13	0.78±0.69	[-1.0,1.9]	19	0.73±0.58	[0.0,2.0]	0	-	-
(-3,-2]	4	0.68±0.79	[0.0,2.0]	6	1.10±0.57	[0.4,2.0]	14	0.91±0.61	[-0.6,2.0]
(-2,-1]	15	0.31±0.73	[-1.0,1.4]	35	0.61±0.63	[-0.8,1.6]	59	0.77±0.85	[-2.0,2.0]
(-1,0]	74	0.69±0.69	[-1.0,2.0]	56	0.77±0.78	[-2.0,2.0]	55	0.88±0.71	[-1.0,2.0]
(0,1]	64	0.69±0.64	[-1.0,2.0]	32	0.80±0.73	[-1.3,2.0]	48	0.85±0.68	[-1.0,2.0]
(1,2]	21	0.59±0.67	[-1.0,2.0]	29	0.85±0.66	[-1.0,2.0]	13	0.92±0.85	[-1.0,2.0]
(2,3]	65	0.58±0.58	[-1.0,1.6]	44	0.54±0.67	[-1.0,2.0]	42	0.76±0.68	[-1.0,2.0]
(3,4]	10	0.18±0.76	[-0.9,2.0]	35	0.31±0.72	[-0.9,2.0]	19	0.14±0.50	[-1.0,1.0]
(4,5]	13	0.14±0.56	[-1.0,1.1]	21	-0.39±0.50	[-1.1,0.6]	23	0.25±0.58	[-1.0,1.2]
(5,6]	25	0.13±0.75	[-1.1,2.0]	46	0.31±0.72	[-0.8,2.0]	43	-0.01±0.98	[-2.0,2.0]
(6,7]	18	-0.53±0.65	[-2.0,0.0]	11	-0.57±0.76	[-2.0,1.5]	3	-0.30±0.51	[-1.0,0.2]
(7,8]	26	-0.24±0.63	[-1.2,1.0]	21	-0.31±0.64	[-1.2,1.4]	41	-0.47±0.79	[-2.0,1.2]
(8,9]	25	0.00±0.81	[-2.0,2.0]	27	-0.42±0.76	[-1.8,1.3]	13	-0.96±0.59	[-2.0,0.1]
(9,10]	21	-0.99±0.49	[-2.0,0.0]	12	-0.93±0.52	[-2.0,-0.3]	13	-0.08±1.00	[-1.4,2.0]
(10,11]	0	-	-	0	-	-	0	-	-
(11,12]	0	-	-	0	-	-	0	-	-
(12,13]	0	-	-	0	-	-	8	-1.89±0.20	[-2.0,-1.5]
Total	**394**	-	-	**394**	-	-	**394**	-	-

Table 5.6 Statistics of TAV in the corresponding UTCI ranges

△UTCI Range	**Corresponding mean TAV at the 0th minute**			**Corresponding mean TAV at the 5th minute**			**Corresponding mean TAV at the 10th minute**		
(K)	**N**	**Mean±SD**	**[Min,Max]**	**N**	**Mean±SD**	**[Min,Max]**	**N**	**Mean±SD**	**[Min,Max]**
(-4,-3]	13	0.52±0.31	[0.0,1.0]	19	0.51±0.30	[0.0,1.0]	0	-	-
(-3,-2]	4	0.53±0.33	[0.1,1.0]	6	0.68±0.25	[0.3,1.0]	14	0.54±0.29	[0.0,1.0]
(-2,-1]	15	0.37±0.36	[-0.4,1.0]	35	0.43±0.35	[-0.1,1.0]	59	0.44±0.38	[-0.4,1.0]
(-1,0]	74	0.45±0.32	[-0.1,1.0]	56	0.46±0.35	[-0.5,1.0]	55	0.51±0.32	[-0.1,1.0]
(0,1]	64	0.44±0.35	[-0.5,1.0]	32	0.47±0.35	[-0.7,1.0]	48	0.46±0.31	[-0.1,1.0]
(1,2]	21	0.44±0.32	[-0.2,1.0]	29	0.55±0.33	[-0.3,1.0]	13	0.53±0.35	[-0.1,1.0]
(2,3]	65	0.40±0.36	[-1.0,1.0]	44	0.32±0.32	[-0.3,1.0]	42	0.48±0.33	[-0.1,1.0]
(3,4]	10	0.21±0.31	[0.0,1.0]	35	0.21±0.29	[0.0,1.0]	19	0.21±0.26	[-0.2,0.8]
(4,5]	13	0.18±0.24	[-0.3,0.6]	21	0.03±0.22	[-0.4,0.5]	23	0.22±0.28	[-0.2,0.9]

(5,6]	25	0.14±0.29	[-0.4,1.0]	46	0.14±0.25	[-0.4,1.0]	43	0.06±0.41	[-0.8,1.0]
(6,7]	18	-0.07±0.36	[-0.9,0.4]	11	-0.22±0.36	[-1.0,0.3]	3	-0.10±0.22	[-0.3,0.2]
(7,8]	26	-0.06±0.30	[-0.7,0.6]	21	-0.12±0.27	[-0.6,0.4]	41	-0.10±0.34	[-1.0,0.7]
(8,9]	25	0.16±0.28	[-0.4,0.9]	27	-0.04±0.33	[-0.6,0.8]	13	-0.44±0.34	[-1.0,0.0]
(9,10]	21	-0.32±0.33	[-0.8,0.7]	12	-0.43±0.32	[-1.0,0.0]	13	-0.02±0.33	[-0.5,0.9]
(10,11]	0	-	-	0	-	-	0	-	-
(11,12]	0	-	-	0	-	-	0	-	-
(12,13]	0	-	-	0	-	-	8	-0.84±0.26	[-1.0,-0.2]
Total	**394**	-	-	**394**	-	-	**394**	-	-

The correlations between TSV_{xmin}\ TSV_{xmin}\$TSV_{xmin}$ and $\triangle UTCI_{xmin\text{-}I}$ are similar to those correlations with $\triangle PET_{xmin\text{-}I}$. As shown in Figure 5.6 (1), the indoor-outdoor UTCI differences ranged from -3.1K to 12.4K, the range of which is narrower than in PET. This is because UTCI gives a smaller absolute value in temperature output when inputting meteorological parameter combinations in extreme weather conditions. Similarly, there exists a positive linear relation between TSV_{xmin} and $\triangle UTCI_{xmin\text{-}I}$ as observed between TSV_{xmin} and $\triangle PET_{xmin\text{-}I}$. Regression R^2 values are 0.85,0.84 and 0.90, respectively for the experimental data at the 0^{th}, 5^{th} and 10^{th} minute of exposure, indicating high fitting qualities.

As shown in Figure 5.6 (2) and Figure 5.6 (3), occupants' mean TCV and TAV are around 0.7 and 0.5, respectively. When $\triangle UTCI_{xmin\text{-}I}$ is under 3K, subjects' mean TCV and TAV values do not show obvious variations, which was similar to the result from $\triangle PET$ regressions. The occupants have the highest level of thermal comfort and thermal acceptability during the 10-minute outdoor exposure if $\triangle UTCI_{xmin\text{-}I}$ is below 3K. When $\triangle UTCI_{xmin\text{-}I}$ exceeds 3K and keeps increasing, occupants' TCV and TAV values drop dramatically. Among three fitting curves in TCV regressions, the 10^{th}-

minute fitting curve showed the highest R^2 values of 0.94. The conclusion was also applicable for the 10^{th}-minute fitting curve in TSV regressions (R^2=0.90) and the 10^{th}-minute fitting curve in TAV regressions (R^2=0.90).

5.5 Summary

This chapter focuses on human thermal perceptions during the 10-minute outdoor after resting in an air-conditioned indoor area. The results can be summarized as follows:

(1) The lift-up shaded sites generally felt more comfortable and acceptable during the short-term exposure. It was also revealed that the seasonal thermal perceptions aggravations were observed only in the sunlit area. The "lift-up" design was able to eliminate this aggravation and maintain the same level of thermal perceptions in summer as in winter during the 10-minute transient process.

(2) There exists a positive linear relation between TSV and PET difference between the outdoor area and the indoor area. The second-order polynomial regression is suitable for fitting TCV/TAV with outdoor-indoor PET difference. This suggests outdoor-indoor environmental difference, which can be presented by $\triangle PET_{xmin\text{-}I}$ or $\triangle UTCI_{xmin\text{-}I}$, is a great indicator of respondent thermal perceptions. Among the correlations aiming at different exposure time, correlations at the 10^{th} minute of exposure showed the best regression quality.

(3) Correlations between TSV\TCV\TAV and outdoor-indoor UTCI differences are similar to those correlations with outdoor-indoor PET differences, except that the calculated △UTCI ranges are narrower than △PET, which is due to the smaller

output absolute values that UTCI model gives.

Chapter 6 Development of TSV and TCV predicting models during short-term outdoor exposure

This chapter presents the development processes of TSV and TCV predicting models incorporating the data acquired from the 10-min exposure experiments. Stepwise regressions were conducted to filter the independent variables in predicting TSV and TCV. Four independent variables were finally selected by the stepwise regression, which were then correlated with TSV and TCV using multiple linear regression to determine the respective impact coefficients.

6.1 Determination of model independent predictors using stepwise regression

15 parameters or factors recorded from the field measurement or questionnaire were examined by stepwise regression to determine the predictors of the predicting models of TCV and TSV, including PET (or UTCI), △PET (or △UTCI), T_{mr}, V_a, subjective sunlight level, subjective wind level, exposure time, emotion, noise, gender, age, weight, height, clothing insulation and metabolism. Entry significant level was set to 0.01 and removal significant level was set to 0.05 to ensure the inclusion of selected predictors significantly improve the regression quality. Models adopting PET and UTCI as predictors were developed separately.

6.6.1 Predictors in TSV predicting models

As shown in Table 6.1, four predictors: △PET, wind level, sunlight level and PET were included in the model in turn, due to their smallest p-values among all predictors that are below 0.01 in each step of stepwise regression adopting PET and △PET as predictors. None of these four selected predictors were removed by the model during the stepwise regression since the p-value of each selected predictor did not exceed 0.05. It can be found from the final model that the four predictors were all highly significant predictors of TSV, with $p < 0.001$ for wind level, sunlight level, PET and $p < 0.01$ for △PET.

Other predictors (time, emotion, noise, T_{mr}, V_a, gender, weight, height, clothing insulation, metabolism) were not included in the model during the regression either because their p values in the t-test were above 0.01 or their p values were not the smallest among all predictors, which means that these predictors have insignificant effects on TSV. However, it can be seen from the 4^{th} model in the stepwise regression that noise ($p = 0.013$), weight ($p = 0.027$) and metabolism ($p = 0.016$) are also marginally significant ($p < 0.05$) if included in the regression model. This indicates these three factors can potentially account for TSV and included in the model if the p-value entry level of the stepwise regression is set to be higher.

Table 6.1 T-test results in stepwise regression process of TSV predicting models adopting PET and △PET as predictors

	Predictors in the model				Predictors not in the model			
Model	Predictors	Beta	t	Sig.	Predictors	Beta	t	Sig.

1	(Constant)		-4.626	.000***	PET	-0.046	-.805	.421
	△PET	.692	32.920	.000***	Sunlight level	0.349	11.456	.000***
					Wind level	-0.293	-14.800	.000***
					Time	0.002	.095	.924
					Emotion	-0.032	-1.523	.128
					Noise	-0.06	-2.819	.005**
					T_{mr}	0.252	3.815	.000***
					Va	-0.05	-2.355	.019*
					Gender	0.004	0.180	.858
					Age	0.013	.635	.526
					Weight	0.062	2.928	.003**
					Height	0.001	0.064	.949
					Clothing insulation	0.068	3.249	.001**
					Metabolism	0.033	1.454	.146
2	(Constant)		-8.431	.000***	PET	0.106	1.988	.047*
	△PET	.627	31.660	.000***	Sunlight level	0.372	13.548	.000***
	Wind level	-.293	-14.800	.000***	Time	0.027	1.415	.157
					Emotion	-0.021	-1.078	.281
					Noise	-0.03	-1.519	.129
					T_{mr}	0.466	7.633	.000***
					Va	0.059	2.858	.004**
					Gender	-0.001	-0.066	.947
					Age	0.031	1.582	.114
					Weight	0.03	1.534	.125
					Height	0.004	0.205	.838
					Clothing insulation	0.04	2.041	.041
					Metabolism	0.059	2.791	.005**
3	(Constant)		-7.952	.000***	PET	0.193	3.868	.000***
	△PET	.343	12.307	.000***	Time	0.019	1.025	.306
	Wind level	-.306	-16.577	.000***	Emotion	-0.015	-.809	.418
	Sunlight level	.372	13.548	.000***	Noise	-0.028	-1.522	.128
					T_{mr}	0.186	2.954	.003**
					Va	0.017	.890	.373
					Gender	0.027	1.508	.132
					Age	0.015	0.807	.420
					Weight	-0.018	-.946	.345
					Height	0.026	1.442	.150
					Clothing insulation	-0.001	-.065	.948
					Metabolism	0.039	1.980	.048*
4	(Constant)		-4.729	.000***	Time	0.019	1.083	.279
	△PET	.151	2.650	.008**	Emotion	-0.02	-1.072	.284
	Wind level	-.320	-17.110	.000***	Noise	-0.046	-2.480	.013*
	Sunlight level	.385	14.003	.000***	T_{mr}	0.118	1.775	.076

	PET	.193	3.868	$.000^{***}$	Va	-0.036	-1.539	.124
					Gender	0.036	1.982	.048
					Age	0.007	0.379	.705
					Weight	0.055	2.217	$.027^{*}$
					Height	0.028	1.564	.118
					Clothing insulation	0.034	1.718	.086
					Metabolism	0.048	2.416	$.016^{*}$

*: p < 0.05; **: p < 0.01; ***: p < 0.001.

The stepwise regressions adopting UTCI and △UTCI as predictors show similar results as that adopting PET and △PET as predictors, which can be inferred from Table 6.2. The final model also included four predictors: △UTCI, wind level, sunlight level and UTCI, each of which showed extremely significant ($p < 0.001$) correlations with TSV. This suggests that the model adopting UTCI and △UTCI as predictors is more powerful than adopting PET and △PET in explaining the relations between TSV and the potential predictors. It can also be found in the final model that T_{mr} ($p = 0.013$) and clothing insulation ($p = 0.032$) are marginally significant ($p < 0.05$) if included in the regression model. Other predictors (time, emotion, noise, T_{mr}, V_a, gender, weight, height, clothing insulation, metabolism) were excluded from the model.

Table 6.2 T-test results in stepwise regression process of TSV predicting models adopting UTCI and △UTCI as predictors

	Predictors in the Model				**Predictors not in the Model**			
Model	Predictors	Beta	t	Sig.	Predictors	Beta	t	Sig.
1	(Constant)		-11.382	$.000^{***}$	Sunlight level	0.355	11.845	$.000^{***}$
	△UTCI	.690	32.731	$.000^{***}$	Wind level	-0.298	-15.098	$.000^{***}$
					Time	0.002	0.087	.931
					Emotion	-0.035	-1.645	.100
					Noise	-0.044	-2.069	$.039^{*}$
					T_{mr}	0.303	5.614	$.000^{***}$
					Va	-0.026	-1.217	.224
					Gender	-0.018	-.838	.402

					Age	0.014	0.658	.510
					Weight	0.031	1.471	.141
					Height	-0.016	-0.746	.456
					Clothing insulation	0.075	3.590	.000***
					Metabolism	0.013	0.569	.569
					UTCI	-0.057	-1.541	.124
2	(Constant)		-14.802	.000***	Sunlight level	0.373	13.813	.000***
	△UTCI	.626	31.689	.000***	Time	0.028	1.431	.153
	Wind level	-.298	-15.098	.000***	Emotion	-0.023	-1.173	.241
					Noise	-0.015	-0.774	.439
					T_{mr}	0.417	8.488	.000***
					Va	0.084	4.133	.000***
					Gender	-0.021	-1.073	.283
					Age	0.031	1.619	.106
					Weight	0.002	.087	.931
					Height	-0.011	-0.591	.555
					Clothing insulation	0.046	2.366	.018*
					Metabolism	0.041	1.899	.058
					UTCI	0.05	1.463	.144
3	(Constant)		-10.993	.000***	Time	0.019	1.032	.302
	△UTCI	.346	12.638	.000***	Emotion	-0.015	-0.837	.403
	Wind level	-.308	-16.785	.000***	Noise	-0.02	-1.109	.268
	Sunlight level	.373	13.813	.000***	T_{mr}	0.174	3.377	.001***
					Va	0.032	1.632	.103
					Gender	0.017	.924	.355
					Age	0.015	.819	.413
					Weight	-0.032	-1.780	.075
					Height	0.018	.982	.327
					Clothing insulation	0.003	.138	.891
					Metabolism	0.027	1.370	.171
					UTCI	0.113	3.512	.000***
4	(Constant)		-4.965	.000***	Time	0.019	1.087	.277
	△UTCI	.240	5.931	.000***	Emotion	-0.019	-1.066	.287
	Wind level	-.322	-17.227	.000***	Noise	-0.035	-1.922	.055
	Sunlight level	.386	14.229	.000***	T_{mr}	0.134	2.498	.013*
	UTCI	.113	3.512	.000***	Va	-0.009	-.369	.712
					Gender	0.022	1.236	.217
					Age	0.009	0.494	.621
					Weight	0.019	0.791	.429
					Height	0.018	1.024	.306
					Clothing insulation	0.045	2.149	.032*
					Metabolism	0.03	1.532	.126

*: $p < 0.05$; **: $p < 0.01$; ***: $p < 0.001$.

6.6.2 Predictors in TCV predicting models

According to the regression results in section 5.4, it is found that $\triangle PET_{xmin\text{-}I}$ (or $\triangle UTCI_{xmin\text{-}I}$) is a great indicator of TCV and the second-order relation is suitable for fitting TCV with $\triangle PET_{xmin\text{-}I}$ (or $\triangle UTCI_{xmin\text{-}I}$). Previously outdoor thermal comfort studies (Hwang & Lin, 2007; Lin & Matzarakis, 2008; Lin et al., 2010) had also demonstrated that a second-order relation is appropriate for correlating thermal comfort indices with occupants' thermal comfort and thermal acceptability. However, stepwise regression is essentially a linear regression model, thus it is necessary to modify the predictor if a second-order polynomial is adopted. In this case, four original predictors for TCV: PET, $\triangle PET_{xmin\text{-}I}$, UTCI and $\triangle UTCI_{xmin\text{-}I}$ was modified into a second-order form, which is expressed by Equation (6.1).

$$\textit{Modified predictor} = (\textit{Original predictor} - \textit{Neutral value})^2 \tag{6.1}$$

The modified predictors of the four potential predictors are (PET – Neutral value of PET)^2, ($\triangle PET_{xmin\text{-}I}$ – Neutral value of $\triangle PET_{xmin\text{-}I}$)^2, (UTCI – Neutral value of UTCI)^2 and ($\triangle UTCI_{xmin\text{-}I}$ – Neutral value of $\triangle UTCI_{xmin\text{-}I}$)^2, respectively. The neutral value denotes the value of the original predictor, in which respondents feel the most comfortable.

To find out the corresponding neutral value of each predictor, second-order polynomial regressions between TCV and the four original predictors were conducted and illustrated in Figure 6.1. Data used for fitting were acquired from the 10-min exposure experiments introduced in Chapter 5 (N=1182). The TCV was calculated in 1 K bin in each of the original predictors.

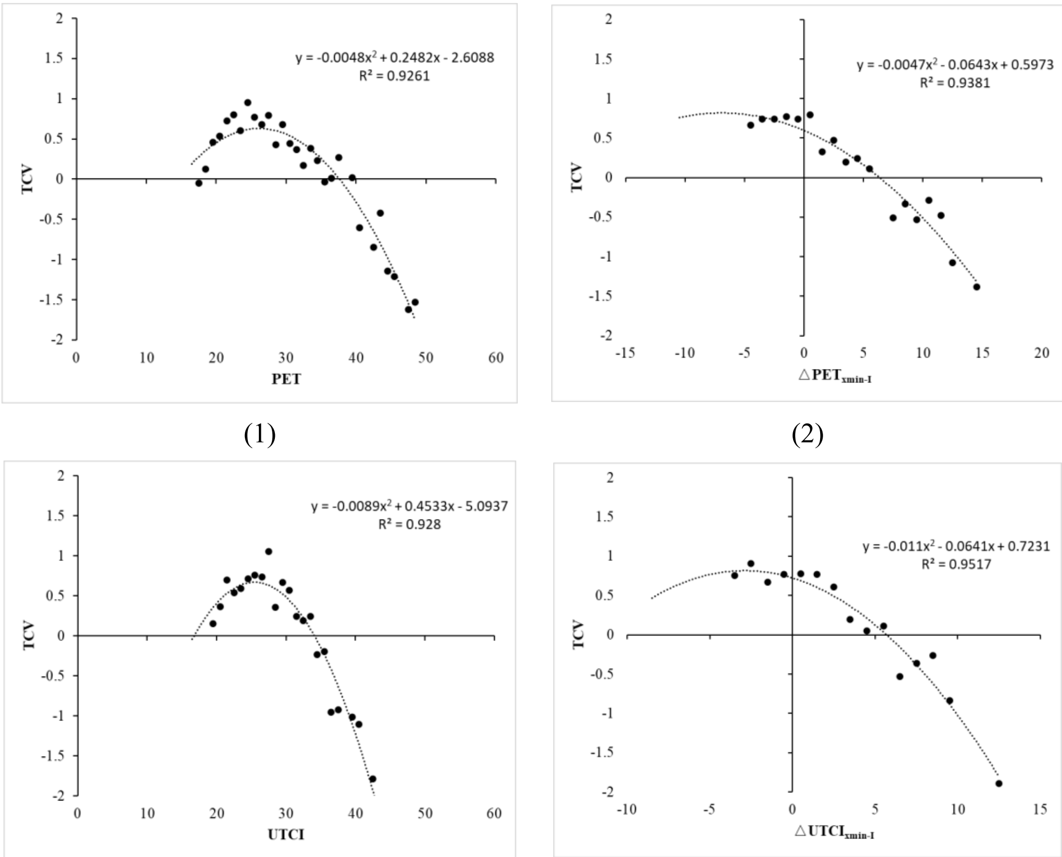

(1) (2)

(3) (4)

Figure 6.1 Second-order polynomial regressions between TCV and the four original predictors. (1) TCV v.s. PET; (2) TCV v.s. $\triangle PET_{xmin\text{-}I}$; (3) TCV v.s. UTCI; (4) TCV v.s. $\triangle UTCI_{xmin\text{-}I}$. Fitting data were obtained from the 10-min exposure experiments. N=1182 in each of the regressions.

It is clear that TCV fits well (R^2>0.9) with all of the four predictors in second-order polynomial regression, which is similar to the results in section 5.4. The neutral values of the corresponding predictors can be obtained by calculating the midpoints of the parabolas, which are 26.4°C for PET, -6.8K for $\triangle PET_{xmin\text{-}I}$, 25.5°C for UTCI and -2.9K for $\triangle UTCI_{xmin\text{-}I}$. Therefore, the modified predictors are $(PET - 26.4)^2$, $(\triangle PET_{xmin\text{-}I} + 6.8)^2$, $(UTCI - 25.5)^2$ and $(\triangle UTCI_{xmin\text{-}I} + 2.9)^2$, respectively.

Similar to the stepwise regressions in developing TSV predicting models, PET and UCTI were examined separately in the development of TCV predicting models. Illustrated in Table 6.3, When adopting $(PET-26.4)^2$ and $(\triangle PET+6.8)^2$ as predictors, four predictors: $(\triangle PET+6.8)^2$, sunlight level, $(PET-26.4)^2$ and wind level were finally included in the model in turn and none of these four selected predictors were removed by the model during the stepwise regression since the p-value of each selected predictors did not exceed 0.05. Among the four final predictors, sunlight level, $(PET-26.4)^2$ and wind level were all highly significant predictors of TCV ($p < 0.001$). The significant level of $(\triangle PET+6.8)^2$ is slightly lower but it is still a significant predictor of TCV ($p < 0.05$).

Other predictors (time, emotion, noise, T_{mr}, V_a, gender, weight, height, clothing insulation, metabolism) were not included in the model during the regression either since their p values in the t-test were above 0.01 or their p values were not the smallest among all predictors, suggesting these predictors have insignificant effects on TCV. Nevertheless, the stepwise regression that weight ($p = 0.046$) and metabolism ($p = 0.041$) is also marginally significant ($p < 0.05$) if included in the regression model.

Table 6.3 T-test results in stepwise regression process of TCV predicting models adopting $(PET-26.4)^2$ and $(\triangle PET+6.8)^2$ as predictors

	Predictors in the Model				**Predictors not in the Model**			
Model	Predictors	Beta	t	Sig.	Predictors	Beta	t	Sig.
1	(Constant)		28.936	.000***	Sunlight level	-0.217	-6.458	.000***
	$(\triangle PET+6.8)^2$	-.579	-24.408	.000***	Wind level	0.105	4.322	.000***

					Time	0.024	0.996	.320
					Emotion	0.019	.772	.440
					Noise	0.032	1.340	.180
					T_{mr}	-0.082	-1.326	.185
					Va	-0.008	-.349	.727
					Gender	0.013	.526	.599
					Age	0.014	0.607	.544
					Weight	0.041	1.719	.086
					Height	-0.002	-0.064	.949
					Clothing insulation	-0.005	-0.202	.840
					$(PET-26.4)^2$	-0.21	-4.999	.000***
					Metabolism	-0.06	-2.037	.042*
2	(Constant)		24.635	.000***	Wind level	0.115	4.814	.000***
	$(\triangle PET+6.8)^2$	-.423	-12.614	.000***	Time	0.029	1.243	.214
	Sunlight level	-.217	-6.458	.000***	Emotion	0.013	0.533	.594
					Noise	0.033	1.410	.159
					T_{mr}	0.155	2.199	.028*
					Va	0.023	.960	.337
					Gender	0.000	0.019	.985
					Age	0.022	0.939	.348
					Weight	0.068	2.877	.004**
					Height	-0.012	-0.516	.606
					Clothing insulation	0.017	0.719	.472
					$(PET-26.4)^2$	-0.293	-6.951	.000***
					Metabolism	-0.005	-0.150	.881
3	(Constant)		20.757	.000***	Wind level	0.108	4.612	.000***
	$(\triangle PET+6.8)^2$	-.139	-2.652	.008**	Time	0.032	1.403	.161
	Sunlight level	-.274	-8.083	.000***	Emotion	0.023	1.007	.314
	$(PET-26.4)^2$	-.293	-6.951	.000***	Noise	0.046	1.976	.048*
					T_{mr}	0.029	0.404	.686
					Va	0.03	1.271	.204
					Gender	-0.018	-.796	.426
					Age	0.038	1.665	.096
					Weight	0.032	1.314	.189
					Height	-0.018	-.803	.422
					Clothing insulation	0.000	.006	.995
					Metabolism	-0.054	-1.756	.079
4	(Constant)		21.234	.000***	Time	0.023	1.010	.313
	$(\triangle PET+6.8)^2$	-.114	-2.178	.030*	Emotion	0.019	0.821	.412
	Sunlight level	-.282	-8.370	.000***	Noise	0.034	1.489	.137
	$(PET-26.4)^2$	-.285	-6.808	.000***	T_{mr}	-0.045	-0.609	.543

	Wind level	.108	4.612	.000***	Va	-0.008	-.329	.742
					Gender	-0.016	-0.677	.499
					Age	0.031	1.371	.171
					Weight	0.048	2.001	.046*
					Height	-0.019	-.841	.400
					Clothing insulation	0.013	.547	.585
					Metabolism	-0.062	-2.041	.041*

*: p < 0.05; **: p < 0.01; ***: p < 0.001.

As shown in Table 6.4, it can be inferred that the stepwise regression adopting $(UTCI\text{-}25.5)^2$ and $(\triangle UTCI+2.9)^2$ as predictors shows similar results that adopting $(PET\text{-}26.4)^2$ and $(\triangle PET+6.8)^2$ as predictors. The final model also included four predictors: $(\triangle UTCI+2.9)^2$, $(UTCI\text{-}25.5)^2$, sunlight level and wind level. But the predictors' entry order is different from that adopting $(PET\text{-}26.4)^2$ and $(\triangle PET+6.8)^2$ as predictors. Three out of the four final predictors: $(UTCI\text{-}25.5)^2$, sunlight level and wind level were highly significant ($p < 0.001$) in predicting TCV. $(\triangle UTCI+2.9)^2$ was only the significant predictor ($p < 0.05$). It can also be found in the final model that noise ($p = 0.045$) is a marginally significant predictor ($p < 0.05$) if included in the regression model. Other predictors (time, emotion, noise, T_{mr}, V_a, gender, weight, height, clothing insulation, metabolism) were not included in the final model.

Table 6.4 T-test results in stepwise regression process of TCV predicting models adopting $(UTCI\text{-}25.5)^2$ and $(\triangle UTCI+2.9)^2$ as predictors

	Predictors in the Model				**Predictors not in the Model**			
Model	Predictors	Beta	t	Sig.	Predictors	Beta	t	Sig.
1	(Constant)		28.936	.000***	Sunlight level	-0.23	-6.746	.000***
	$(\triangle UTCI+2.9)^2$	-.579	-24.408	.000***	Wind level	0.112	4.580	.000***
					Time	0.026	1.077	.282
					Emotion	0.019	.771	.441
					Noise	0.02	0.844	.399

					Tmr	-0.171	-2.886	.004**
					Va	-0.015	-.630	.529
					Gender	0.026	1.071	.284
					Age	0.014	0.586	.558
					Weight	0.065	2.695	.007**
					Height	0.008	0.331	.741
					Clothing insulation	-0.003	-0.145	.885
					Metabolism	-0.06	-1.990	.047*
					(UTCI-25.5)^2	-0.276	-7.467	.000
	(Constant)		28.790	.000***	Sunlight level	-0.259	-7.775	.000***
	(△UTCI+2.9)^2	-.355	-9.614	.000***	Wind level	0.123	5.135	.000***
	(UTCI-25.5)^2	-.276	-7.467	.000***	Time	0.027	1.150	.250
					Emotion	0.03	1.259	.208
					Noise	0.05	2.111	.035*
					Tmr	-0.156	-2.689	.007**
2					Va	0.033	1.375	.170
					Gender	0.02	0.844	.399
					Age	0.032	1.338	.181
					Weight	-0.029	-1.063	.288
					Height	0.011	0.482	.630
					Clothing insulation	-0.073	-2.918	.004**
					Metabolism	-0.082	-2.769	.006**
	(Constant)		24.450	.000***	Wind level	0.135	5.782	.000***
	(△UTCI+2.9)^2	-.144	-3.202	.001**	Time	0.033	1.433	.152
	(UTCI-25.5)^2	-.305	-8.415	.000***	Emotion	0.025	1.069	.285
	Sunlight level	-.259	-7.775	.000***	Noise	0.058	2.499	.013*
					Tmr	0.079	1.219	.223
3					Va	0.085	3.487	.001***
					Gender	0.001	.037	.970
					Age	0.042	1.841	.066
					Weight	-0.011	-.401	.689
					Height	-0.004	-.163	.871
					Clothing insulation	-0.052	-2.110	.035*
					Metabolism	-0.022	-.738	.460
	(Constant)		25.187	.000***	Time	0.021	0.945	.345
	(△UTCI+2.9)^2	-.094	-2.065	.039*	Emotion	0.02	0.878	.380
	(UTCI-25.5)^2	-.318	-8.879	.000***	Noise	0.046	2.010	.045*
	Sunlight level	-.271	-8.227	.000***	Tmr	0.014	0.222	.824
4	Wind level	.135	5.782	.000***	Va	0.043	1.671	.095
					Gender	0.003	0.111	.912
					Age	0.035	1.541	.124
					Weight	0.004	0.134	.893
					Height	-0.005	-.237	.813

		Clothing insulation	-0.039	-1.601	.110
		Metabolism	-0.035	-1.168	.243

*: $p < 0.05$; **: $p < 0.01$; ***: $p < 0.001$.

The final predictors determined in the TCV predicting models are similar to those in the TSV predicting models. Sunlight level and wind level are selected by all of the TSV and TCV predicting models with a high significant level ($p < 0.001$). The modified predictors which were calculated by Equation (6.1) were all included in the final models, but the modified predictors $(\triangle PET+6.8)^2$ and $(\triangle UTCI+2.9)^2$ did not show a very high level of significance ($p < 0.05$) compared to the other selected predictors ($p < 0.001$). This is presumably because respondent TCV is asymmetrical between the cold weather side and the hot weather side. The regressions concerning TCV in Figure 6.1 mainly involved weather conditions on the right half of the parabolas. There is a lack of data in the cold weather conditions, which may lead to predicting errors on the left side of the parabolas if adopting second-order polynomials.

6.2 Determination of the impact coefficient of each predictor

Table 6.5 Summary of the predictor impact coefficients of TCV and TSV predicting models adopting 4 predictors.
(N=1183 in each regression.)

Model		Predictor	Coefficient	SE	R^2
1	TSV=f (PET, △PET, Wind level, Sunlight level)	PET	.039	.010	.624
		△PET	.045	.017	
		Sunlight level	.344	.025	
		Wind level	-.365	.021	
		(Constant)	-1.253	.265	
2	TSV=f (UTCI, △UTCI, Wind level, Sunlight level)	UTCI	.034	.010	.626
		△UTCI	.096	.016	
		Sunlight level	.345	.024	

		Wind level	-.367	.021	
		(Constant)	-1.259	.254	
3	TCV=f [(PET-26.4)^2, (△PET+6.8)^2, Wind level, Sunlight level]	(PET-26.4)^2	-.00261	.038	.394
		(△PET+6.8)^2	-.00094	.043	
		Sunlight level	-.160	.019	
		Wind level	.078	.017	
		(Constant)	.714	.034	
4	TCV=f [(UTCI-25.5)^2, (△UTCI+2.9)^2, Wind level, Sunlight level]	(UTCI-25.5)^2	-.00541	.061	.402
		(△UTCI+2.9)^2	-.00175	.085	
		Sunlight level	-.154	.019	
		Wind level	.098	.017	
		(Constant)	.758	.030	

Multiple linear regressions were conducted to determine the impact coefficients of each of the independent variables (the selected predictors) in the corresponding linear models, the result of which is summarized in Table 6.5. The multiple linear equations (Equation 6.2 – 6.5) for TSV and TCV prediction can be obtained. The TSV predicting models show better fitting quality (R^2 around 0.6) than the TCV predicting models (R^2 around 0.4). This may be due to the asymmetrical predicting errors explained in Section 6.6.2.

$$TSV=0.039PET+0.045\triangle PET_{xmin-1}+0.344SL-0.365WL-1.253 \quad (6.2)$$

$$TSV=0.034UTCI+0.096\triangle UTCI_{xmin-1}+0.345SL-0.367WL-1.259 \quad (6.3)$$

$$TCV=-0.00261(PET-26.4)^2-0.00094\ (\triangle PET_{xmin-1}+6.8)^2-0.16SL+0.078WL+0.714 \quad (6.4)$$

$$TCV=-0.00541(UTCI-25.5)^2-0.00175\ (\triangle UTCI_{xmin-1}+2.9)^2-0.154SL+0.098WL+0.758 \quad (6.5)$$

SL and WL denote sunlight level and wind level, respectively in Equation (6.2) – (6.5). It can be inferred from the corresponding impact coefficient in Equation (6.2) and Equation (6.3) that TSV is in positive relation with PET, △PET and sunlight level, while it is in negative relation with wind level. The opposite effects that sunlight level and wind level have on TSV suggest that in a city located in a subtropical climate, the higher sunlight level tends to make subjects feel hotter, while the higher wind level can make subjects feel cooler.

It can be seen from Equation (6.4) and (6.5) that all the impact coefficients of the second-order terms are negative, which suggests that subjects feel less comfortable if the thermal indices (PET, UTCI) or the indoor-outdoor thermal index differences (△PET, △UTCI) deviate from their neutral value (the corresponding index value when subjects have highest TCV). This also indicates that these second-order terms adopted can be reasonably related to TCV. It can also be observed that wind level and sunlight level are in opposite relations with TCV in both equations. The increase in wind level results in a higher level of thermal comfort, while the increase in sunlight level leads to a reduction in thermal comfort.

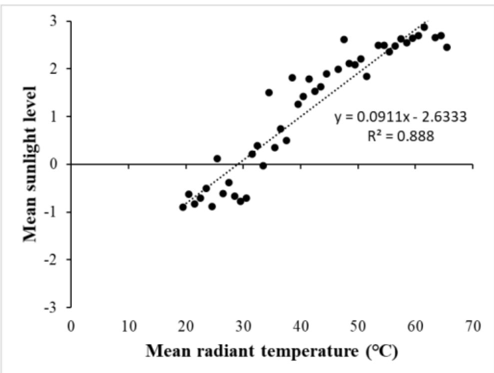

(1)

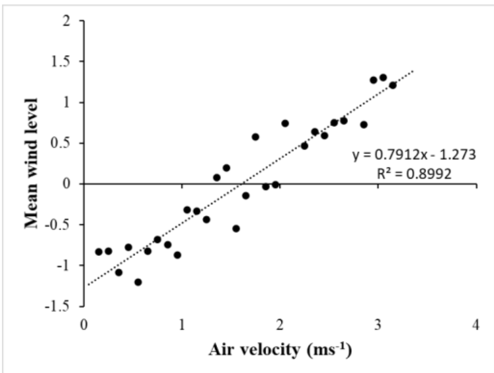

(2)

Figure 6.2 Linear regressions between mean sunlight (wind) level and mean radiant temperature (air velocity).

(1) mean sunlight level v.s. T_{mr}; (2) mean wind level v.s. V_a. Fitting data were obtained from the 10-min exposure experiments. N=1182 in each of the regressions.

The 4 equations obtained by multiple linear regressions include independent variables that can be directly calculated by objective parameters (PET, UTCI, △PET, △UTCI) and independent variables that cannot be calculated by objective parameters (sunlight level and wind level). Therefore, extra regressions were conducted to convert the subjective predictors, sunlight level and wind level, into objective predictors that can be measured or calculated. As illustrated in Figure 6.2, mean sunlight level is obtained by calculating the average sunlight level in 1 K mean radiant temperature difference bin, while mean wind level is obtained by calculating the average wind level in 0.1 ms^{-1} air velocity difference bin. The fitting data were acquired from the 10-min exposure experiments introduced in Chapter 5. The sample size is 1182. Both regressions show a high fitting quality (R^2 around 0.9), indicating strong linear relations between mean sunlight level and T_{mr} and between mean wind level and V_a.

The linear equation converting sunlight level and wind level into T_{mr} and V_a can thus be obtained and demonstrated in Equation (6.7) and (6.8), where SL denotes sunlight level and WL denotes wind level.

$$SL=0.0911T_{mr} - 2.6333 \tag{6.7}$$

$$WL=0.7912V_a - 1.273 \tag{6.8}$$

By combining Equation (6.2) – (6.8), the final TSV and TCV predicting models during short-term outdoor exposure can be obtained and illustrated in Equation (6.9) – (6.12), where PET, UTCI, $\triangle PET_{xmin-I}$, $\triangle UTCI_{xmin-I}$, T_{mr} and V_a are expressed in °C, °C, K, K, °C and ms^{-1}, respectively.

$$TSV=0.039PET+0.045\triangle PET_{xmin-I}+0.0313T_{mr}-0.289V_a-1.69 \quad (6.9)$$

$$TSV=0.034UTCI+0.096\triangle UTCI_{xmin-I}+0.0314T_{mr}-0.29V_a-1.7 \quad (6.10)$$

$$TCV=-0.00261(PET-26.4)^2-0.00094\ (\triangle PET_{xmin-I}+6.8)^2-0.0146T_{mr}+0.0617V_a+0.82 \quad (6.11)$$

$$TCV=-0.00541(UTCI-25.5)^2-0.00175\ (\triangle UTCI_{xmin-I}+2.9)^2-0.014T_{mr}+0.0775V_a+1.039 \quad (6.12)$$

6.3 Model verification with extra field experimental data in the 0-min, 5-min, 10-min and 15-min outdoor exposure

A series of extra on-site thermal comfort experiments were conducted in contrast to verify the TSV and TCV predicting models obtained in Section 6.2. The experiments were conducted during Jul-2018 and Dec-2018 on 12 different days. The research subjects were asked to experience 3 different outdoor sites in a university campus in Hong Kong in turn, filling in questionnaires to record their TSV and TCV at the 0^{th}, 5^{th}, 10^{th} and 15^{th} minute of exposure in each of the 3 sites. 61 subjects participated in the experiments and 244 copies of questionnaires were collected.

6.6.1 Verification on the accuracy of model prediction

Predicting TSV and TCV obtained from the four predicting models adopted 4 predictors expressed in Equation (6.9) – (6.12) was compared with actual TSV and TCV from the extra experimental data. Data from experiments in the 0^{th} minute, 5^{h}

minute, 10th minute and 15th minute were analyzed separately. It is assumed that the TSV (TCV) prediction is correct if the predicting TSV (TCV) is within actual TSV (TCV) ±1 (±0.67). Verifications of TSV prediction accuracy are illustrated in Figure 6.3 and 6.4 and verifications of TCV prediction accuracy are illustrated in Figure 6.5 and 6.6.

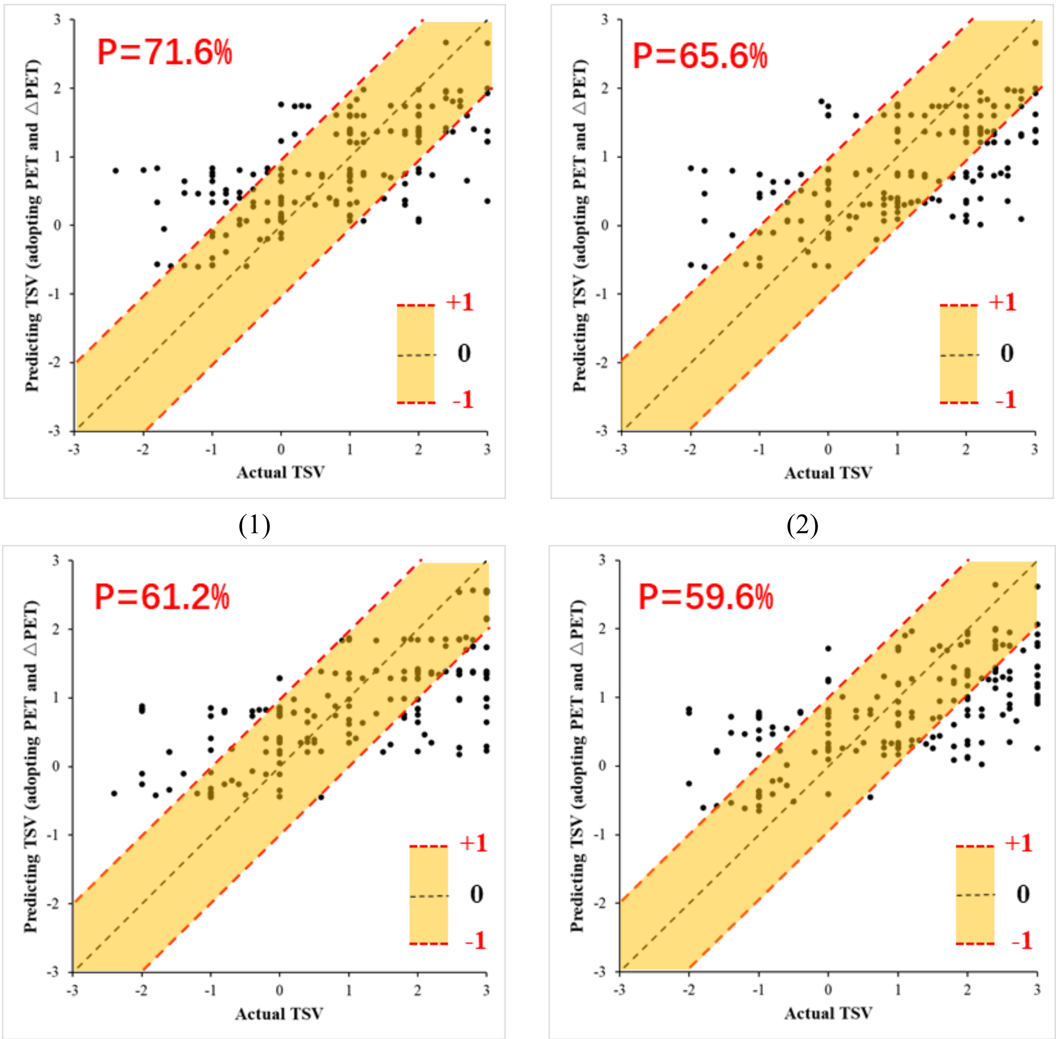

(1) (2)

(3) (4)

Figure 6.3 Verification on TSV prediction accuracy adopting the model (model 1 in Table 6.5) that includes PET, △PET, T_{mr} and V_a as predictors.

Subject's actual TSV was shown on x-axis and the model predicting TSV was shown on y-axis. The black dashed line denotes the coordinates in which predicting TSV = Actual TSV. The red dashed lines denote black dashed line ±1 in ordinate and the orange area between the two red dashed lines denote the area in which the prediction is correct. P stands for the percentage of correct predictions among all predictions. Data acquired at different time of outdoor exposure

were verified separately. N=183 in each of the verifications.
(1) 0th minute; (2) 5th minute; (3) 10th minute; (4) 15th minute.

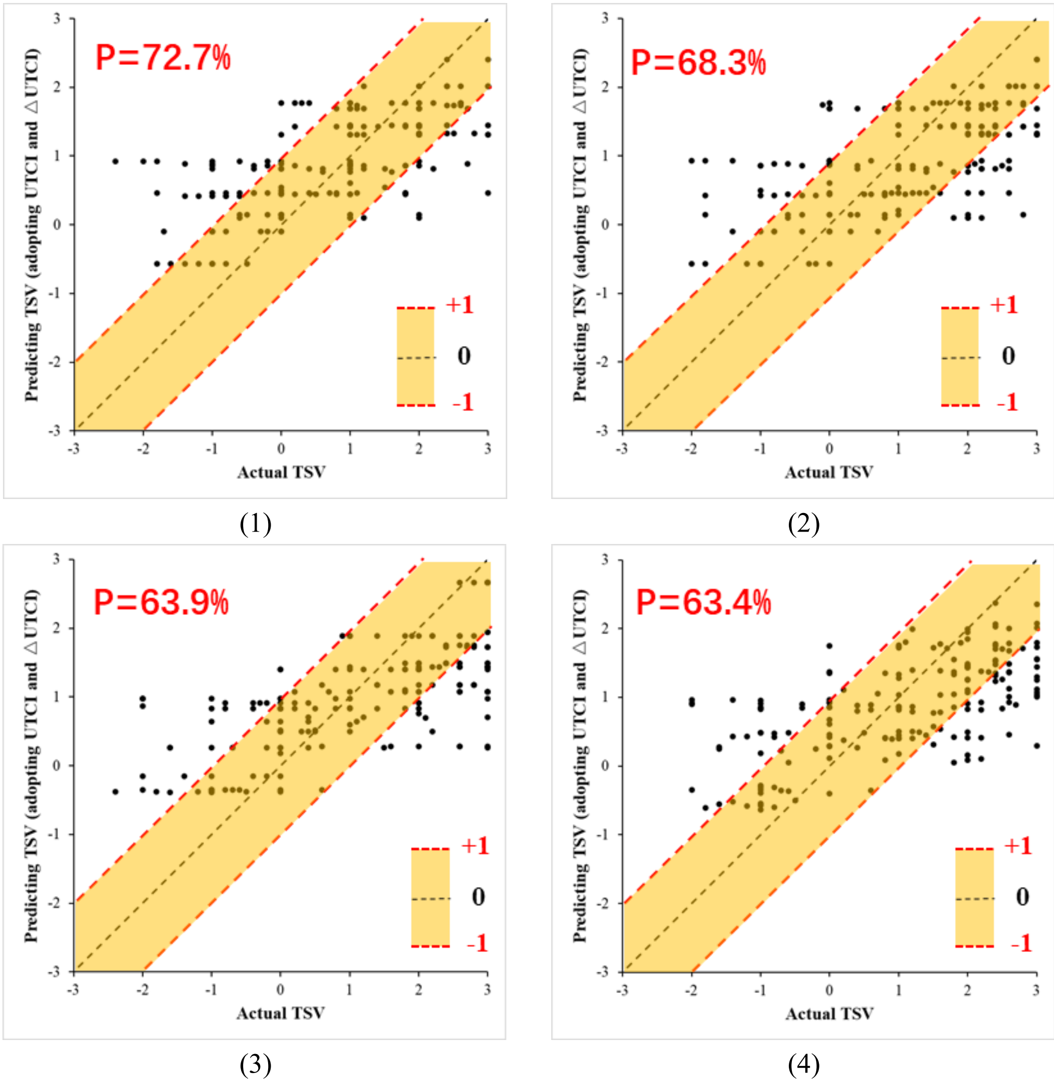

Figure 6.4 Verification on TSV prediction accuracy adopting the model (model 2 in Table 6.5) that includes UTCI, △UTCI, T_{mr} and V_a as predictors.
Subject's actual TSV was shown on x-axis and the model predicting TSV was shown on y-axis. The black dashed line denotes the coordinates in which predicting TSV = Actual TSV. The red dashed lines denote black dashed line ±1 in ordinate and the orange area between the two red dashed lines denote the area in which the prediction is correct. P stands for the percentage of correct predictions among all predictions. Data acquired at different time of outdoor exposure were verified separately. N=183 in each of the verifications.
(1) 0th minute; (2) 5th minute; (3) 10th minute; (4) 15th minute.

The TSV predictions made by the model adopting four predictors (model 1 and model 2 in Table 6.5) show an acceptable percentage of correct prediction (59.6%~72.7%).

Model 2 that adopts UTCI, △UTCI, T_{mr} and V_a as predictors is slightly better than model 1 that adopts PET, △PET, T_{mr} and V_a in terms of TSV predicting accuracy since the percentage of correct predictions from model 2 are 1%~4% higher than those from model 1. In both model 1 and model 2, the prediction accuracy decreases as the outdoor exposure time increases. Verifications in the 15^{th} minute of exposure show the lowest prediction accuracy. This is presumably since the predicting models were developed according to the data collected during the 10-minute exposure. TSV calculated by the models may not be quite suitable for the predictions of respondent TSV in outdoor exposure that is over 15 minutes.

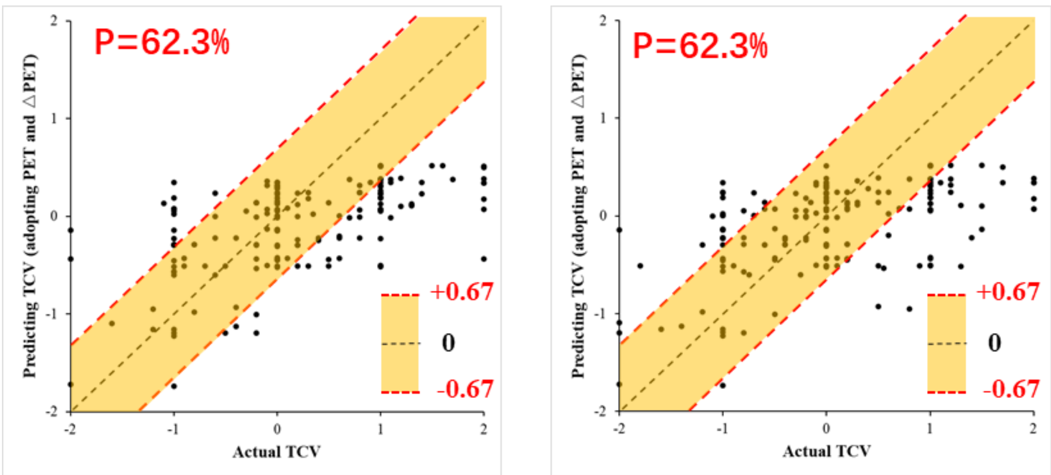

(1) (2)

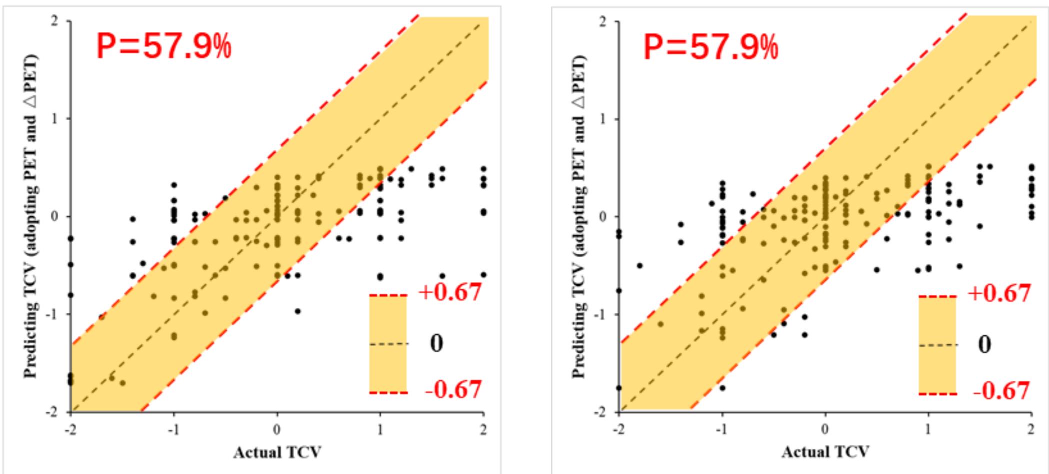

(3) (4)

Figure 6.5 Verification on TCV prediction accuracy adopting the model (model 3 in Table 6.5) that includes PET, △PET, T_{mr} and V_a as predictors.

Subject's actual TCV was shown on x-axis and the model predicting TCV was shown on y-axis. The black dashed line denotes the coordinates in which predicting TCV = Actual TCV. The red dashed lines denote black dashed line ±0.67 in ordinate and the orange area between the two red dashed lines denote the area in which the prediction is correct. P stands for the percentage of correct predictions among all predictions. Data acquired at different time of outdoor exposure were verified separately. N=183 in each of the verifications.

(1) 0^{th} minute; (2) 5^{th} minute; (3) 10^{th} minute; (4) 15^{th} minute.

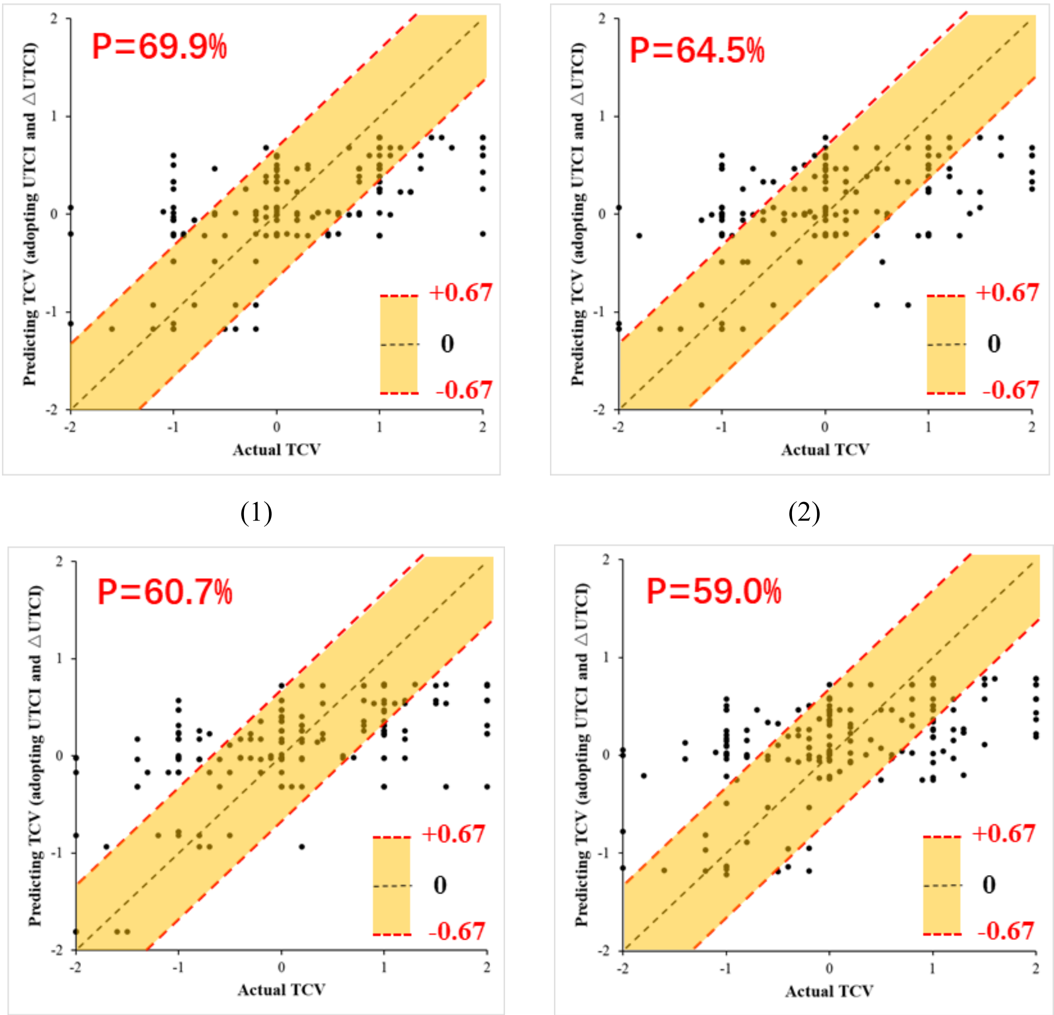

(1) (2)

(3) (4)

Figure 6.6 Verification on TCV prediction accuracy adopting the model (model 4 in Table 6.5) that includes UTCI, △UTCI, T_{mr} and V_a as predictors.

Subject's actual TCV was shown on x-axis and the model predicting TCV was shown on y-axis. The black dashed line denotes the coordinates in which predicting TCV = Actual TCV. The red dashed lines denote black dashed line ±0.67 in ordinate and the orange area between the two red dashed lines denote the area in which the prediction is correct. P stands for the percentage of correct predictions among all predictions. Data acquired at different time of outdoor exposure

were verified separately. N=183 in each of the verifications.
(1) 0^{th} minute; (2) 5^{th} minute; (3) 10^{th} minute; (4) 15^{th} minute.

The TCV predictions made by the model adopting four predictors (model 3 and model 4 in Table 6.5) also show an acceptable percentage of correct prediction (57.9%~69.9%). Similar to TSV predicting models, model 4 that adopts UTCI, △UTCI, T_{mr} and V_a as predictors is slightly better than model 3 that adopts PET, △PET, T_{mr} and V_a in terms of TCV predicting accuracy. The percentage of correct predictions from model 4 are 1%~7% higher than those from model 3 and verifications in the 15^{th} minute of exposure also show the lowest prediction accuracy.

In general, TSV predicting accuracy is slightly higher (1%~9%) than TCV predicting accuracy. Both TSV and TCV predicting models are highly accurate if the actual TSV or TCV is around 0. The high values of actual TSV or TCV lead to underestimations of predicting TSV or TCV, while the low values of actual TSV or TCV lead to overestimations of predicting TSV or TCV.

6.6.2 Verification on the model improvement when including extra predictors

The above-mentioned models adopting 4 predictors (model 1-4 in Table 6.5) are compared with the models that only adopt 1 predictor (either PET or UTCI) in terms of predicting accuracy to verify whether the inclusion of the 3 extra predictors can improve the model regression quality and the predicting accuracy. Regression results of the models that adopt 1 predictor each were summarized in Table 6.6. Data used to develop these models were the same as the data used for developing model 1 to model 4. the equations of the 1-predictor models were illustrated in Equation (6.13) – (6.16)

Table 6.6 Summary of the predictor impact coefficients of TCV and TSV predicting models adopting 1 predictor.
(N=1183 in each regression.)

Model		Predictor	Coefficient	SE	R^2
5	TSV=f (PET)	PET	0.131	.005	.406
		(Constant)	-3.440	.136	
6	TSV=f (UTCI)	UTCI	0.163	.007	.300
		(Constant)	-4.453	.215	
7	TCV=f [$(PET-26.4)^2$]	$(PET-26.4)^2$	-0.00499	.022	.298
		(Constant)	.635	.025	
8	TCV=f [$(UTCI-25.5)^2$]	$(UTCI-25.5)^2$	-0.00936	.041	.302
		(Constant)	.712	.027	

$$TSV=0.131PET-3.44 \tag{6.13}$$

$$TSV=0.163UTCI-4.453 \tag{6.14}$$

$$TCV=-0.00499(PET-26.4)^2+0.635 \tag{6.15}$$

$$TCV=-0.00936(UTCI-25.5)^2 +0.712 \tag{6.16}$$

By comparing the 1-predictor models in Table 6.6 with the 4-predictor models in Table 6.5, it is clear that the regression R^2 values in the 4-predictor models are higher than those in the 1-predictor models. R^2 values in model 3 and 4 (4-predictor models for TCV prediction) are 0.1 higher than in model 7 and 8 (1-predictor models for TCV prediction), while R^2 values in model 1 and 2 (4-predictor models for TSV prediction) are 0.2~0.3 higher than in model 5 and 6 (1-predictor models for TSV prediction). It can be inferred that the inclusion of the 3 extra predictors (△PET or △UTCI, sunlight level, wind level) obviously improves the regression quality, especially in TSV predictions.

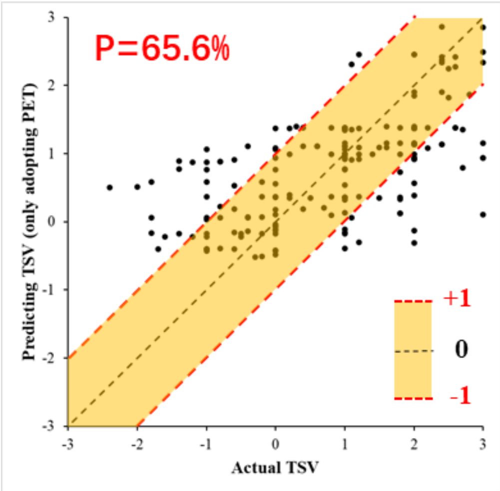

(1)

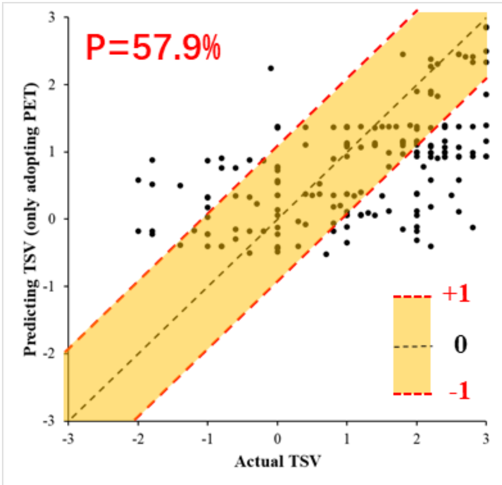

(2)

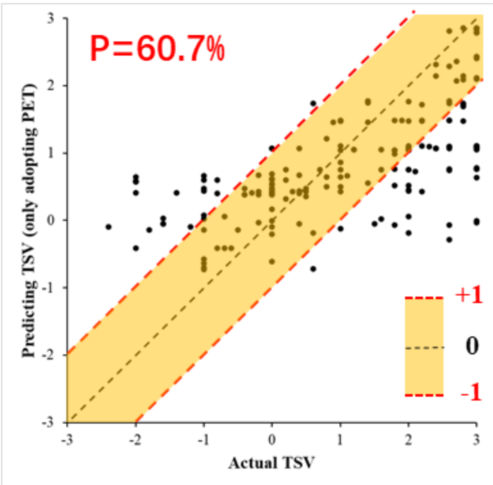

(3)

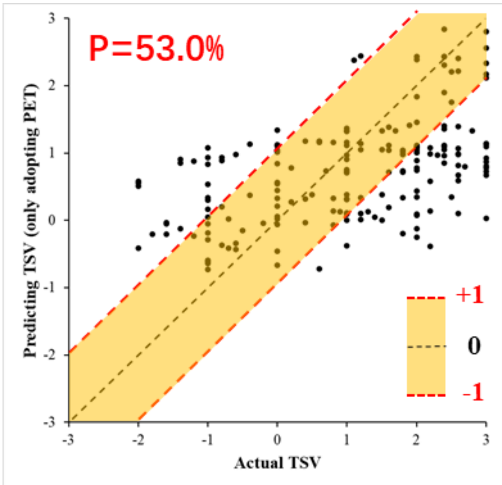

(4)

Figure 6.7 Verification on TSV prediction accuracy adopting the model (model 5 in Table 6.6) that includes only PET as predictor.

Subject's actual TSV was shown on x-axis and the model predicting TSV was shown on y-axis. The black dashed line denotes the coordinates in which predicting TSV = Actual TSV. The red dashed lines denote black dashed line ±1 in ordinate and the orange area between the two red dashed lines denote the area in which the prediction is correct. P stands for the percentage of correct predictions among all predictions. Data acquired at different time of outdoor exposure were verified separately. N=183 in each of the verifications.

(1) 0^{th} minute; (2) 5^{th} minute; (3) 10^{th} minute; (4) 15^{th} minute.

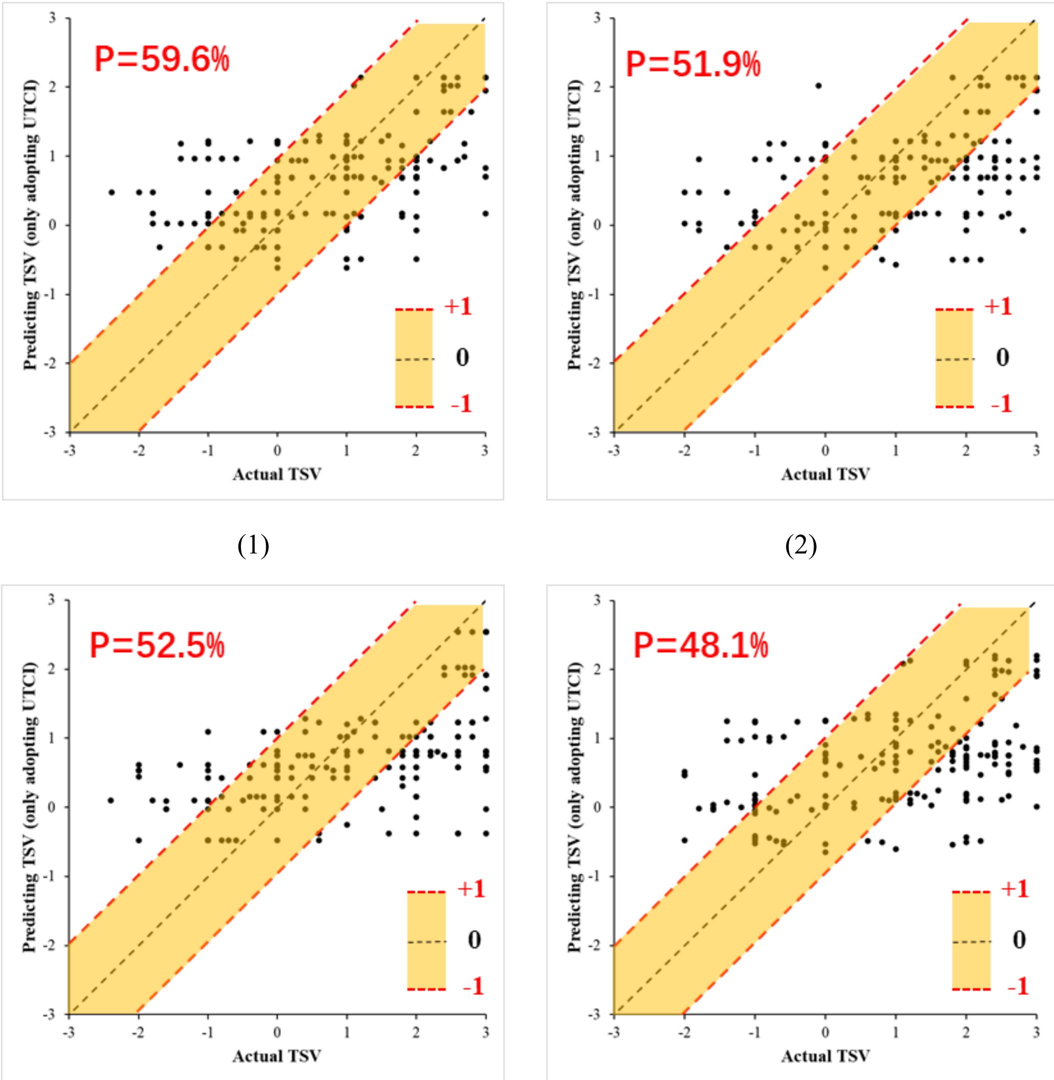

(1) (2) (3) (4)

Figure 6.8 Verification on TSV prediction accuracy adopting the model (model 6 in Table 6.6) that includes only UTCI as predictor.

Subject's actual TSV was shown on x-axis and the model predicting TSV was shown on y-axis. The black dashed line denotes the coordinates in which predicting TSV = Actual TSV. The red dashed lines denote black dashed line ±1 in ordinate and the orange area between the two red dashed lines denote the area in which the prediction is correct. P stands for the percentage of correct predictions among all predictions. Data acquired at different time of outdoor exposure were verified separately. N=183 in each of the verifications.

(1) 0^{th} minute; (2) 5^{th} minute; (3) 10^{th} minute; (4) 15^{th} minute.

As illustrated in Figure 6.7 and 6.8, the TSV predictions made by model adopting one predictor (model 5 and model 6 in Table 6.6) show a normal percentage of correct prediction (48.1%~65.6%). The 1-predictor model 5 and model 6 are lower in predicting accuracy compared to the 4-predictor model 1 and 2. Model 5 shows a 5.2% of accuracy drop in average compared to model 1. The accuracy differences between model 6 and model 2 are up to 16.4% (14.1% on average). This suggests that the inclusion of the 3 extra predictors increases the predicting accuracy when predicting TSV.

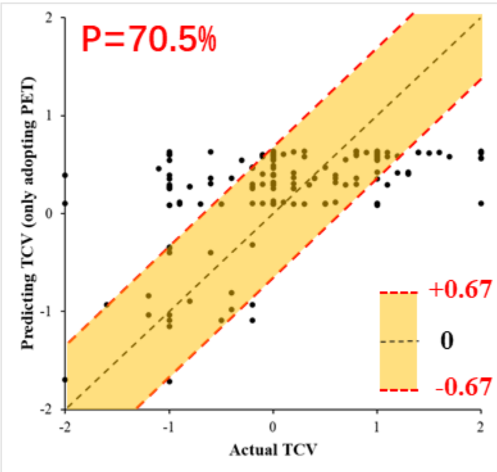

(1)

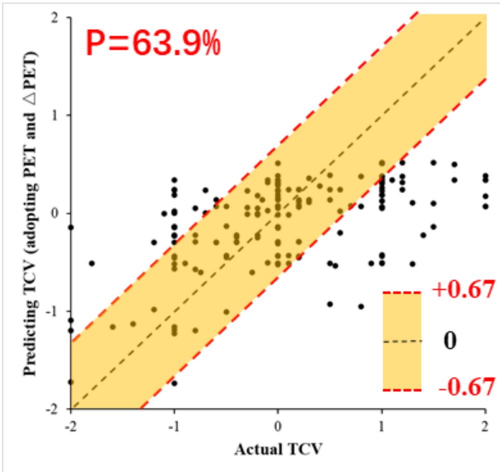

(2)

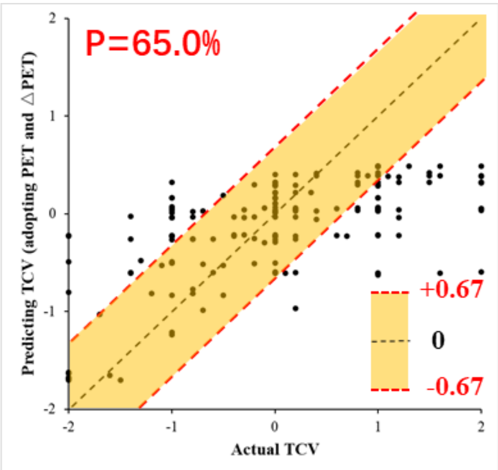

(3)

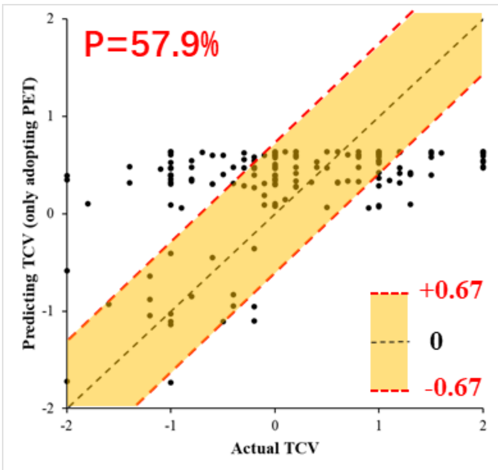

(4)

Figure 6.9 Verification on TCV prediction accuracy adopting the model (model 7 in Table 6.6) that includes only PET as predictor.

Subject's actual TCV was shown on x-axis and the model predicting TCV was shown on y-axis. The black dashed line denotes the coordinates in which predicting TCV = Actual TCV. The red dashed lines denote black dashed line ±0.67 in ordinate and the orange area between the two red dashed lines denote the area in which the prediction is correct. P stands for the percentage of correct predictions among all predictions. Data acquired at different time of outdoor exposure

were verified separately. N=183 in each of the verifications.
(1) 0^{th} minute; (2) 5^{th} minute; (3) 10^{th} minute; (4) 15^{th} minute.

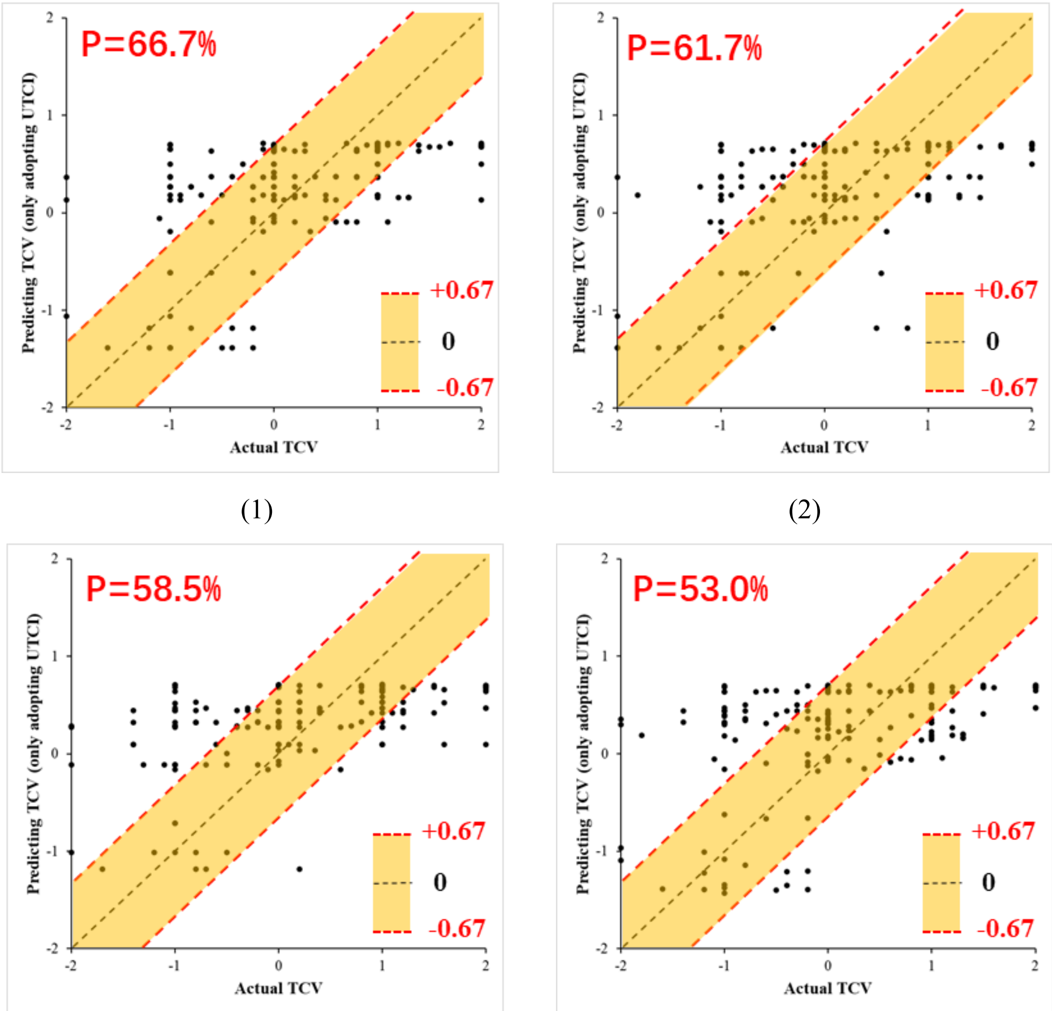

(1) (2)

(3) (4)

Figure 6.10 Verification on TCV prediction accuracy adopting the model (model 8 in Table 6.6) that includes only UTCI as predictor.
Subject's actual TCV was shown on x-axis and the model predicting TCV was shown on y-axis. The black dashed line denotes the coordinates in which predicting TCV = Actual TCV. The red dashed lines denote black dashed line ±0.67 in ordinate and the orange area between the two red dashed lines denote the area in which the prediction is correct. P stands for the percentage of correct predictions among all predictions. Data acquired at different time of outdoor exposure were verified separately. N=183 in each of the verifications.
(1) 0^{th} minute; (2) 5^{th} minute; (3) 10^{th} minute; (4) 15^{th} minute.

The TCV predictions made by the model adopting four predictors (model 7 and model 8 in Table 6.5) show an acceptable percentage of correct prediction (53.0%~70.5%).

The 1-predictor model 8 shows worse accuracy in TCV prediction compared to the 4-predictor model 4, with an accuracy drop of 3.6% on average. However, the 1-predictor model 7 shows better accuracy in TCV prediction compared to the 4-predictor model 3, with an accuracy increase of 4.2%. It can be inferred that in the TCV predictions, the 4-predictor models are not always better than the 1-predictor models in terms of predicting accuracy. When adopting UTCI as a predictor, the predicting accuracy of the 1-predictor model is worse than the 4-predictor model. But when adopting PET as a predictor, the result is the opposite.

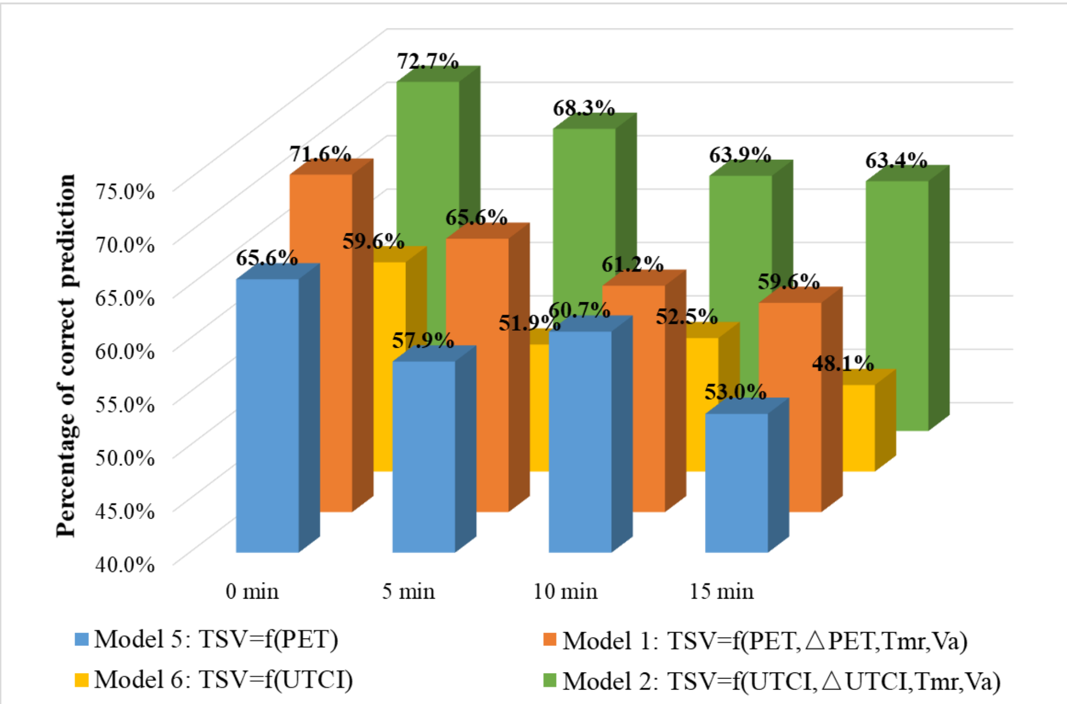

Figure 6.11 Overall comparison in TSV predicting accuracy between the 1-predictor models (model 5 and model 6) and the 4-predictor models (model 1 and model 2).

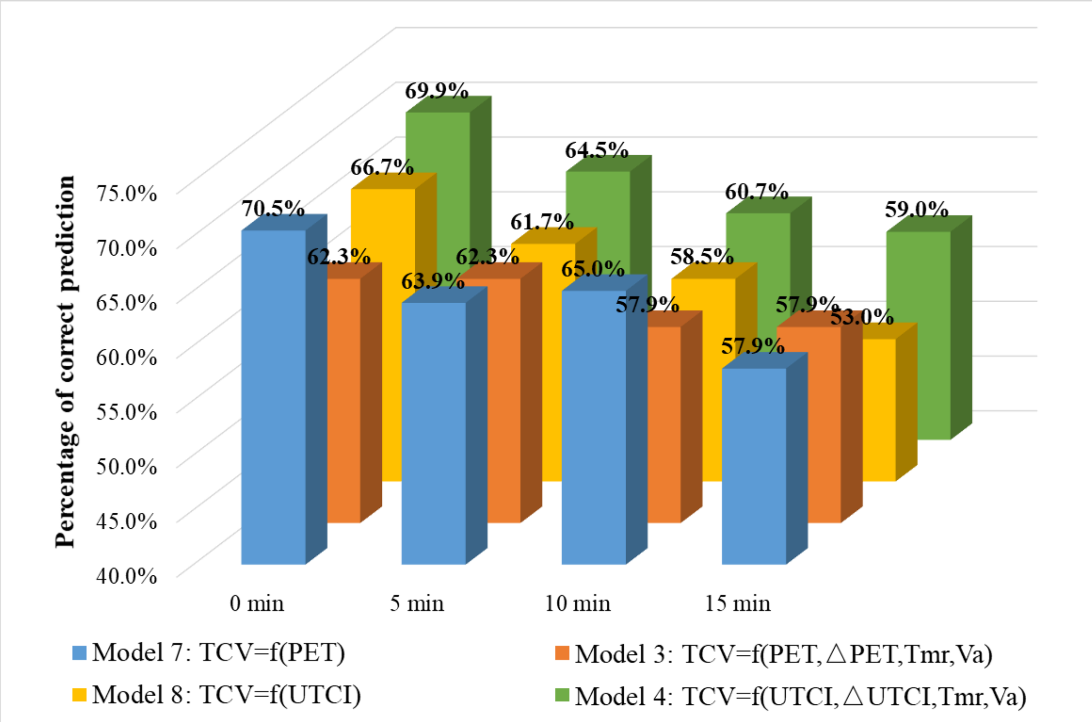

Figure 6.12 Overall comparison in TCV predicting accuracy between the 1-predictor models (model 7 and model 8) and the 4-predictor models (model 3 and model 4).

The overall comparisons in terms of TSV and TCV predicting accuracy between the 1-predictor models and the 4-predictor models are demonstrated in Figure 6.11 and 6.12. To summarize, the 4-perdictor models have better predicting accuracy in TSV prediction than the 1-predictor model. However, the inclusion of the three extra predictors does not always improve the model predicting accuracy in TCV prediction.

6.4 Summary

This chapter illustrates the development process of TSV and TCV predicting models during short-term outdoor exposure. Verifications on the model predicting accuracy and the model improvement in terms of fitting quality and predicting accuracy by including three extra predictors are also conducted. The results can be summarized as follows:

(1) According to the stepwise regression in which entry significant level is 0.01 and removal significant level is 0.05, 4 predictors are finally selected out of 15 potential predictors in each of the TSV and TCV predicting models includes. The predictors include PET (or UTCI), $\triangle PET_{xmin\text{-}I}$ (or $\triangle UTCI_{xmin\text{-}I}$), sunlight level and wind level.

(2) Respondents' subjective sunlight level and wind level were correlated with mean radiant temperature and wind velocity, respectively, to convert all the independent variables in the models into measurable parameters. Thus, the TSV and TCV predicting models finally include 4 measurable predictors: PET (or UTCI), $\triangle PET_{xmin\text{-}I}$ (or $\triangle UTCI_{xmin\text{-}I}$), mean radiant temperature and wind velocity.

(3) The impact coefficients of each predictor in the TSV and TCV predicting models were determined by multiple linear regression. Combined with the converting equations between sunlight level (wind level) and mean radiant temperature (wind velocity), the equations of TSV and TCV predicting models were obtained.

(4) The 4-predictor TSV and TCV predicting models show an acceptable predicting accuracy of 57.9%~72.7%. The prediction accuracy decreases as the outdoor exposure time increases and the predicting accuracies in the 15^{th} minute of exposure are the lowest. The TSV predicting accuracies are generally higher (1.7%~9.3%, 4.0% on average) than TCV. The predicting model adopting UTCI and △UTCI as predictors shows better accuracy than the predicting models adopting PET and △PET as predictors in both TSV (1.1%~3.8%, 2.6% in average) and TCV (1.1%~7.6%, 3.4% in average) predictions.

(5) The 4-predictor models show better fitting quality than the 1-predictor model. The 4-predictor models also have better predicting accuracy (5.2% or 14.1% higher) in TSV prediction than the 1-predictor model. However, the inclusion of the three extra predictors does not always improve the model predicting accuracy (3.6% higher or 4.2% lower) in TCV prediction.

Chapter 7 Conclusions and suggestions for future work

7.1 Summary of the main contributions

This thesis performs comprehensive investigations on the urban residents' outdoor thermal perceptions and thermal comfort during the short-term exposure in different outdoor sites in the hot subtropical climate across all seasons. Models for predicting subjects' thermal sensation and thermal comfort during the transitional outdoor exposure are presented and verified. The main contributions are summarized as follows.

(1) Field measurements and subject questionnaire surveys in both 10-min and 15-min exposure are conducted, which demonstrates the major differences in meteorological parameters between the underneath elevated building sites and the sunlit sites, among which solar irradiance and wind velocity showed the most significant differences. This serves as a shred of strong evidence that the lift-up design provides significant wind amplification and shadings to the occupants.

(2) TSV and TCV distribution comparisons were established with Ridit and ANOVA analyses, indicating significant differences in occupants' TSV and TCV values between the lift-up shaded areas and the sunlit areas. It is proven that in the underneath elevated building areas, subjects have significantly

cooler and more comfortable perceptions in hot conditions, without extra uncomfortable responses in cold weather conditions. It is recommended that such lift-up design be adopted in urban building design to enhance local microclimate and improve residents' thermal comfort in the outdoor exposure.

(3) All-season linear regressions between MTSV and PET/UTCI are obtained according to the data acquired from field studies conducted in the underneath elevated building shaded areas and the sunlit open areas in Hong Kong. MTSV is found to be in good linear relationship with the two selected thermal comfort indices, but extra considerations on the factors affecting human's expectations on neutral states should be taken into account for thermal comfort assessing indices to present better predictions of subjects' thermal perceptions.

(4) Correlations between TSV/TCV/TAV and outdoor-indoor PET difference were performed, results of which suggesting that outdoor-indoor environmental difference is a great indicator of respondent thermal perceptions during the transitional short-term outdoor exposure. Among the correlations from different periods of outdoor exposure, the fitting curves at the 10^{th} minute of exposure are in the highest regression qualities.

(5) Multiple-predictor models for the predictions of TSV and TCV are developed. It is found that 4 predictors out of 15 potential predictors are significant predictors of TCV and TSV during the 10-min transitional outdoor exposure. The TSV and TCV predicting models including 4 predictors: PET (or UTCI), $\triangle PET_{xmin-I}$ (or $\triangle UTCI_{xmin-I}$), mean radiant temperature and wind velocity

available for the thermal perception prediction during the transitional short-term outdoor exposure are developed.

(6) The 4-predictor TSV and TCV predicting models are verified with data acquired from extra field experiments. The models perform acceptable predicting accuracies of 57.9%~72.7%. The predicting model adopting UTCI and △UTCI as predictors shows better accuracy than the predicting models adopting PET and △PET as predictors in both TSV and TCV predictions. The models that adopted UTCI and △UTCI as predictors have a better predicting performance in general.

(7) The 4-predictor models are found to improve the fitting quality and predicting accuracy compared with the 1-predictor models in most cases. However, the inclusion of the three extra predictors does not always improve the model predicting accuracy in TCV prediction. In general, the 4-predictor models are recommended as a predicting tool of occupants' thermal perceptions during the transitional outdoor exposure.

The study provides abundant experimental data concerning human transient state thermal perceptions in the outdoor areas in the hot and humid subtropical climate. The output of the research can be used to predict subjective thermal perceptions during short-term outdoor exposure in any combinations of environmental parameters and personal details in the subtropical regions. It is also helpful in the development of advanced design tools concerning urban outdoor microclimate, which is believed to be beneficial for developers, city planners and the government in designing a more comfortable and livable urban environment.

7.2 Summary of the conclusions

7.2.1 Thermal perceptions after 15-min outdoor exposure

This study performs simultaneous field monitoring on meteorological parameters and subject questionnaire surveys of 1,107 research subjects in a university campus located in Hong Kong. A comprehensive investigation of subjects' TSV and TCV conditions in underneath elevated building shaded areas in contrast with the sunlit open areas after the 15-min outdoor exposure was performed. Outdoor thermal comfort assessing indices PET, UTCI were compared in terms of correlations with subjects' MTSV to examine the predicting availability of the selected thermal comfort assessing indices in the assessed outdoor conditions. The main findings are summarized as follows:

a) The underneath-elevated-building shaded sites and open sunlit sites are distinct mainly in solar irradiance and wind conditions.
b) The shaded areas are significantly more comfortable in hot weather, compared with the open sunlit areas. In winter, both areas are equally comfortable.
c) PET and UTCI are in great linear relations with MTSV, but additional considerations of other factors that affect subjects' thermal perceptions need to be covered to improve the predicting accuracies.

7.2.2 Thermal comfort assessment during 10-min outdoor exposure

This study demonstrates the assessment of subjects' thermal sensation, thermal comfort and thermal acceptability during a 10-minute outdoor exposure transferred from an air-conditioned indoor condition. The experimental sites were all pedestrian-level locations on a university campus in Hong Kong, where students frequently transfer from the building indoor area to the outer spaces of the buildings. Two typical outdoor locations with different building geometries, the sunlit sites and the "lift-up" shaded sites, were compared according to seasons and exposure time. The occupants' thermal perceptions were correlated with PET and UTCI differences between outdoor and indoor environments to discover the relations between outdoor-indoor environmental differences and subjective TSV, TCV and TAV in the transitional short-term outdoor exposure. The main findings are summarized as follows:

a) In winter, the lift-up shaded areas are in the same level of thermal perceptions compared with the sunlit areas, while the thermal perceptions in lift-up shaded areas are significantly better in summer.
b) A strong linear relationship is observed between TSV and PET/UTCI difference between the outdoor area and the indoor area, while second-order regression is suitable for the regression of TCV and TAV.
c) The calculated △UTCI ranges are narrower than △PET, except for which △PET and △UTCI regression lines are almost the same.

7.2.3 Development of TSV and TCV predicting models

This study illustrates the development process of TSV and TCV predicting models during short-term outdoor exposure by means of stepwise regression and multiple linear regression. 4 out of 15 predictors are recognized as significant independent variables to calculate TSV or TCV and they are selected as the predictors of each predicting models. Verifications on the model predicting accuracy and the model improvement in terms of fitting quality and predicting accuracy by including three extra predictors are also conducted. The main findings are summarized as follows:

a) 4 predictors including PET (or UTCI), $\triangle PET_{xmin-I}$ (or $\triangle UTCI_{xmin-I}$), sunlight level and wind level are selected out of 15 potential predictors by the stepwise regression in each of the TSV and TCV predicting models. Sunlight level and wind level are converted into mean radiant temperature and wind velocity, respectively and the final TSV and TCV predicting models that include 4 measurable predictors: PET (or UTCI), $\triangle PET_{xmin-I}$ (or $\triangle UTCI_{xmin-I}$) are obtained by multiple linear regression.
b) The 4-predictor TSV and TCV predicting models show an acceptable predicting accuracy of 57.9%~72.7%. The predicting model adopting UTCI and △UTCI as predictors shows better accuracy than the predicting models adopting PET and △PET as predictors.
c) In general, the 4-predictor models show better fitting quality and accuracy than the 1-predictor models, except the TCV predicting model, where the 4-predictor model adopting PET and △PET show lower predicting accuracy compared with that

adopting UTCI and △UTCI.

7.3 Suggestions for future work

The studies established so far are still limited in various aspects. It is recommended that supplemental research in the corresponding aspects be conducted in the future. The suggested future work is illustrated as follows:

i. Most of the research subjects who participated in the field experiments are young students. Only a small portion (about 10%) of the research subjects consists of middle-aged and elder people. The predicting models developed according to field experimental data may thus be inappropriate for the thermal perception prediction of middle-aged and elder people. It is recommended that research subjects with a wider age range be surveyed to establish widely applicable thermal perception predicting models.

ii. The logging internal of the questionnaire surveys was 5 minutes, which was too long to be not able to describe the variations of thermal perceptions due to the thermal effects during the transient process. Therefore, it is recommended that a shorter interval (1-2min) of the questionnaire survey be applied in the field experiments for a better evaluation of thermal perception variations during the transitional short-term exposure.

iii. Except for the regular thermal perception indicator TSV, TCV and TAV, this study also evaluated another 4 subjective factors: sunlight level, wind level, emotion and noise. However, the potential factors that may affect the subjects' response to the thermal environment during transient outdoor exposure are much more than what we have included. It is suggested that visit frequency, lifestyle preference, air quality, odor, glare or other factors be considered and added to the regression models to improve the fitting qualities of the regression models.

iv. This study employed the traditional regression method, i.e. multiple linear regression to develop the thermal perceptions predicting models. The regression technic itself may not be appropriate since the internal relations between predicting parameters and the predictors may be nonlinear. It is suggest that more advanced technics such as machine learning and cluster analysis be adopted to develop predicting models that perform better in nonlinear regression and with higher level of predicting accuracies.

v. The TSV and TCV predicting models in this study were developed based on PET/UTCI and their corresponding energy balance and thermal regulation models, but the model PET and UTCI themselves may not be perfectly accurate when evaluating the complex outdoor thermal conditions in the transient process. The inaccuracy induced by PET and UTCI can also be the limitation on the accuracy of the thermal perception predicting models obtained in this study. Therefore, the models that perform a better assessment of the outdoor environment in transient conditions are recommended to be the basis of the thermal perception prediction.

References

Abraham, A., Sommerhalder, K., & Abel, T. (2010). Landscape and well-being: a scoping study on the health-promoting impact of outdoor environments. *International journal of public health*, *55*(1), 59-69.

Abreu-Harbich, L. V., Labaki, L. C., & Matzarakis, A. (2014). Thermal bioclimate in idealized urban street canyons in Campinas, Brazil. *Theoretical and applied climatology*, *115*(1), 333-340.

Alexandri, E., & Jones, P. (2008). Temperature decreases in an urban canyon due to green walls and green roofs in diverse climates. *Building and Environment*, *43*(4), 480-493.

Ali-Toudert, F., & Mayer, H. (2006). Numerical study on the effects of aspect ratio and orientation of an urban street canyon on outdoor thermal comfort in hot and dry climate. *Building and Environment*, *41*(2), 94-108.

Ali-Toudert, F., & Mayer, H. (2007). Effects of asymmetry, galleries, overhanging facades and vegetation on thermal comfort in urban street canyons. *Solar Energy*, *81*(6), 742-754.

Aminipouri, M., Knudby, A. J., Krayenhoff, E. S., Zickfeld, K., & Middel, A. (2019). Modelling the impact of increased street tree cover on mean radiant temperature across Vancouver's local climate zones. *Urban forestry & urban greening*, *39*, 9-17.

Amiri, S. S., Mottahedi, M., & Asadi, S. (2015). Using multiple regression analysis to develop energy consumption indicators for commercial buildings in the US. *Energy and Buildings*, *109*, 209-216.

ASHRAE. (2009). *ASHRAE handbook: Fundamentals*. Atlanta, GA: American Society of Heating, Refrigeration and Air-Conditioning Engineers.

Berkovic, S., Yezioro, A., & Bitan, A. (2012). Study of thermal comfort in courtyards in a hot arid climate. *Solar Energy*, *86*(5), 1173-1186.

Blocken, B. (2014). 50 years of computational wind engineering: past, present and future. *Journal of Wind Engineering and Industrial Aerodynamics*, *129*, 69-102.

Bourbia, F., & Boucheriba, F. (2010). Impact of street design on urban microclimate for semi arid climate (Constantine). *Renewable Energy*, *35*(2), 343-347.

Bouyer, J., Vinet, J., Delpech, P., & Carré, S. (2007). Thermal comfort assessment in semi-outdoor environments: application to comfort study in stadia. *Journal of Wind Engineering and Industrial Aerodynamics*, *95*(9-11), 963-976.

Bowler, D. E., Buyung-Ali, L. M., Knight, T. M., & Pullin, A. S. (2010). A systematic review of evidence for the added benefits to health of exposure to natural environments. *BMC public health*, *10*(1), 1-10.

Bröde, P., Krüger, E. L., & Fiala, D. (2013). UTCI: validation and practical application to the assessment of urban outdoor thermal comfort. *Geographia Polonica*, *86*(1), 11-20.

Bröde, P., Krüger, E. L., Rossi, F. A., & Fiala, D. (2012). Predicting urban outdoor thermal comfort by the Universal Thermal Climate Index UTCI—a case study in Southern Brazil. *International journal of biometeorology*, *56*(3), 471-480.

Bross, I. D. (1958). How to use ridit analysis. *Biometrics*, 18-38.

Campra, P., Garcia, M., Canton, Y., & Palacios-Orueta, A. (2008). Surface temperature cooling trends and negative radiative forcing due to land use change toward greenhouse farming in southeastern Spain. *Journal of Geophysical Research: Atmospheres*, *113*(D18).

Chang, C.-R., & Li, M.-H. (2014). Effects of urban parks on the local urban thermal environment. *Urban forestry & urban greening*, *13*(4), 672-681.

Chang, C.-R., Li, M.-H., & Chang, S.-D. (2007). A preliminary study on the local cool-island intensity of Taipei city parks. *Landscape and urban planning*, *80*(4), 386-395.

Chatzidimitriou, A., & Yannas, S. (2015). Microclimate development in open urban spaces: The influence of form and materials. *Energy and Buildings*, *108*, 156-174.

Chen, H., Ooka, R., Harayama, K., Kato, S., & Li, X. (2004). Study on outdoor thermal environment of apartment block in Shenzhen, China with coupled simulation of convection, radiation and conduction. *Energy and Buildings*, *36*(12), 1247-

1258.

Chen, H., Ooka, R., Huang, H., & Tsuchiya, T. (2009). Study on mitigation measures for outdoor thermal environment on present urban blocks in Tokyo using coupled simulation. *Building and Environment*, *44*(11), 2290-2299.

Chen, X., Xue, P., Liu, L., Gao, L., & Liu, J. (2018). Outdoor thermal comfort and adaptation in severe cold area: A longitudinal survey in Harbin, China. *Building and Environment*, *143*, 548-560.

Cheung, P. K., & Jim, C. Y. (2019). Improved assessment of outdoor thermal comfort: 1-hour acceptable temperature range. *Building and Environment*, *151*, 303-317.

Cohen, P., Potchter, O., & Matzarakis, A. (2013). Human thermal perception of Coastal Mediterranean outdoor urban environments. *Applied Geography*, *37*, 1-10.

Dahlan, N. D., & Gital, Y. Y. (2016). Thermal sensations and comfort investigations in transient conditions in tropical office. *Applied ergonomics*, *54*, 169-176.

De Dear, R. (2011). Revisiting an old hypothesis of human thermal perception: alliesthesia. *Building Research & Information*, *39*(2), 108-117.

De Dear, R., & Pickup, J. (2000). An outdoor thermal comfort index (OUT_SET*)-part I-the model and its assumptions. In *Biometeorology and urban climatology at the turn of the millenium. Selected papers from the Conference ICB-ICUC* (Vol. 99, pp. 279-283)

Deng, J.-Y., & Wong, N. H. (2020). Impact of urban canyon geometries on outdoor thermal comfort in central business districts. *Sustainable Cities and Society*, *53*, 101966.

Dimoudi, A., & Nikolopoulou, M. (2003). Vegetation in the urban environment: microclimatic analysis and benefits. *Energy and Buildings*, *35*(1), 69-76.

Doulos, L., Santamouris, M., & Livada, I. (2004). Passive cooling of outdoor urban spaces. The role of materials. *Solar Energy*, *77*(2), 231-249.

Du, Y., Mak, C. M., Huang, T., & Niu, J. (2017). Towards an integrated method to assess effects of lift-up design on outdoor thermal comfort in Hong Kong. *Building and Environment*, *125*, 261-272.

Elnabawi, M. H., Hamza, N., & Dudek, S. (2016). Thermal perception of outdoor urban spaces in the hot arid region of Cairo, Egypt. *Sustainable Cities and Society*, *22*, 136-145.

Emmanuel, R., Rosenlund, H., & Johansson, E. (2007). Urban shading—a design option for the tropics? A study in Colombo, Sri Lanka. *International Journal of Climatology: A Journal of the Royal Meteorological Society*, *27*(14), 1995-2004.

Fang, Z., Feng, X., Liu, J., Lin, Z., Mak, C. M., Niu, J., Tse, K.-T., & Xu, X. (2019). Investigation into the differences among several outdoor thermal comfort indices against field survey in subtropics. *Sustainable Cities and Society*, *44*, 676-690.

Fang, Z., Lin, Z., Mak, C. M., Niu, J., & Tse, K.-T. (2018). Investigation into sensitivities of factors in outdoor thermal comfort indices. *Building and Environment*, *128*, 129-142.

Fanger, P. O. (1967). Calculation of thermal comfort-introduction of a basic comfort equation. *ASHRAE Transacions*, *73*.

Fanger, P. O. (1970). Thermal comfort. Analysis and applications in environmental engineering. *Thermal comfort. Analysis and applications in environmental engineering.*

Feyisa, G. L., Dons, K., & Meilby, H. (2014). Efficiency of parks in mitigating urban heat island effect: An example from Addis Ababa. *Landscape and urban planning*, *123*, 87-95.

Fiala, D. (1998). *Dynamic simulation of human heat transfer and thermal comfort* (Doctoral dissertation, De Montfort University).

Fiala, D., Havenith, G., Bröde, P., Kampmann, B., & Jendritzky, G. (2012). UTCI-Fiala multi-node model of human heat transfer and temperature regulation. *International journal of biometeorology*, *56*(3), 429-441.

Fiala, D., Lomas, K. J., & Stohrer, M. (1999). A computer model of human thermoregulation for a wide range of environmental conditions: the passive system. *Journal of applied physiology*, *87*(5), 1957-1972.

Fiala, D., Lomas, K. J., & Stohrer, M. (2001). Computer prediction of human thermoregulatory and temperature responses to a wide range of environmental conditions. *International journal of biometeorology*, *45*(3), 143-159.

Fiala, D., Psikuta, A., Jendritzky, G., Paulke, S., Nelson, D. A., van Marken Lichtenbelt, W. D., & Frijns, A. J. (2010). Physiological modeling for technical, clinical and research applications. *Frontiers in bioscience*, *2*(6), 939-968.

Gagge, A., Fobelets, A., & Berglund, L. (1986). A standard predictive Index of human reponse to thermal enviroment. *Transactions/American Society of Heating, Refrigerating and Air-Conditioning Engineers, 92*(2B), 709-731.

Gagge, A. P. (1971). An effective temperature scale based on a simple model of human physiological regulatory response. *Ashrae Trans.*, *77*, 247-262.

Gagge, A. P., Fobelets, A., & Berglund, L. (1986). A standard predictive Index of human reponse to thermal enviroment. *Transactions/American Society of Heating, Refrigerating and Air-Conditioning Engineers*, *92*(2B), 709-731.

Gehl, J. (1987). *Life between buildings* (Vol. 23). New York: Van Nostrand Reinhold.

Giannopoulou, K., Santamouris, M., Livada, I., Georgakis, C., & Caouris, Y. (2010). The impact of canyon geometry on intra urban and urban: suburban night temperature differences under warm weather conditions. *Pure and applied geophysics*, *167*(11), 1433-1449.

Gulyás, Á., Unger, J., & Matzarakis, A. (2006). Assessment of the microclimatic and human comfort conditions in a complex urban environment: modelling and measurements. *Building and Environment*, *41*(12), 1713-1722.

Hadianpour, M., Mahdavinejad, M., Bemanian, M., & Nasrollahi, F. (2018). Seasonal differences of subjective thermal sensation and neutral temperature in an outdoor shaded space in Tehran, Iran. *Sustainable Cities and Society*, *39*, 751-764.

Höppe, P. (1994). Die Wärmebilanzmodelle MEMI und IMEM zur Bewertung der thermischen Beanspruchung am Arbeitsplatz. *Verh. Dtsch. Ges. Arbeitsmed. Umweltmed*, *34*, 153-158.

Höppe, P. (1999). The physiological equivalent temperature–a universal index for the biometeorological assessment of the thermal environment. *International* *journal of biometeorology*, *43*(2), 71-75.

Höppe, P. R. (1993). Heat balance modelling. *Experientia*, *49*(9), 741-746.

Huang, J., Zhou, C., Zhuo, Y., Xu, L., & Jiang, Y. (2016). Outdoor thermal environments and activities in open space: an experiment study in humid subtropical climates. *Building and Environment*, *103*, 238-249.

Huang, T., Li, J., Xie, Y., Niu, J., & Mak, C. M. (2017). Simultaneous environmental parameter monitoring and human subject survey regarding outdoor thermal comfort and its modelling. *Building and Environment*, *125*, 502-514.

Huang, T., Niu, J., Xie, Y., Li, J., & Mak, C. M. (2020). Assessment of “lift-up” design's impact on thermal perceptions in the transition process from indoor to outdoor. *Sustainable Cities and Society*, *56*, 102081.

Hwang, R.-L., & Lin, T.-P. (2007). Thermal comfort requirements for occupants of semi-outdoor and outdoor environments in hot-humid regions. *Architectural Science Review*, *50*(4), 357-364.

ISO, S. (2005). Ergonomics of the thermal environment, analytical determination and interpretation of thermal comfort using calculations of the PMV and PPD indices and local thermal comfort criteria.

Jamei, E., Rajagopalan, P., Seyedmahmoudian, M., & Jamei, Y. (2016). Review on the impact of urban geometry and pedestrian level greening on outdoor thermal comfort. *Renewable and Sustainable Energy Reviews*, *54*, 1002-1017.

Jendritzky, G., de Dear, R., & Havenith, G. (2012). UTCI—why another thermal index? *International journal of biometeorology*, *56*(3), 421-428.

Johansson, E. (2006). Influence of urban geometry on outdoor thermal comfort in a hot dry climate: A study in Fez, Morocco. *Building and Environment*, *41*(10), 1326-1338.

Johansson, E., & Emmanuel, R. (2006). The influence of urban design on outdoor thermal comfort in the hot, humid city of Colombo, Sri Lanka. *International journal of biometeorology*, *51*(2), 119-133.

Johansson, E., Yahia, M. W., Arroyo, I., & Bengs, C. (2018). Outdoor thermal comfort in public space in warm-humid Guayaquil, Ecuador. *International journal of* *biometeorology*, *62*(3), 387-399.

Klemm, W., Heusinkveld, B. G., Lenzholzer, S., Jacobs, M. H., & Van Hove, B. (2015). Psychological and physical impact of urban green spaces on outdoor thermal comfort during summertime in The Netherlands. *Building and Environment*, *83*, 120-128.

Kong, L., Lau, K. K.-L., Yuan, C., Chen, Y., Xu, Y., Ren, C., & Ng, E. (2017). Regulation of outdoor thermal comfort by trees in Hong Kong. *Sustainable Cities and Society*, *31*, 12-25.

KOPPEN, W. d. (1936). Das geographische system der klimat. *Handbuch der klimatologie*, 46.

Krüger, E., Drach, P., & Bröde, P. (2015). Implications of air-conditioning use on thermal perception in open spaces: a field study in downtown Rio de Janeiro. *Building and Environment*, *94*, 417-425.

Lai, D., Guo, D., Hou, Y., Lin, C., & Chen, Q. (2014). Studies of outdoor thermal comfort in northern China. *Building and Environment*, *77*, 110-118.

Lai, D., Liu, W., Gan, T., Liu, K., & Chen, Q. (2019). A review of mitigating strategies to improve the thermal environment and thermal comfort in urban outdoor spaces. *Science of the total environment*, *661*, 337-353.

Lai, D., Zhou, C., Huang, J., Jiang, Y., Long, Z., & Chen, Q. (2014). Outdoor space quality: A field study in an urban residential community in central China. *Energy and Buildings*, *68*, 713-720.

Lam, C. K. C., & Lau, K. K.-L. (2018). Effect of long-term acclimatization on summer thermal comfort in outdoor spaces: a comparative study between Melbourne and Hong Kong. *International journal of biometeorology*, *62*(7), 1311-1324.

Lam, J. C., Hui, S. C., & Chan, A. L. (1997). Regression analysis of high-rise fully air-conditioned office buildings. *Energy and Buildings*, *26*(2), 189-197.

Lau, K. K.-L., Chung, S. C., & Ren, C. (2019). Outdoor thermal comfort in different urban settings of sub-tropical high-density cities: An approach of adopting local climate zone (LCZ) classification. *Building and Environment*, *154*, 227-238.

Liao, C. J., & Cech, I. I. (1977). Effect of abrupt exposure to outdoor heat on humans accustomed to air conditioning. *Urban Ecology*, *2*(4), 355-369.

Lin, T.-P. (2009). Thermal perception, adaptation and attendance in a public square in hot and humid regions. *Building and Environment*, *44*(10), 2017-2026.

Lin, T.-P., De Dear, R., Matzarakis, A., & Hwang, R. L. (2009). Prediction of thermal acceptability in hot-humid outdoor environments in Taiwan. In *The seventh International Conference on Urban Climate*.

Lin, T.-P., & Matzarakis, A. (2008). Tourism climate and thermal comfort in Sun Moon Lake, Taiwan. *International journal of biometeorology*, *52*(4), 281-290.

Lin, T.-P., Matzarakis, A., & Hwang, R.-L. (2010). Shading effect on long-term outdoor thermal comfort. *Building and Environment*, *45*(1), 213-221.

Lin, T. P., De Dear, R., & Hwang, R. L. (2011). Effect of thermal adaptation on seasonal outdoor thermal comfort. *International journal of climatology*, *31*(2), 302-312.

Lin, W., Yu, T., Chang, X., Wu, W., & Zhang, Y. (2015). Calculating cooling extents of green parks using remote sensing: Method and test. *Landscape and urban planning*, *134*, 66-75.

Lin, Y., Zhong, S., Yang, W., Hao, X., & Li, C.-Q. (2021). Multi-objective design optimization on building integrated photovoltaic with Trombe wall and phase change material based on life cycle cost and thermal comfort. *Sustainable Energy Technologies and Assessments*, *46*, 101277.

Liu, H., Liao, J., Yang, D., Du, X., Hu, P., Yang, Y., & Li, B. (2014). The response of human thermal perception and skin temperature to step-change transient thermal environments. *Building and Environment*, *73*, 232-238.

Liu, J., Niu, J., & Xia, Q. (2016). Combining measured thermal parameters and simulated wind velocity to predict outdoor thermal comfort. *Building and Environment*, *105*, 185-197.

Liu, W., Zhang, Y., & Deng, Q. (2016). The effects of urban microclimate on outdoor thermal sensation and neutral temperature in hot-summer and cold-winter climate. *Energy and Buildings*, *128*, 190-197.

Lloyd, K., & Auld, C. (2003). Leisure, public space and quality of life in the urban environment. *Urban policy and research*, *21*(4), 339-356.

Mahmoud, A. H. A. (2011). Analysis of the microclimatic and human comfort conditions in an urban park in hot and arid regions. *Building and Environment*, *46*(12), 2641-2656.

Matzarakis, A., & Mayer, H. (1996). Another kind of environmental stress: thermal stress. *WHO newsletter*, *18*(January 1996), 7-10.

Matzarakis, A., & Mayer, H. (1997). Heat stress in Greece. *International journal of biometeorology*, *41*(1), 34-39.

Matzarakis, A., Mayer, H., & Iziomon, M. G. (1999). Applications of a universal thermal index: physiological equivalent temperature. *International journal of biometeorology*, *43*(2), 76-84.

Matzarakis, A., Rutz, F., & Mayer, H. (2007). Modelling radiation fluxes in simple and complex environments—application of the RayMan model. *International journal of biometeorology*, *51*(4), 323-334.

Mayer, H., & Höppe, P. (1987). Thermal comfort of man in different urban environments. *Theoretical and applied climatology*, *38*(1), 43-49.

Middel, A., & Krayenhoff, E. S. (2019). Micrometeorological determinants of pedestrian thermal exposure during record-breaking heat in Tempe, Arizona: Introducing the MaRTy observational platform. *Science of the total environment*, *687*, 137-151.

Middel, A., Selover, N., Hagen, B., & Chhetri, N. (2016). Impact of shade on outdoor thermal comfort—a seasonal field study in Tempe, Arizona. *International journal of biometeorology*, *60*(12), 1849-1861.

Mihara, K., Sekhar, C., Tham, K. W., Takemasa, Y., & Lasternas, B. (2019). Effects of temperature, air movement and initial metabolic rate on thermal sensation during transient state in the tropics. *Building and Environment*, *155*, 70-82. https://doi.org/10.1016/j.buildenv.2019.03.030

Morakinyo, T. E., Lau, K. K.-L., Ren, C., & Ng, E. (2018). Performance of Hong Kong's common trees species for outdoor temperature regulation, thermal comfort and energy saving. *Building and Environment*, *137*, 157-170.

Nagano, K., & Horikoshi, T. (2011). New index indicating the universal and separate effects on human comfort under outdoor and non-uniform thermal conditions. *Energy and Buildings*, *43*(7), 1694-1701.

Nazarian, N., Fan, J., Sin, T., Norford, L., & Kleissl, J. (2017). Predicting outdoor thermal comfort in urban environments: A 3D numerical model for standard effective temperature. *Urban climate*, *20*, 251-267.

Ng, E., Chen, L., Wang, Y., & Yuan, C. (2012). A study on the cooling effects of greening in a high-density city: An experience from Hong Kong. *Building and Environment*, *47*, 256-271.

Ng, E., & Cheng, V. (2012). Urban human thermal comfort in hot and humid Hong Kong. *Energy and Buildings*, *55*, 51-65.

Niachou, K., Livada, I., & Santamouris, M. (2008). Experimental study of temperature and airflow distribution inside an urban street canyon during hot summer weather conditions. Part II: Airflow analysis. *Building and Environment*, *43*(8), 1393-1403.

Nikolopoulou, M., & Lykoudis, S. (2006). Thermal comfort in outdoor urban spaces: analysis across different European countries. *Building and Environment*, *41*(11), 1455-1470.

Niu, J., Liu, J., Lee, T.-c., Lin, Z. J., Mak, C., Tse, K.-T., Tang, B.-s., & Kwok, K. C. (2015). A new method to assess spatial variations of outdoor thermal comfort: Onsite monitoring results and implications for precinct planning. *Building and Environment*, *91*, 263-270.

Oke, T. R., Mills, G., Christen, A., & Voogt, J. A. (2017). *Urban climates*. Cambridge University Press.

Parkinson, T., & De Dear, R. (2015). Thermal pleasure in built environments: physiology of alliesthesia. *Building Research & Information*, *43*(3), 288-301.

Parkinson, T., & de Dear, R. (2016). Thermal pleasure in built environments: spatial alliesthesia from contact heating. *Building Research & Information*, *44*(3), 248-262.

Parkinson, T., & de Dear, R. (2017). Thermal pleasure in built environments: spatial alliesthesia from air movement. *Building Research & Information*, *45*(3), 320-335.

Parkinson, T., de Dear, R., & Candido, C. (2016). Thermal pleasure in built environments: alliesthesia in different thermoregulatory zones. *Building Research & Information*, *44*(1), 20-33.

Pickup, J., & de Dear, R. (2000). An outdoor thermal comfort index (OUT_SET*)-part I-the model and its assumptions. In *Biometeorology and urban climatology at the turn of the millenium. Selected papers from the Conference ICB-ICUC* (Vol. 99, pp. 279-283)

Provençal, S., Bergeron, O., Leduc, R., & Barrette, N. (2016). Thermal comfort in Quebec City, Canada: sensitivity analysis of the UTCI and other popular thermal comfort indices in a mid-latitude continental city. *International journal of biometeorology*, *60*(4), 591-603.

Qaid, A., Lamit, H. B., Ossen, D. R., & Shahminan, R. N. R. (2016). Urban heat island and thermal comfort conditions at micro-climate scale in a tropical planned city. *Energy and Buildings*, *133*, 577-595.

Rosenfeld, A. H., Akbari, H., Bretz, S., Fishman, B. L., Kurn, D. M., Sailor, D., & Taha, H. (1995). Mitigation of urban heat islands: materials, utility programs, updates. *Energy and Buildings*, *22*(3), 255-265.

Rosso, F., Golasi, I., Castaldo, V. L., Piselli, C., Pisello, A. L., Salata, F., Ferrero, M., Cotana, F., & de Lieto Vollaro, A. (2018). On the impact of innovative materials on outdoor thermal comfort of pedestrians in historical urban canyons. *Renewable Energy*, *118*, 825-839.

Salata, F., Golasi, I., de Lieto Vollaro, R., & de Lieto Vollaro, A. (2016). Outdoor thermal comfort in the Mediterranean area. A transversal study in Rome, Italy. *Building and Environment*, *96*, 46-61.

Santamouris, M. (2013). Using cool pavements as a mitigation strategy to fight urban heat island—A review of the actual developments. *Renewable and Sustainable Energy Reviews*, *26*, 224-240.

Santamouris, M. (2014). Cooling the cities–a review of reflective and green roof mitigation technologies to fight heat island and improve comfort in urban environments. *Solar Energy*, *103*, 682-703.

Shashua-Bar, L., & Hoffman, M. E. (2000). Vegetation as a climatic component in the design of an urban street: An empirical model for predicting the cooling effect of urban green areas with trees. *Energy and Buildings*, *31*(3), 221-235.

Skoulika, F., Santamouris, M., Kolokotsa, D., & Boemi, N. (2014). On the thermal characteristics and the mitigation potential of a medium size urban park in Athens, Greece. *Landscape and urban planning*, *123*, 73-86.

Song, J., & Wang, Z.-H. (2015). Impacts of mesic and xeric urban vegetation on outdoor thermal comfort and microclimate in Phoenix, AZ. *Building and Environment*, *94*, 558-568.

Sonne, J. K., & Vieira, R. K. (2000). Cool neighborhoods: the measurement of small scale heat islands. In *Proceedings of* (pp. 650-655).

Spagnolo, J., & De Dear, R. (2003). A field study of thermal comfort in outdoor and semi-outdoor environments in subtropical Sydney Australia. *Building and Environment*, *38*(5), 721-738.

Standard, A. (1992). 55, Thermal environmental conditions for human occupancy. *American Society of Heating, Refrigerating and Air conditioning Engineers*, *145*.

Standardization, I. O. f. (1998). *Ergonomics of the Thermal Environment: Instruments for Measuring Physical Quantities*. ISO.

Svensson, M. K., Thorsson, S., & Lindqvist, S. (2003). A geographical information system model for creating bioclimatic maps–examples from a high, mid-latitude city. *International journal of biometeorology*, *47*(2), 102-112.

Takahashi, K., Yoshida, H., Tanaka, Y., Aotake, N., & Wang, F. (2004). Measurement of thermal environment in Kyoto city and its prediction by CFD simulation. *Energy and Buildings*, *36*(8), 771-779.

Taleghani, M. (2018). Outdoor thermal comfort by different heat mitigation strategies-A review. *Renewable and Sustainable Energy Reviews*, *81*, 2011-2018.

Taleghani, M., Kleerekoper, L., Tenpierik, M., & Van Den Dobbelsteen, A. (2015). Outdoor thermal comfort within five different urban forms in the Netherlands. *Building and Environment*, *83*, 65-78.

Taleghani, M., Sailor, D. J., Tenpierik, M., & van den Dobbelsteen, A. (2014). Thermal assessment of heat mitigation strategies: The case of Portland State University, Oregon, USA. *Building and Environment*, *73*, 138-150.

Thorsson, S., Honjo, T., Lindberg, F., Eliasson, I., & Lim, E.-M. (2007). Thermal comfort and outdoor activity in Japanese urban public places. *Environment and Behavior*, *39*(5), 660-684.

Toparlar, Y., Blocken, B., Maiheu, B., & Van Heijst, G. (2017). A review on the CFD analysis of urban microclimate. *Renewable and Sustainable Energy Reviews*, *80*, 1613-1640.

Toudert, F. A. (2005). Dependence of outdoor thermal comfort on street design in hot and dry climate.

Vailshery, L. S., Jaganmohan, M., & Nagendra, H. (2013). Effect of street trees on microclimate and air pollution in a tropical city. *Urban forestry & urban greening*, *12*(3), 408-415.

Villadiego, K., & Velay-Dabat, M. A. (2014). Outdoor thermal comfort in a hot and humid climate of Colombia: A field study in Barranquilla. *Building and Environment*, *75*, 142-152.

Watanabe, S., Nagano, K., Ishii, J., & Horikoshi, T. (2014). Evaluation of outdoor thermal comfort in sunlight, building shade, and pergola shade during summer in a humid subtropical region. *Building and Environment*, *82*, 556-565.

Xi, T., Li, Q., Mochida, A., & Meng, Q. (2012). Study on the outdoor thermal environment and thermal comfort around campus clusters in subtropical urban areas. *Building and Environment*, *52*, 162-170.

Xie, Y. (2020). A quantitative analysis and modeling of human thermal sensation and comfort in outdoor spaces.

Xiong, J., Zhou, X., Lian, Z., You, J., & Lin, Y. (2016). Thermal perception and skin temperature in different transient thermal environments in summer. *Energy and*

Buildings, *128*, 155-163.

Xu, M., Hong, B., Jiang, R., An, L., & Zhang, T. (2019). Outdoor thermal comfort of shaded spaces in an urban park in the cold region of China. *Building and Environment*, *155*, 408-420.

Yahia, M. W., & Johansson, E. (2013). Evaluating the behaviour of different thermal indices by investigating various outdoor urban environments in the hot dry city of Damascus, Syria. *International journal of biometeorology*, *57*(4), 615-630.

Yang, F., Lau, S. S., & Qian, F. (2011). Thermal comfort effects of urban design strategies in high-rise urban environments in a sub-tropical climate. *Architectural Science Review*, *54*(4), 285-304.

Yin, J., Zheng, Y., Wu, R., Tan, J., Ye, D., & Wang, W. (2012). An analysis of influential factors on outdoor thermal comfort in summer. *International journal of biometeorology*, *56*(5), 941-948.

Yu, Z. J., Yang, B., & Zhu, N. (2015). Effect of thermal transient on human thermal comfort in temporarily occupied space in winter–A case study in Tianjin. *Building and Environment*, *93*, 27-33.

Zhang, Y., Liu, J., Zheng, Z., Fang, Z., Zhang, X., Gao, Y., & Xie, Y. (2020). Analysis of thermal comfort during movement in a semi-open transition space. *Energy and Buildings*, *225*. https://doi.org/10.1016/j.enbuild.2020.110312

Zhou, Z., Chen, H., Deng, Q., & Mochida, A. (2013). A field study of thermal comfort in outdoor and semi-outdoor environments in a humid subtropical climate city. *Journal of Asian Architecture and Building Engineering*, *12*(1), 73-79.